NTNU
Norwegian University of
Science and Technology

Integrated energy system for Granåsen Snow Arena, Hotel and Supermarket

Jostein Birkeland

Master of Science in Mechanical Engineering
Submission date: June 2018
Supervisor: Armin Hafner, EPT

Norwegian University of Science and Technology
Department of Energy and Process Engineering

NTNU

Norwegian University
of Science and Technology

Department of Energy
and Process Engineering

EPT-M-2018-07

MASTER THESIS

for

student Jostein Birkeland

Spring 2018

Integrated energy system for Granåsen Snow Arena, Hotel and Supermarket

Integrert energisentral for helårs langrennsløype, hotell og butikk i Granåsen

Background and objective

Large investments will be made in the near future to further develop the skiing area (cross country, jump, biathlon, etc.) around Granåsen in Trondheim. This will enable to host world cup events and utilise the arena for training activities of local, national and international teams.

REMA1000 plans to build a supermarket in the area. The building will also host a hotel with approximately 200 rooms. As a gimmick and attraction, the hotel will provide its guests a 1 km cross country slope available all year.

The objective of the Master Thesis is to develop and describe how the energy system with a centralised heat pumping unit should be designed to provide all major heating and cooling demands of the building and for snow (ice) production.

The following tasks are to be considered:

1 Literature review on state of the art supermarket refrigeration systems, heat pumping systems for hotels, snow production methods and snow demands for all year ski slopes.
2. Describe and calculate the ice demand for an operative ski slope on a daily base for a normal year with typical climatic data for Granåsen (with and without shading).
3. Describe and calculate the cooling, heating and hot water demand for a hotel building with 200 rooms at Granåsen.
4. Describe and calculate the refrigeration demand for a standard REMA1000 supermarket at Granåsen (Basement location, no AC demand).
5. Develop a calculation tool to integrate and analyse the various energy flows to be able to describe the design specification of the centralised refrigeration unit (providing heating, cooling and hot water) and required energy (hot and cold) storage devices.
5. Discussion, conclusions and proposals for further work
6. Make a draft scientific paper based on the main results

-- ” --

Within 14 days of receiving the written text on the master thesis, the candidate shall submit a research plan for his project to the department.

When the thesis is evaluated, emphasis is put on processing of the results, and that they are presented in tabular and/or graphic form in a clear manner, and that they are analyzed carefully.

The thesis should be formulated as a research report with summary both in English and Norwegian, conclusion, literature references, table of contents etc. During the preparation of the text, the candidate should make an effort to produce a well-structured and easily readable report. In order to ease the evaluation of the thesis, it is important that the cross-references are correct. In the making of the report, strong emphasis should be placed on both a thorough discussion of the results and an orderly presentation.

The candidate is requested to initiate and keep close contact with his/her academic supervisor(s) throughout the working period. The candidate must follow the rules and regulations of NTNU as well as passive directions given by the Department of Energy and Process Engineering.

Risk assessment of the candidate's work shall be carried out according to the department's procedures. The risk assessment must be documented and included as part of the final report. Events related to the candidate's work adversely affecting the health, safety or security, must be documented and included as part of the final report. If the documentation on risk assessment represents a large number of pages, the full version is to be submitted electronically to the supervisor and an excerpt is included in the report.

Pursuant to "Regulations concerning the supplementary provisions to the technology study program/Master of Science" at NTNU §20, the Department reserves the permission to utilize all the results and data for teaching and research purposes as well as in future publications.

The final report is to be submitted digitally in DAIM. An executive summary of the thesis including title, student's name, supervisor's name, year, department name, and NTNU's logo and name, shall be submitted to the department as a separate pdf file. Based on an agreement with the supervisor, the final report and other material and documents may be given to the supervisor in digital format.

☐ Work to be done in lab (Water power lab, Fluids engineering lab, Thermal engineering lab)
☐ Field work

Department of Energy and Process Engineering, 15. January 2018

_____
Prof. Dr.-Ing. Armin Hafner
Academic Supervisor

Research Advisor: Prof. Trygve M. Eikevik (trygve.m.eikevik@ntnu.no)
Prof. Petter Nekså (Petter.Neksa@sintef.no>)

Preface

This master's thesis is the final dissertation for my M.Sc. degree at the Department of Energy and Process Engineering at the Norwegian University of Science and Technology (NTNU), in the spring of 2018.

The topic for the thesis is based on challenges associated with energy consumption in commercial buildings and for snow production, with the aim to minimize the power demand of a centralized heat pumping unit.

I contacted my main supervisor, Prof. Dr.-Ing. Armin Hafner at NTNU, with the aim to write my thesis within the subject of commercial refrigeration after attending a course he lectured during the fall of 2017. I am very grateful for his positive response and the guidance I have received from him and my research advisors, Prof. Trygve M. Eikevik and Prof. Petter Nekså, during my work. I would also like to thank my friend and fellow student Espen Halvorsen Verpe for the discussions we have had during all our years at NTNU.

Thanks to my family for complete support during all my six years as a student in Trondheim.

Finally, I would like to express that I am very happy to have written a thesis touching the subjects of winter sports and environmental challenges, which are of my personal interest.

Jostein Birkeland Trondheim, July 28th 2018

Abstract

Granåsen in Trondheim is the chosen location for Norway's application to host the 2023 FIS Nordic Ski World Championships. One of the investments to develop the area around Granåsen is a new building accommodating a REMA1000 supermarket and a 200 room hotel. A key feature for the hotel is to offer its guests a cross-country slope available all year. This thesis aims to describe how a centralized heat pumping unit should be designed to provide all major thermal demands of the building in addition for the snow production to the cross-country slope.

The snow demand of the cross-country slope with and without provided shade is calculated using a degree-day method which includes radiation. Meteorological data is collected from the database Meteonorm. A model of the hotel is created in the building simulation software SIMIEN, to obtain heating and cooling demands. A numerical model of the centralized R744 heat pump integrated with a flake ice machine is created in Microsoft Excel, utilizing the free library RnLib for thermodynamic data. Four cases are defined to investigate costs and performance. In cases 1 and 2, all available heat is recovered. In cases 3 and 4, heat is only recovered to cover the demand of the building. In cases 1 and 3, snow is produced continuously, whereas in cases 2 and 4, snow is produced during the hours of the day with cheaper electricity.

In annual simulations, shading was found to reduce the snow demand from 80 406 m^3 to 47 036 m^3. The required snow storage volume to overcome the snow demand in summer is 20 000 m^3. The annual average energy efficiency of the heat pump was found to be 4.62, with 8 times more heat available in the gas cooler than the demand of the building. Sale of the excess heat to local clients is therefore considered. A 30 m^3 thermal storage tank is required to cover the heating demand. Parameter studies altering the high-side pressure and evaporation temperature in the flake ice machine were carried out and found to increase the efficiency from 4.62 to 5.02 and 5.79, respectively. This is higher than traditional heat pumps and similar to existing R744 systems. The current design should be improved by reducing the high-side pressure, in accordance with the findings of the parameter study. The results also suggest that one-stage compression of the discharge from the flake ice machine, especially in combination with a higher evaporation temperature in the flake ice machine, will improve performance. The sale of excess energy will cover a large part of the electricity cost and greatly increase the profitability of the investment.

Sammendrag

Granåsen i Tronhdheim er valgt som arena for Norges søknad til VM på ski i 2023. En av investeringene for å utvikle området rundt Granåsen er en bygning med en REMA1000-butikk i kjelleren og et 200-roms hotell i etasjene over. Hotellet vil tilby gjestene sine en langrennsløype tilgjengelig hele året. Denne oppgaven tar sikte på å beskrive hvordan en sentralisert varmepumpe bør designes for å dekke alle de viktigste varme- og kjølebehovene til bygningen, samt snøproduksjon.

Snøbehovet til langrennsløypa er regnet ut med og uten solskjerming ved hjelp av en graddagsmetode som inkluderer stråling. Meteorologiske data er hentet fra databasen Meteonorm. En modell av hotellet er opprettet i bygningssimuleringsprogrammet SIMIEN for å finne hotellets varme- og kjølebehov. En numerisk modell av R744-varmepumpen, integrert med en flakismaskin, er laget i Excel, med bruk av det frie biblioteket RnLib for termodynamiske data. Fire caser er definert for å undersøke kostnader og ytelse av systemet. I case 1 og 2 gjenvinnes all tilgjengelig varme. I case 3 og 4 gjenvinnes varme kun for å dekke bygningens varmebehov. Case 1 og 3 er simulert med jevn snøproduksjon, mens i case 2 og 4 produseres snø i perioder på døgnet med lavere strømpriser.

Årlige simuleringer viser at solskjermingen reduserer snøbehovet fra 80 406 m^3 til 47 036 m^3. For å overkomme snøbehovet om sommeren trengs et 20 000 m^3 snølager. Varmepumpens gjennomsnittelige årlige energieffektivitet er regnet ut til å være 4.62, med 8 ganger mer varme tilgjengelig i gasskjøleren enn det totale varmebehovet til bygningen. Salg av overskuddsvarme til lokale kunder er derfor vurdert. Parameterstudier av høysidetrykket og fordampningstemperaturen i flakismaskinen er utført og resultatene viser en henholdsvis økning av effektiviteten til 5.02 og 5.79. Dette er høyere ytelse enn tradisjonelle systemer og lik som andre R744-varmepumper. Det nåværende designet burde forbedres ved å redusere høysidetrykket, i tråd med resultatet av parameterstudiet. Resultatene peker også mot at en-trinns komprimering av utløpet fra flakismaskinen, særlig i kombinasjon med en økning av fordampningstemperaturen i flakismaskinen, vil forbedre ytelsen. Salget av overskuddsvarme vil dekke en stor del av strømkostnadene og øke lønnsomheten av investeringen betraktelig.

Contents

Preface v

Abstract vii

Sammendrag ix

Nomenclature xv

1 Introduction **1**

1.1 Background 1

1.2 Objective 2

1.3 Outline of the thesis 2

2 Heat pump and refrigeration systems **5**

2.1 Supermarket refrigeration systems 6

2.1.1 Environmental impact of refrigerants and the reintroduction of CO_2 . . . 7

2.1.2 Energy performance 8

2.1.3 Common refrigeration systems using CO_2 9

2.1.4 Transcritical CO_2 booster system 10

2.1.5 Heat recovery from the gas cooler 11

2.2 Heat pump systems in hotels 13

2.2.1 Drainage water heat recovery 15

2.2.2 Thermal energy storage tanks and PCMs 17

3 Snow production methods and snow demand **19**

3.1 Snow guns 19

3.2 Temperature independent snowmaking machines 22

3.2.1 Flake ice machines 22

3.2.2 Plate ice machines . . . 23
3.2.3 Ice slurry methods . . . 24
3.2.4 Connecting snowmaking equipment to a refrigeration system . . . 25
3.3 Snow storage methods . . . 28
3.3.1 Outdoor snow storage . . . 28
3.3.2 Indoor snow storage . . . 29
3.4 Snow demand for all year ski slopes . . . 30

4 Simulation model and system design **33**
4.1 Shading and snow production . . . 34
4.2 Building models and supermarket refrigeration demand . . . 36
4.2.1 AC and space heating . . . 37
4.2.2 Domestic hot water . . . 39
4.2.3 Supermarket refrigeration demand . . . 40
4.3 Transcritical CO_2 heat pump . . . 40
4.3.1 Heat pump design . . . 41
4.3.2 Control strategy . . . 47
4.3.3 Hourly electricity price variation and power fees . . . 53
4.4 Thermal storages and PCM integration . . . 55

5 Results and discussion **57**
5.1 Shading and snow production . . . 57
5.2 Building simulation . . . 59
5.3 Transcritical CO_2 heat pump . . . 63
5.3.1 Seasonal performance . . . 67
5.3.2 DHW and space heat storages . . . 71
5.3.3 Economical considerations . . . 73
5.4 Parameter study . . . 76
5.4.1 High-side pressure during heat recovery . . . 76
5.4.2 Evaporation temperature in the flake ice machine . . . 77
5.5 Remarks and further discussion . . . 79

6 Summary and conclusion **83**

6.1 Suggestions for further work 84

Bibliography **86**

Appendices **95**

A Risk Assessment **97**

B Draft Scientific Paper **99**

Nomenclature

Abbreviations

AC	Air conditioning
a.s.l.	Above sea level
CFC	Chlorofluorocarbon
COP	Coefficient of performance
DHW	Domestic hot water
E.E.	Energy efficiency
F-gases	Fluorinated greenhouse gases
FID	Flake ice drum
GWP	Global warming potential
HCFC	Hydrochlorofluorocarbon
HFC	Hydrofluorocarbon
LT	Low temperature
MT	Medium temperature
ODP	Ozone depletion potential
PCM	Phase change material
TIS	Temperature independent snowmaking

Greek letters

η_{is}	Isentropic efficiency of compressors	[-]
ρ	Density	[kg/m^3]

Roman letters

A	Area	[m^2]
$a_{snow/ice}$	Irradiance coefficient	[-]
c_p	Specific heat at constant pressure	[kJ/kgK]
C	Cooling contribution	[MWh]
E	Energy	[kJ]
$f_{heat\ loss}$	Heat loss factor	[-]
$F_{i,j}$	View factor	[-]
G_s	Measured global irradiance	[W/m^2]
h	Enthalpy per unit mass	[kJ/kg]
h_{sf}	Heat of solidification per unit mass	[kJ/kg]
H	Heating contribution	[MWh]
I	Potential clear-sky irradiance	[W/m^2]
I_s	Potential clear-sky direct solar irradiance	[W/m^2]
m	Mass	[kg]
$\dot{m}$	Mass flow	[kg/s]
M	Melt rate	[mm/h]
MF	Melt factor	[mm/day°C]
n	Number of time steps	[1/day]
P	Pressure	[bar]
PR	Pressure ratio	[-]
ΔP	Pressure difference	[bar]
$\dot{Q}$	Heat transfer rate	[kW]
T	Temperature	[°C]
ΔT_{lm}	Logarithmic mean temperature difference	[K]
U	Overall heat transfer coefficient	[W/m^2K]
$\dot{V}$	Volumetric flow rate	[L/s]
$\dot{W}$	Rate of work, or power	[kW]
W	Work	[MWh]
$W_{i,j}$	Relative width	[-]

1. Introduction

1.1 Background

The Norwegian Ski Federation and the Municipality of Trondheim are together applying to host the 2023 FIS Nordic World Ski Championships. To host such events and provide a training arena for local, national and international teams, large investments will be made in the near future to further develop the skiing area around Granåsen in Trondheim.

One of these investments is a new REMA1000 supermarket. The building will also host a hotel with approximately 200 rooms. As an attraction, the hotel will provide its guests with a 1 km cross-country slope available all year. This will require temperature independent snow production, which has been criticized for having a high electricity demand and not being environmentally friendly (Müller, 2015). Taking into consideration that the number of days with snow in central Norway is expected to drop from 150 to 70-80 by 2100 (Hanssen-Bauer et al., 2009), investigation of TIS systems in Granåsen is of interest beyond a short summer slope. In light of increasing global temperatures, energy efficiency naturally becomes a focus area of the new investments in the area. Therefore, the supermarkets' centralized refrigeration unit will be designed to provide all major heating and cooling demands of the building and for snow production in order to minimize the total electricity demand of the building.

Figure 1.1: An illustration of a Nordic World Championship in Granåsen, Trondheim (Trondheim Kommune, 2018)

Supermarkets represent 3-4 % of the national electricity used in western countries (Arias, 2005; Tassou et al., 2011). Additionally, their environmental impact is increased by leakages of the refrigerant in their refrigeration systems. The most common refrigerant in supermarkets worldwide is HCFC-22, and annual leakages are as high as 30 % of the total installed charge (Hafner et al., 2012). In Europe, the figure is about 15-20 % with HFC-404a being the main refrigerant in use. Such fluids have high GWP and ODP values, which has induced regulations to phase out and ban their use. One example is the 2016 Kigali Amendment, introducing specific timetables worldwide for the phase-down on substances that deplete the ozone layer (United Nations Environmental Program, 2016). Another is the 2015 EU F-gas regulation, which will cut the emissions from HFCs and HCFCs to one-third by 2030, compared to 2014 levels (European Union, 2016). This has led to research on natural refrigerants such as CO_2, ammonia and hydrocarbons. CO_2 has emerged as the best option and its reintroduction as a refrigerant will reduce the consequence of emissions from refrigeration systems, as it has a GWP value more than a thousand times lower than the current day's most used refrigerants.

1.2 Objective

This master thesis aims to map the demands to be covered by the centralized refrigeration unit using CO_2 as the working fluid, before developing its design. Methods to improve energy efficiency will be investigated as well as strategies to reduce the operational costs. The design specifications and the requirements for energy storage devices will be presented.

1.3 Outline of the thesis

Chapter 2 is a literature review of state of the art supermarket refrigeration systems and heat pump systems in hotels. The motivation for the reintroduction of CO_2 as a refrigerant is introduced before examples of methods to improve efficiency and reduce costs of hotel heat pump systems are discussed.

Chapter 3 is a literature review of snow production methods and snow storing. Snow producing equipment both dependent and independent of ambient temperature is presented followed by examples and experimental data of outdoor snow storage. A calculation method for snowmelt is suggested to estimate the yearly snow demand for a cross-country slope.

In Chapter 4, assumptions and theory used in calculations are presented along with the components of the model. The design and control strategy of the heat pump is explained.

In Chapter 5, results from calculations and simulations are treated and presented. Four cases are defined to evaluate the heat pump. A parameter study is performed to investigate measures to improve the heat pump's performance. Limitations of the model and the validity of the results are discussed.

Chapter 6 comprises the summary, conclusion and suggestions for further work.

2. Heat pump and refrigeration systems

In order to discuss heating and refrigeration systems, one needs to know the basic principle of a heat pumping unit. Figure 2.1 shows the components of a simple, one-stage heat pump. A phase-changing fluid circulates through the components. It typically enters the evaporator

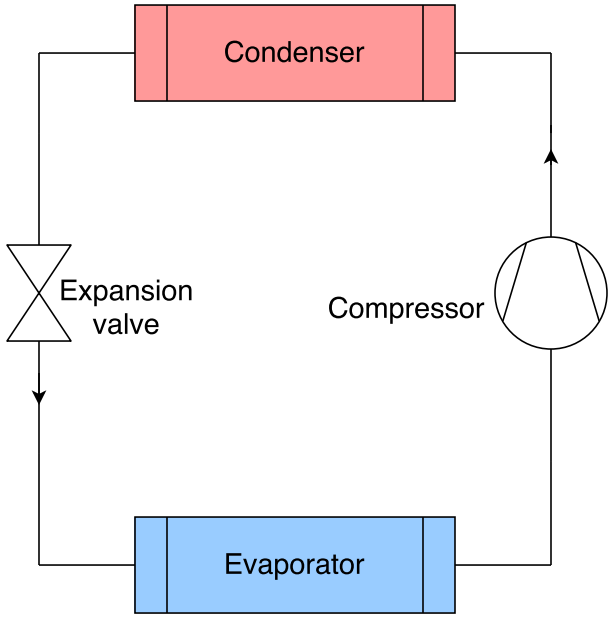

Figure 2.1: A basic heat pump and its components

in a mixed state of gas and liquid. The fluid is evaporated by heat added to the system. This heat can be added at a low temperature, allowing heat to be extracted from low-temperature sources such as sea-water. If the heat pump is used for refrigeration purposes, the evaporator is used to extract heat from a reservoir where there is a cooling demand. As the compressor can be damaged if it sucks in a liquid instead of a gas, the fluid is fully evaporated to gas state before entering the compressor. It is normal to super-heat the fluid to make sure it is in gas state. This means to add additional heat even after gas state is reached. In the compressor, the pressure and temperature are increased by mechanical work. The compressor can be powered by electricity. The fluid, now at high pressure and temperature in gas state, enters the condenser. Latent heat is extracted as the fluid condenses into the two-phase state. Both the evaporation and condensation happens at constant pressure and temperature. The fluid is expanded to a lower temperature and pressure in the valve before entering the evaporator again and starting a

new cycle through the components. In both ideal heat pump and ideal refrigeration cycles, the sum of the heat added in the evaporator and the power input in the compressor is equal to the rejected heat in the condenser (Moran et al., 2012):

$$\dot{Q}_{condenser} = \dot{Q}_{evaporator} + \dot{W}_{cycle} \tag{2.1}$$

This relation is illustrated in figure Figure 2.2:

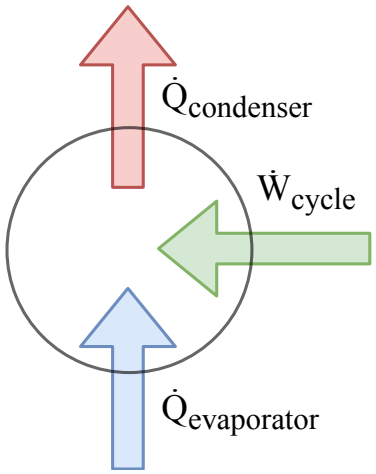

Figure 2.2: A basic heat pump/refrigeration cycle

2.1 Supermarket refrigeration systems

Modern supermarkets use refrigeration systems to maintain low temperatures for goods that need to be kept chilled or frozen. Typical goods are meat, milk, fish and frozen vegetables. There are three types of refrigeration systems used in supermarkets:

- Stand-alone units
- Condensing units
- Centralized systems

In small supermarkets, the goods are commonly kept in stand-alone units, such as ice-cream freezers. In these units, the refrigeration system is integrated into the unit, and heat from the

condenser is rejected directly to the store. Condensing units offer refrigeration to a small group of display cabinets or freezers. The condenser and the compressor are installed out of the sales area, normally on the roof or in a machine room. In larger supermarkets, there are centralized refrigeration systems, able to offer both cooling and freezing to several units on different locations in the store. The components are placed in a separate machine room. Condensers are typically placed on the roof in these systems as well. Centralized systems can either be indirect or direct. Indirect systems contain two fluids, where the secondary fluid circulates between the machine room and display cabinets, providing refrigeration. The direct system operates with one fluid, which provides cooling through evaporators placed in the display cabinets. Centralized systems are highly configurable and have the possibility to be connected to other systems, which makes them suited for an integrated energy system. Therefore, centralized systems will be investigated further in this thesis, after the environmental impact of refrigerants and systems using CO_2 as the working fluid are discussed.

2.1.1 Environmental impact of refrigerants and the reintroduction of CO_2

The majority of refrigeration systems today use refrigerants that can damage the environment. The refrigerants circulate in closed loops, but there are leakages, allowing the refrigerants to enter the atmosphere. Their impact on the environment is rated to their Global Warming Potential (GWP) and Ozone Depletion Potential (ODP). Table 2.1 presents the GWP and ODP of common refrigerants, with data gathered from The Linde Group (2017).

Table 2.1: GWP and ODP of common refrigerants

ASHRAE Number	Molecular formula	Refrigerant type	GWP	ODP
R-12	CCl_2F_2	CFC	10900	0,82
R-22	$CHClF_2$	HCFC	1810	0,06
R-134a	$C_2H_2F_4$	HFC	1430	0
R-404a	C_2HF_5+$C_2H_3F_3$+$C_2H_2F_4$	HFC	3920	0
R-717	NH_3	Natural	0	0
R-744	CO_2	Natural	1	0

HFC-404a is the most commonly used refrigerant in Europe, while HCFC-22 is the most common North-American refrigerant (Emerson Climate Technologies, 2010). The increased con-

cern for the environment has sparked phase-outs of refrigerants with high GWP and ODP, such as HFCs and HCFCs in both Europe and North America. The 2016 Kigali Amendment to the Montreal Protocol on Substances that Deplete the Ozone Layer introduces specific timetables for the phase-down of HFC for different parts of the world, based on wealth and climate. Warmer countries are more dependent on cooling and have received a longer phase-down schedule than Europe and the US. The Kigali Amendment is expected to have a greater impact on the parties' impact to reduce climate change than the Paris Agreement (United Nations Environmental Program, 2016). In the US, the Environmental Protection Agency (EPA) will restrict production and import of all HCFCs by 2030. In Europe, the 2015 EU F-gas regulation will cut the emission of HFCs and HCFCs to one-third by 2030, compared to 2014 levels (European Union, 2016). These phase-downs create a need for alternative refrigerants. Natural refrigerants such as ammonia, hydrocarbons and CO_2 are viable options. Ammonia (NH_3) is climate neutral, but not ideal due to its toxicity. Using hydrocarbons is another option but requires thorough safety measures as they are flammable.

CO_2 has emerged as the best alternative. It was reintroduced as a refrigerant around 1990. Since then, development has shown that CO_2 refrigeration systems have competitive potential regarding both efficiency and cost (Nekså et al., 2010). In operation in high ambient temperatures, the high-side pressure of CO_2 systems needs to be regulated and often raised so that the temperature in the gas cooler is above the critical temperature to avoid a high gas-fraction, and thus, a lower efficiency. A high operating pressure is seen as a disadvantage, setting a high demand for components, raising their cost. However, CO_2 has a low viscosity in the liquid face, reducing pressure drop and a good COP in practice. It also has the possibility for low evaporating temperatures, making it a suitable refrigerant for many applications.

2.1.2 Energy performance

Supermarkets are big electricity consumers. They represent an estimated 4% of the national electricity use in France and the US, and 3% in Sweden and the UK (Arias, 2005; Tassou et al., 2011). Within the supermarket, refrigeration is normally the biggest contributor to electricity use, followed by lighting. A typical Swedish supermarket uses between 35% and 50% of its electricity consumption for refrigeration purposes. A study by Johnsen (2013) on a REMA1000 su-

permarket in Trondheim, Norway found that the refrigeration system only accounted for 18% of the total energy demand of the store. This system is a centralized system using CO_2. However, this is based on measurements done during the winter, and a higher percentage can be expected annually, due to less heat demand in the summer.

2.1.3 Common refrigeration systems using CO_2

In the description of refrigeration systems, two temperature levels will be referred to: LT (Low Temperature) and MT (High Temperature). These abbreviations are used to differentiate between the evaporators operating at different temperatures and the compressors downstream of them. The three most common refrigeration systems using CO_2 are:

- Indirect/Secondary systems
- Cascade systems
- Booster systems

As stated previously, there are two fluids in an indirect system, where CO_2 circulates in the low-side cycle of the system. The CO_2 is cooled by the high-side fluid through a heat exchanger connecting the two cycles. In such a system, CO_2 is very volatile and partially evaporates. This offers good cooling capacity and low pumping power compared to other secondary fluids, such as glycol (Emerson Climate Technologies, 2015).

In a cascade system, the high side offers cooling for both the MT evaporator and for the low-side circuit. CO_2 is the refrigerant in the low-side circuit, similar to indirect systems, flowing through the LT evaporator. The two circuits are connected through a cascade heat exchanger. In both cascade and indirect systems, the high-side fluid is often an HFC.

Systems with one closed fluid circuit and two evaporator temperatures are commonly referred to as booster systems. These systems have a two-stage compression of the fluid. One advantage of the booster system is the absence of HFC. Another is the absence of an internal heat exchanger and related loss in efficiency, as can be found in both indirect systems and cascade systems. Booster systems are considered state of the art and will be described further in the following section.

2.1.4 Transcritical CO_2 booster system

A CO_2 booster system is a centralized system. Figure 2.3 shows a schematic of such a system with parallel compression. In Figure 2.4, the process is sketched in a logarithmic pressure-enthalpy diagram. It is drawn with a LT temperature of −30 °C, a MT temperature of −5 °C and 5 K su-

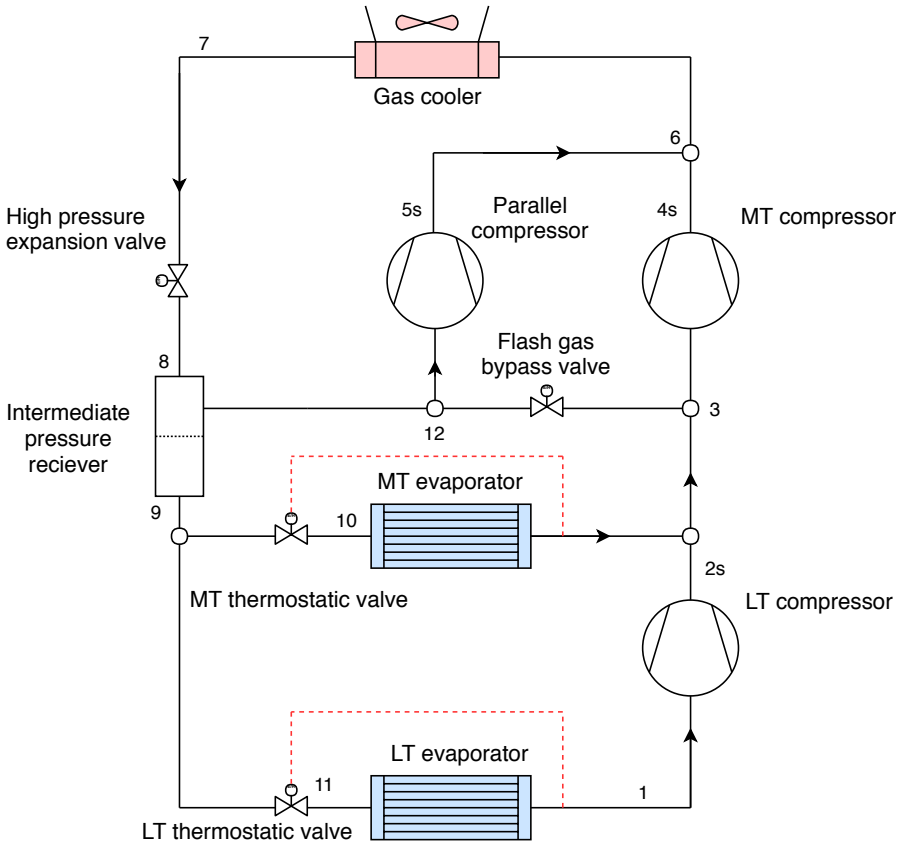

Figure 2.3: CO_2 booster system with parallel compression

perheat out of the evaporators. The gas cooler pressure is 90 bar and there is a 10 bar pressure difference between the intermediate pressure receiver and the MT evaporator. Compression is drawn isentropically for all three compressors. The state points in Figure 2.4 are marked with numbers that correspond to the numbers in Figure 2.3. The ambient temperature influences the pressure and outlet temperature of the gas cooler. This does not affect the low-side of the system. A higher ambient temperature will result in a higher outlet temperature of the gas cooler, which will move state point 7 to the right in Figure 2.4. The consequence is a higher vapor fraction. Without the parallel compressor, this vapor needs to be expanded in the flash gas bypass

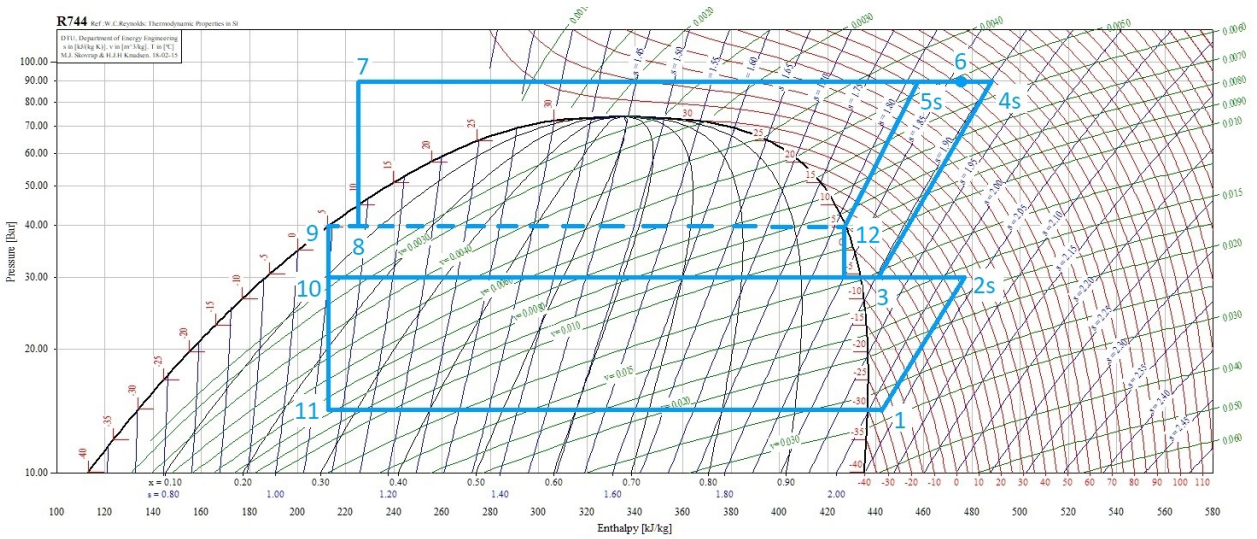

Figure 2.4: Logarithmic pressure-enthalpy diagram of the CO_2 booster system with parallel compression

valve and compressed by the MT compressor. The principle idea of the parallel compressor is to avoid expanding the gas before compressing it, hence increasing the efficiency of the system. In practice, there needs to be sufficient flash gas for the parallel compressor to operate at good efficiency for this configuration to be beneficial.

Another configuration with a potential to increase the COP is replacing the high-pressure expansion valve with an ejector. The ejector lifts the pressure of a part of the fluid originally destined for the MT compressor, allowing it to rather be compressed by the parallel compressor. It does so by using the high-pressure flow out of the gas cooler. It is measured to yield approximately a 10% increase in the COP tested in identical conditions as an expansion valve (Elbel and Hrnjak, 2004). These conditions were COP maximizing compressor discharge pressures.

2.1.5 Heat recovery from the gas cooler

In transcritical operation, CO_2 is cooled as a single phase gas at a supercritical pressure. This is why the component where heat is rejected is called a gas cooler, not a condenser. The gas cooler is very well suited for heating water due to its gliding temperature. The gas cooler inlet temperature (6) of the system sketched in Figure 2.4 is 75 °C, while the outlet temperature (7) is approximately 10 °C. This is a good match to heat water from 10 °C to 70 °C, a typical hot water storage temperature. At the beginning of the 2000's, millions of heat pumps for water heating

using CO_2 as the refrigerant were installed in Japan in order to replace fossil fuel heating of hot water. The aim was to reduce the emission of CO_2 from the existing heaters (Katsumi, 2006).

Several REMA1000 supermarkets in Trondheim already use a CO_2 refrigeration system with heat recovery. Examples are stores at locations Prinsens Gate, Dragvoll and Kroppanmarka. These integrated systems use surplus heat for preparation of hot water, space heating and ice-melting on sidewalks outside the store. The system at REMA1000 at Kroppanmarka is a result of a cooperation between SINTEF and Danfoss. This system won Trondheim Municipality's energy-saving price in 2014 for its 30% energy saving, compared to similar REMA supermarkets in Trondheim (Danfoss, 2016).

A study by Selvnes (2017) evaluates the use of excess heat from a supermarket refrigeration system and a hydrogen refueling station for hydrogen cars. The supermarket refrigeration system was designed as a transcritical CO_2 heat pump. Figure 2.5 shows the refrigeration demand of the modeled supermarket.

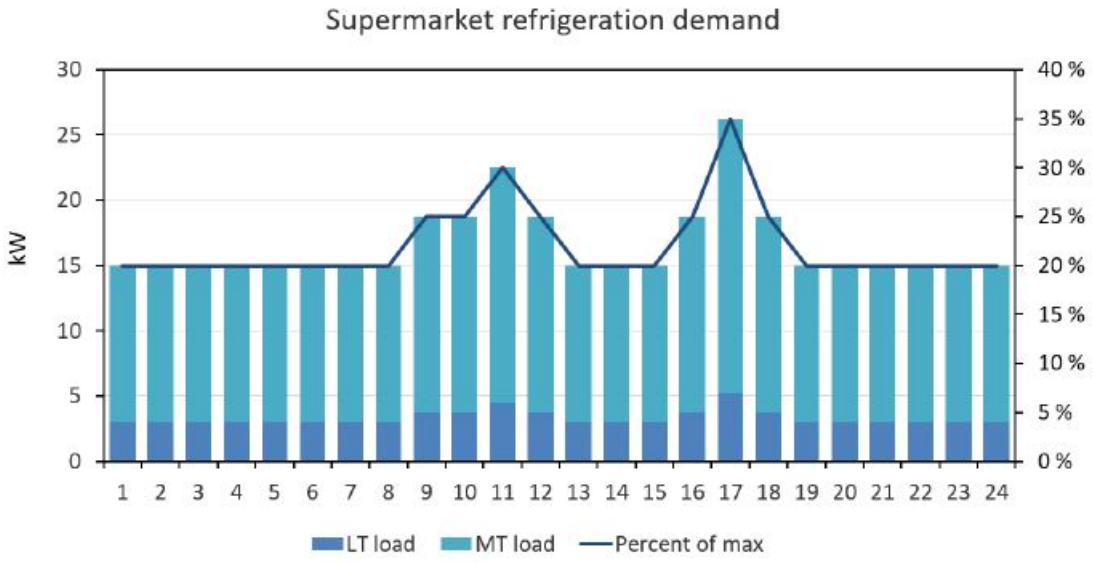

Figure 2.5: The supermarket refrigeration demand modeled by Selvnes (2017)

The excess heat from the supermarket refrigeration system was recovered to provide space heating and hot water preparation for 30 apartments. It was found that the heat demand for the apartments increases linearly with the ventilation air flow rate. The apartments in the study were modeled with an air exchange rate of 0.5 times/hour, which was considered too low despite it being a value from the Norwegian passive house standard (StandardNorge, 2012). It was

increased to 1.5 in the study. The heat recovered from the supermarket refrigeration system was found to cover all the heat demand in both a typical summer and a typical spring week, 75 % of the heat demand in a fall week and only 25 % of the heat demand during a winter week.

2.2 Heat pump systems in hotels

Refrigeration systems utilizing surplus heat and heat pump systems consist of the same components and may even be designed similarly. Smitt (2017) proposed a heat pump system design where a CO_2 heat pump supported by a propane heat pump covers the heating and cooling demands of Britannia Hotel in Trondheim. The hotel has 247 rooms, 4 restaurants, a conference room and a spa center. The CO_2 system proposed is a transcritical booster system with parallel compression, as described in subsection 2.1.4. Its evaporators offer cooling directly to refrigerated rooms and freezers, while heating is supplied through indirect sub-systems using hot water. The system can change its focus from heating to cooling, adapting to the dominating demand. While in cooling mode, it bypasses the space heating circuit, rejecting heat to the domestic hot water circuit while meeting the cooling demand. Not considering fans and pumps, simulations of the CO_2 system yielded an average annual energy efficiency of 5.55. As expected, it measured lower performance in summer due to higher ambient temperatures and thus lower space heating demand. The centralized system was compared to a traditional solution where 80% of the heating demand is covered by a heat pump (COP = 4), the remaining 20% and heating of domestic hot water (DHW) is covered by electric heating and all refrigeration demands are covered by a separate heat pump (COP = 3). It was found to reduce the yearly operational cost by 68%, highlighting the energy efficiency of a centralized system. The thermal energy budget of the simulated system is presented in Table 2.2

Table 2.2: Simulated thermal energy budget of Britannia Hotel

	Annual thermal demand [kWh]	Percentage
Domestic hot water	311 334	36%
Space heating	252546	29%
Space cooling	174 617	20%
Refrigerated rooms	43 800	5%
Freezer rooms	87 600	10%

The Q-ton heat pump by Mitsubishi is designed to heat water, using CO_2 as a refrigerant. It has been installed in student accommodations, sports centres and hotels throughout Europe. Two 30 kW units were installed in Lancaster Hall Hotel in London, able to supply 12 000 litres of hot water per day, at 65 °C, catering for 250 people. Reducing the hotel's gas consumption, the installation resulted in a 40% reduction in the hotels annual energy spending (Tasiou, 2014). The heat pump is reported to have a COP of 4.3.

A case study was performed by Lam and Chan (2003) on three R134a water-to-water heat pumps in a hotel in subtropical Hong Kong. The heat pump evaporator was connected to the heat rejection side of the hotel's HVAC system and the condenser supplied heat for hot water preparation, as seen in Figure 2.6. Estimations yielded a heating energy output and electricity

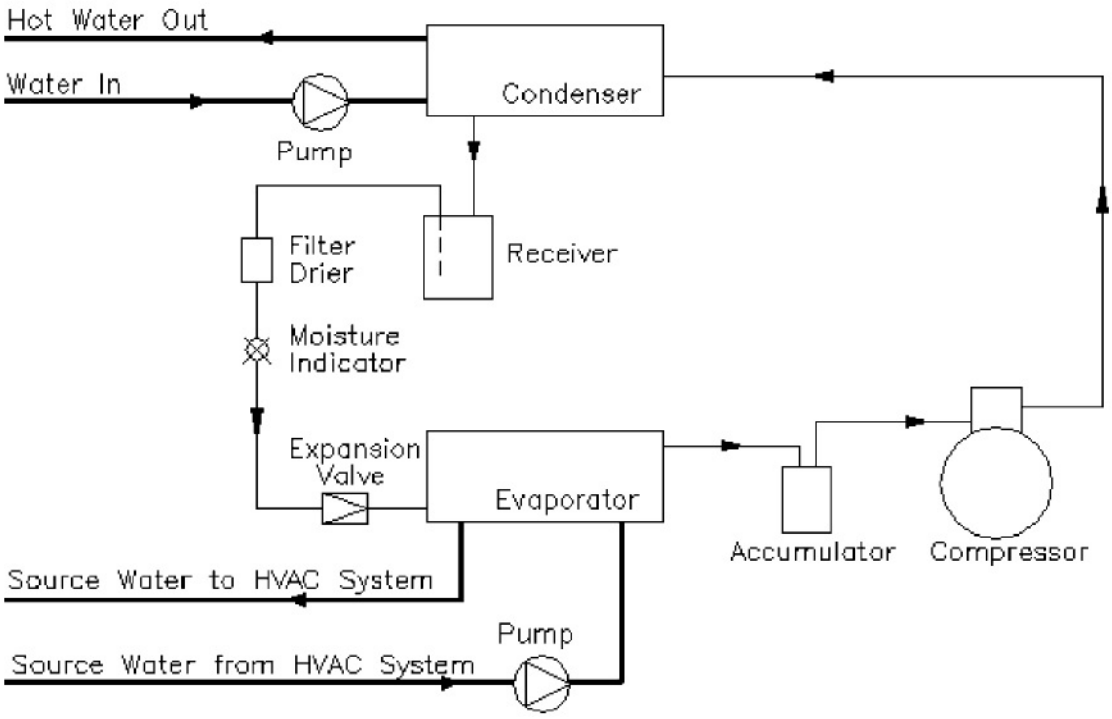

Figure 2.6: Water-to-water heat pump system in Hong Kong (Lam and Chan, 2003)

consumption of 952 and 544 MWh, respectively, resulting in an average annual energy efficiency of 1.75. Figure 2.6 shows a schematic of this system.

Also located in Hong Kong, a swimming pool center was the reference case of the study of a solar assisted heat pump system for an indoor swimming pool, water and space heating (Chow et al., 2012). The refrigerant in the heat pump is R22, achieving a heating capacity of 27 kW.

The solar water heating system reheats the pool water, able to reach a temperature difference of almost 9 K, maintaining the reheated pool water between 30 °C and 35 °C before it's further heated. Simulation of the heating period from November to March shows a mean heating COP of 4.52. The calculated payback period is 5 years, expected to decrease if the system is extended to cover cooling and dehumidification during summer time. Swimming pools are common in hotels, but the heat demand of a swimming pool center is expected to be different than that of a hotel. However, the system solution can be relevant for hotel application.

2.2.1 Drainage water heat recovery

One example of a measure to improve the energy efficiency for a hotel heat pump system is heat recovery from the drainage water. Similar to heat recovery from the exhaust air in ventilation, heat can be recovered from drainage water. This water is commonly referred to as grey water and is drainage water from installations using hot water, such as showers, sinks, washing machines and dishwashers. Connecting the grey water to the evaporator in a heat pump cycle enables utilization of this surplus heat. This can be done either directly or indirectly. A key challenge with grey water heat recovery is the impurity of the water, often containing much grease. This poses a challenge for the heat exchanger, which must be cleaned regularly. Having several heat exchangers in parallel enables operation during cleaning of one of the exchangers. Shell-and-tube heat exchangers are the most common choice in grey water heat recovery applications (Kleven, 2012).

(Baek et al., 2005) conducted a study on the use of wastewater from saunas and public baths as a heat source for instant hot water supply to a Korean hotel. The heat pump, using refrigerant R-134a, was simulated using the software TRNSYS. A hot water storage tank volume of 200 m^3 was used to a daily hot water consumption of 229 500 L (229.5 m^3). The design condition temperature of the wastewater was 28 °C and the hot water temperature was 50 °C. The wastewater was filtered before entering a tank and later pumped to the evaporator. A cost-saving strategy of this system was to use cheap off-peak electricity to charge the storage tanks during the night-time (22:00-08:00), as can be seen in Figure 2.7 on the next page.

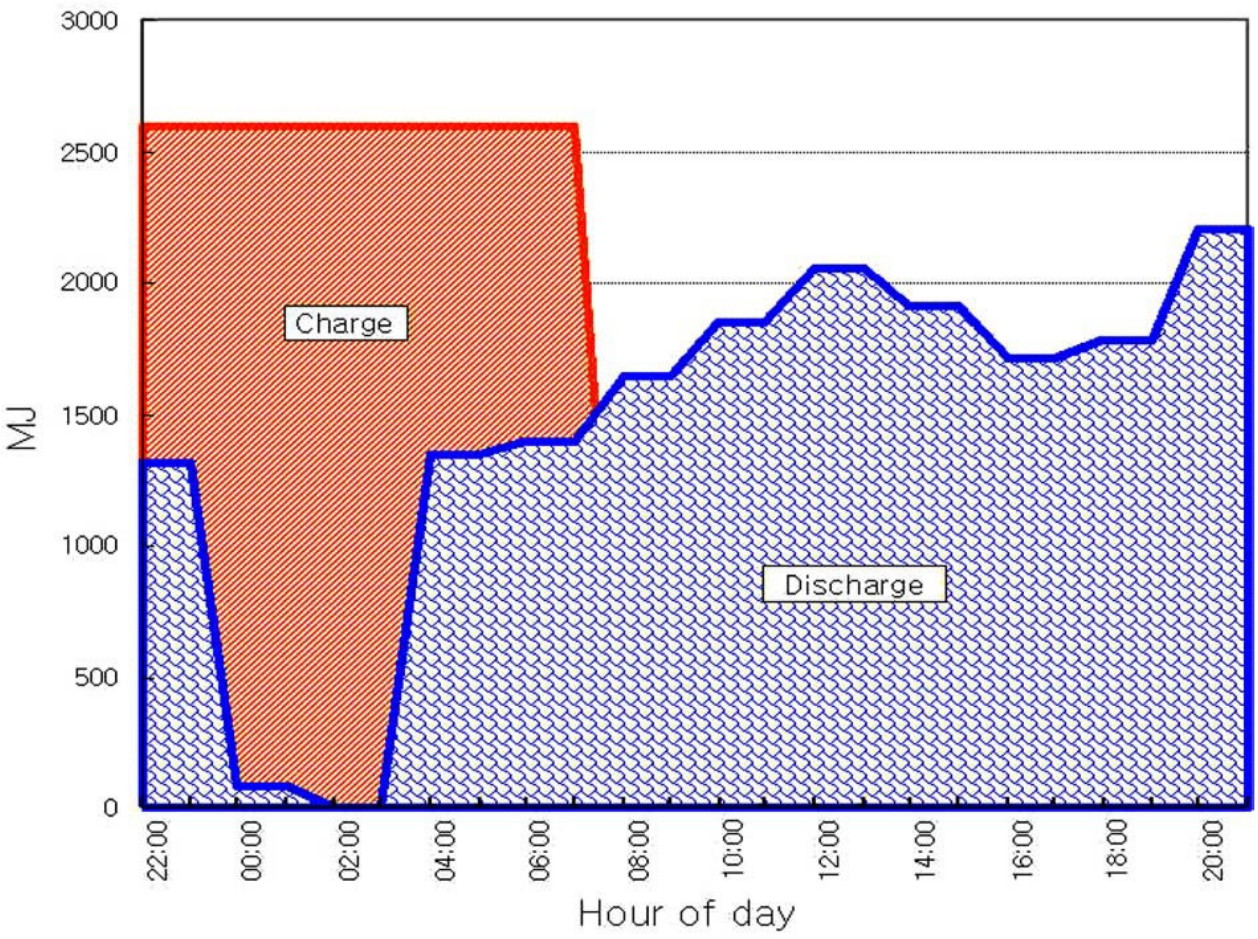

Figure 2.7: Night-time charge and discharge of hot water in a Korean hotel (Baek et al., 2005)

Results of the simulations showed a mean operating COP of 4.5-5.0 and that 90% of the instant hot water load was covered, with winter weekends having the largest loads. The study concludes that the system is particularly suitable for countries with a similar climate to Korea and that it can be effectively applied to space heating as well, as decreasing the temperature difference between the evaporator and condenser will benefit the system.

(Ni et al., 2012) studied an energy-recovery system where the grey water was indirectly connected to the evaporator of a heat pump offering cooling, space heating and hot water. Performance data of a compressor by Copeland Scroll for the refrigerant R410a was used. Simulation of a typical residential house with four family members and three bedrooms in New York showed a total energy saving of 33.9 % after implementing drainage water heat recovery. The decrease of energy consumption of cooling, space heating and water heating was 2.7%, 23.5% and 76.0%, respectively.

2.2.2 Thermal energy storage tanks and PCMs

Another measure to increase the energy efficiency for a hotel heat pump system is to use thermal energy storage tanks. The principle of an energy storage is to store energy when there is a surplus of it and distribute it when there is a need. A general benefit of an energy storage is that it lowers the necessary installed capacity of the heat pump system where it is installed, by distributing the energy during peak demands. Also, it can substitute auxiliary heating or cooling. In the tanks, a liquid is stored at a temperature, T_s, suitable for its application. The amount of energy, E, possible to store in the tank depends on m, the available mass of the fluid, its specific heat c_p, and the temperature difference for its application. In the case where a thermal storage tank is to aid a heating system, the total heat in the tank is found by Equation 2.2, where T_s is the temperature of the fluid in the storage and T_i is the temperature of the fluid after its application:

$$E = m \cdot c_p \cdot \left(T_s - T_i\right) \tag{2.2}$$

Water is a common fluid to use in thermal energy storage tanks due to its availability and high specific heat. It also has the possibility to be used directly in applications where water is the circulation fluid, such as district heating and domestic hot water. Statkraft Varme installed a 5000 m^3 water tank to act as a thermal energy storage for their district heating network in Trondheim in 2017 (Graver, 2016). The tank will be used to cover peak loads in place of oil boilers and electricity, providing an estimated extra 8 GWh of heating energy from renewable sources per year.

Phase change Materials (PCM) represent another method to store energy, also both for heating and cooling purposes. PCMs absorb heat through the phase change of the PCM, in contrast to ordinary energy storage tanks, which are charged by raising or lowering the temperature of a fluid before admitting it into an insulated tank. The most common phase change in PCM systems is solid-liquid and liquid-solid. The large change in volume between the gas and liquid state of most fluids makes liquid-gas phase change less practical. Due to the fact that the latent heat of fusion is often much larger than the sensible heat of fluids, this method has a higher energy density than traditional storage tanks. In turn, this reduces the required volume of the storage, increasing the storage capacity at a given storage volume. The PCMs can either be kept

in a separate tank or added in the storage tank of the fluid in circulation. A study performed by Nkwetta and Haghighat (2014) on the performance of residential hot water tanks shows that the improvement in thermal energy storage is directly proportional to the amount of PCM in the storage. In this study, the PCM was added to the hot water tank. In a 270 L water tank, the addition of 52.8 kg of the PCM increased the stored energy by 12 %. With a density of 1260 kg/m^3 in its liquid state, the volume of the PCM is 42 L, 16 % of the water tank volume. With more PCM added to the tank, more energy can be stored for a fixed tank volume.

The most important criteria for chosing a PCM is the temperature at which it changes phase. Secondly, it should release and absorb a large amount of energy in the phase change. Furthermore, it is desirable that the phase change occurs at a fixed temperature, that the PCM doesn't supercool, is non-hazardous and can remain stable through many freezing/melting cycles. PCM Products offers PCMs such as hydrated salts and organic solutions (PCM Products, 2013). They have phase changing temperatures between 7 °C and 117 °C, suitable for residential purposes such as space heating and domestic hot water. Table 2.3 shows key numbers for 5 selected hydrated salt PCMs from PCM Products:

Table 2.3: Key numbers for selected PCMs from PCM Products (2013)

	PCM name				
	S89	**S83**	**S72**	**S34**	**S32**
Phase Change Temperature [°C]	89	83	72	34	32
Latent heat capacity [kJ/kg]	151	141	127	115	200
Volumetric heat capacity [MJ/m^3]	234	226	212	242	292

3. Snow production methods and snow demand

This chapter contains descriptions of snow production methods and snow storing principles, followed by a suggested method to estimate the snow demand of a cross-country slope. In today's winter sports facilities, the demand for snow is covered by four sources:

- Natural snowfall
- Temperature dependent snow machines (snow guns)
- Temperature independent snowmaking machines (TIS machines)
- Stored snow from cold periods

Natural snowfall and snow guns are both dependent on cold temperatures. TIS machines can produce snow at positive ambient temperatures. Two resorts in Norway, Sjusøen and Geilo, have invested in these machines with the objective of an earlier season opening. The combination of TIS-produced snow and snow stored from the previous season made Sjusjøen able to open a 1,2 km cross-country slope the 25^{th} of September 2017. However, most sports facilities today rely only on natural snowfall and snow cannons, making their guarantee for skiing conditions dependent on low temperatures and precipitation.

3.1 Snow guns

Snow production by snow guns is a temperature dependent technology. The required condition for snow production by snow guns is a wet-bulb temperature of -2°C, as indicated by snow gun manufacturers (Spandre et al., 2016). The wet-bulb temperature is a function of dry-bulb temperature (standard measured temperature) and relative humidity and is always lower or equal to the dry-bulb temperature. The common principle for all snow guns is combining water droplets and cold air to form snow. To ensure small droplets, the water is pressurized and sprayed through a small diameter nozzle to the surrounding air at atmospheric pressure.

The pressure difference accelerates the water to a high speed and turbulence breaks the jet, creating droplets. The droplets enter the cold air where they exchange heat through convection and evaporation. According to Fauve and Rhyner (2004), they will freeze if the following three conditions are met:

1. Sufficient energy exchange to freeze the whole volume of water
2. Presence of freezing nuclei which trigger the freezing process
3. Sufficient flight time to allow a complete freezing of the droplets

Chemically pure water can remain liquid until −45 °C. Normal nucleation temperature in clouds is −12 °C, while commercial freezing nuclei used in snowmaking enables freezing as high as −3 °C. Figure 3.1 shows how the temperature changes with time in the freezing of a droplet:

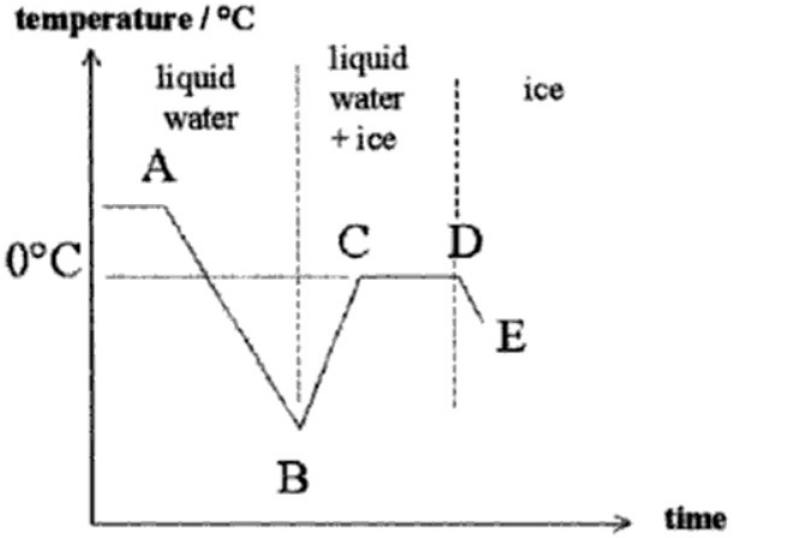

Figure 3.1: Water droplet temperature during snowmaking (Fauve and Rhyner, 2004)

The existing types of snow guns vary in principle and design. High-pressure towers require little maintenance and can produce high-quality snow, but are being phased out of the market due to high energy cost and noise (Gjerland and Olsen, 2014). Today, the two most widely used snow gun types in resorts are fan guns and lances, seen on the next page in Figure 3.2 and Figure 3.3.

Figure 3.2: A mobile fan gun unit (Gjerland and Olsen, 2014)

Fan guns are high capacity snowmakers with an operating water pressure between 15 and 17 bar. These guns do not use pressurized air. Instead, an air jet created by a fan is used to throw the droplets into the air. This allows good control of the snow produced: the machine's vertical and horizontal angle can be changed to avoid piling of snow in front of the snow gun. It also increases the flight time of the droplets and makes production less vulnerable to wind.

Figure 3.3: Snow piles behind the lance model Sky Giant by Ratnik Industries (Ratnik Industries, 2014)

The snow produced is of high quality due to the possibility of adjustment according to conditions. The noise level is acceptable. Fan guns are mobile, but difficult to transport due to their size and weight. Additionally, fan guns require a lot of maintenance. (Gjerland and Olsen, 2014).

Lances require less energy than fan guns. However, the production capacity is also lower. The water pressure for lances is in the range of 17 to 40 bar. Lances do not produce much noise. They have a smaller degree of adjustment than fan guns, resulting in poorer snow quality in marginal conditions. In addition to low a power demand, lances require little need for maintenance. The most common models are stationary, but mobile units exist (Gjerland and Olsen, 2014).

3.2 Temperature independent snowmaking machines

The existing technologies of TIS machines will be presented in this section, followed by an evaluation of the possibility to add a TIS machine to an integrated energy system.

3.2.1 Flake ice machines

The ice produced by flake ice machines is dry, subcooled ice. Water kept in a tank is sprinkled onto the inner walls of the flake ice drum (FID). The walls of the FID are cooled and act as the evaporator in the system. The flake ice machine requires a refrigerant and an evaporating temperature around $-30\,^{\circ}\mathrm{C}$ to keep the FID cold enough. Inside the FID, the ice formed on the surface is scraped away mechanically by a rotating scraper, with ice layers up to 3 mm thick (Graham et al., 1993). The excess water in the FID is collected and transported back to the tank. This is a continuous process. Due to the low temperature required, the compressor power demand is high compared to other methods. However, this is somewhat compensated for as flake ice machines do not require a defrost mechanism (Dieseth, 2016). The inside of a flake ice machine is shown in Figure 3.4 on the next page. Water sprinkled on the FID can be seen in the top right as well as ice shaved off by a rotating blade following the sprinkler. The ice is collected in the bottom of the FID.

Figure 3.4: The SFE20T flake ice machine by Snowell Ice Systems (2016)

3.2.2 Plate ice machines

The freezing principle of the plate ice machines is similar to the flake ice machines. Water is sprinkled onto a cold metal surface. The ice is removed by defrosting, not mechanical scraping. Defrosting is achieved by running water down the other face of the cold surface. Hence, plate ice production is a sequential process, not a continuous one. Figure 3.5 shows a design with vertical plates in pairs, with the defrost water sprayed on the inside during defrost.

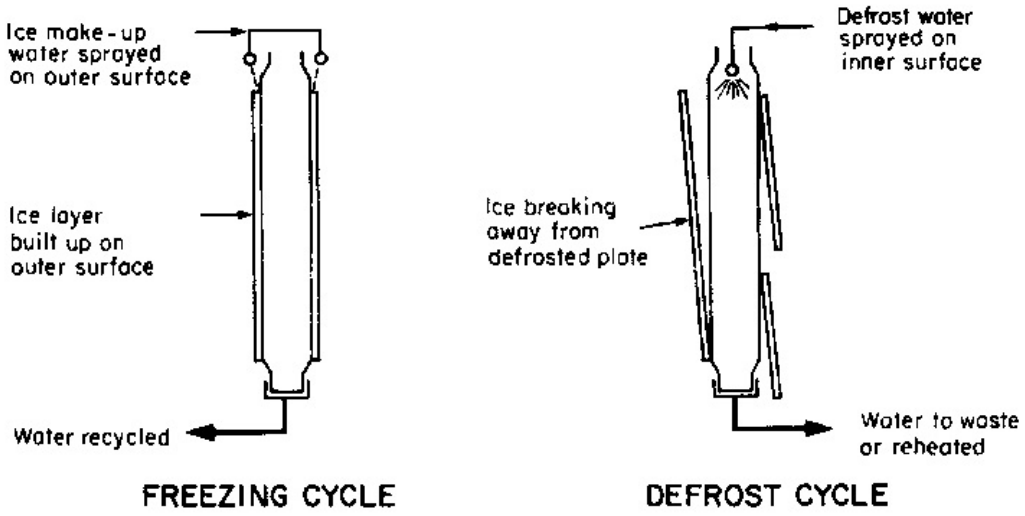

Figure 3.5: Freezing and defrosting of a plate ice machine (Graham et al., 1993)

The plate ice will fall off and have a wet surface, in contrast to the flake ice which is dry. The defrosting process increases the energy consumption. This is the main reason that the plate ice is removed at a thickness of 10-12 mm. It is economically unprofitable to produce thinner ice.

3.2.3 Ice slurry methods

Ice slurry is a liquid containing small ice particles with diameters between 0.1 and 1 mm in diameter (Hägg, 2005). The liquid can be pure water or a brine of water and a freezing point depressant (Dieseth, 2016). The numerous particles contained in the liquid give a large surface area for heat transfer.

Vacuum Ice Makers

The principle of a vacuum ice maker is to produce ice at water's triple point condition. The triple point is where all three phases of water are present: solid, liquid and gas. The triple point conditions are 611 Pa (less than 1% of atmospheric pressure) and 0.01 °C (Van Orshoven et al., 1993). When water reaches its triple point, some water will evaporate, and release heat. This lowers the temperature of the remaining water (Dieseth, 2016) and freezing begins around nuclei in the water. The latent heat of evaporation (2500 kJ/kg) of water is 7.5 times the latent heat of freezing (333 kJ/kg). Hence, the mass of produced ice is 7.5 times the mass of produced vaporized water (Van Orshoven et al., 1993). The ice slurry is continuously pumped into a tank where ice and water can be separated. The ice from vacuum ice makers is thus also wet when produced. To maintain the low pressure in the vacuum tank, the vapor is evacuated by a compressor. An alternative method is to deposit the vapor on refrigerated plates inside the vacuum freezer, condensing it back to liquid state. The existing models of vacuum ice makers vary a lot with respect to production capacity, from 20 m^3/day to 1720 m^3/day (Dieseth, 2016). The specific electricity consumption decreases with increasing capacity. This technology requires no refrigerant, as the working fluid is water itself.

Scraped Surface Ice Slurry Generator

Scraped surface ice slurry makers also produce a slurry of ice and water. Its technology is different from the vacuum ice maker as it does not lower the pressure to the triple point. A typical scraped surface ice slurry generator is a shell-and-tube heat exchanger (Dieseth, 2016). The refrigerant flows inside the outer shell, while the ice slurry flows inside. The ice is created on the inside walls and mechanically removed by rotating blades. The SnowGen model from the Finnish company SnowTek was used during the 2014 Winter Olympic games in Sochi. Three units with a capacity of 220 m^3/day were needed. The scraped surface ice slurry generators have high maintenance costs and are quite expensive (Bédécarrats et al., 2010).

3.2.4 Connecting snowmaking equipment to a refrigeration system

Traditional snow guns are not suitable to be connected to a refrigeration system as they rely on low ambient temperatures to produce snow. In order to connect a commercially available TIS machine to a refrigeration system, it must be possible to supply the cooling in the TIS machine directly using the refrigerant or with an indirect cycle. This leaves out the vacuum ice makers where water vapor is compressed. The vacuum ice makers with refrigerated plates can possibly be used. The evaporating temperature must be within what is achievable by the refrigeration system. A viable option will be the flake ice model SF220 by the Italian company TechnoAlpin AG. This model can operate in ambient temperatures between −5 °C and 25 °C. The evaporation temperature is −30 °C, similar to that of freezers in a refrigeration system. However, the model is designed for low pressure, as ammonia is the working fluid. A direct connection to a refrigeration system using CO_2 will therefore not be possible. In Figure 3.6 on the following page the outlet of the SF220 is seen during production in ambient temperatures above 0 °C.

Figure 3.6: TIS production by a flake ice machine (SF220) at Sjusjøen, Norway (Müller, 2015)

Bergwitz-Larsen (2017) performed a study where an outdoor flake ice system using CO_2 as the refrigerant was modeled. The location was Granåsen, Trondheim. The snow production capacity of the system was 100 tonnes/day, which corresponds to 8.3 m^3/hour of snow with density 500 kg/m^3. The flake ice machine was integrated with heat recovery from the gas cooler. The surplus heat was to be used for heating water to be sold to local customers with high hot water demand. The pre-study leading up to the master's thesis investigated the market potential of selling hot water in Trondheim. In the study, the water is transported in hot water tanks stacked inside 40' containers to the customer. The tanks inside the container have a capacity of 24 000 L. Pirbadet, a local swimming hall, and the hotel Scandic Lerkendal are possible customers with a sufficiently high hot water demand to avoid extensive heat loss during emptying of the containers. The water flow was adapted to the water outlet temperature at 80 °C. A schematic of the proposed CO_2 system is presented on the next page in Figure 3.7.

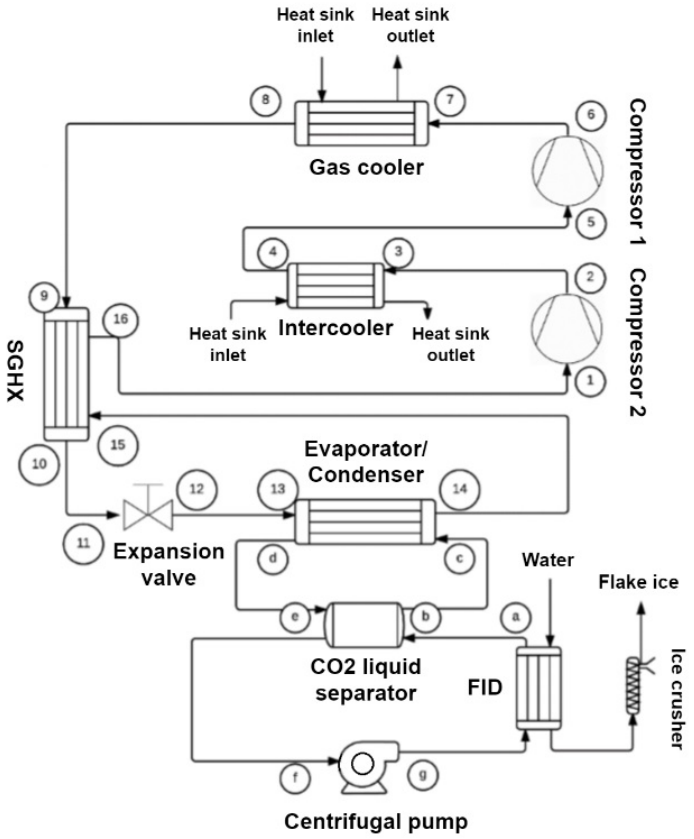

Figure 3.7: Flake ice system with heat recovery using CO_2 as the refrigerant (Bergwitz-Larsen, 2017)

Energy efficiency measures such as two-stage compression with an intercooler and a suction gas heat exchanger, enabling use of internal heat, was implemented. The electricity consumption of the system was measured to be 16.3 % higher than commercially available flake ice models. That is regarded as very acceptable, as heat from commercial models is rejected to the ambient, while the system proposed by Bergwitz-Larsen (2017) produces useful heat. Further data of the flake ice system is shown in Table 3.1:

Table 3.1: Key performance data of the flake ice system modelled by Bergwitz-Larsen (2017)

Characteristic	Value	Unit
$COP_{heating}$	2.37	[-]
$COP_{cooling}$	1.66	[-]
$\dot{Q}_{gas\ cooler}$	629	kW
$\dot{Q}_{evaporator}$	442	kW
$\dot{W}_{total}$	266	kW

3.3 Snow storage methods

3.3.1 Outdoor snow storage

For outdoor snow storages, the snow melt can be reduced using sawdust (wooden chips) as a cover over a pile of snow. A study by Strand (2014) on a storage in Beitostølen shows that the insulation capacity of sawdust is reduced when it gets wet. However, a lot of the heat added to a wet layer of sawdust is used to evaporate the water contained in the layer. In a sensitivity analysis done by Grünewald et al. (2018) in Davos, on snow covered by sawdust, added precipitation was found not to increase the snow melt significantly. The study shows that reducing the precipitation completely, thus keeping the sawdust dry, increased the melt drastically. Hence, the loss in insulation capacity due to wet sawdust is lower than the benefits of evaporation of water in a wet layer. The volume of melted snow in storages covered by sawdust during the summer season for four locations is presented in Table 3.2 (Strand, 2014; Vagle, 2016; Gisselman and Cole, 2016; Grünewald et al., 2018).

Table 3.2: Melted snow in different storages

Location	Snow volume melted	Year
Beitostølen	10% - 15%	2013, 2014
Granåsen	22%	2015
Østersund	40%	-
Davos	26% - 37%	2015

Outdoor snow storage is most commonly used to store a certain amount of snow during the summer, to ensure skiing conditions at the start of the following season, not for continuous supply during the summer season. A study by Lintzén (2016) on snow piles stored during the summer in Arjeplog, Sweden concludes that outdoor storages should be covered with a sufficiently thick insulation layer, preferably with good evaporation properties, which agrees with the findings of Grünewald et al. (2018) and Strand (2014). Experiments in the study include a 190 m^3 snow pile left uncovered, which was found to have melted completely from April the 15th to May the 27th. The pile was shaped as a cut-off cone with a bottom diameter of 12 m, top diameter of 6 m and a depth of 3 m.

3.3.2 Indoor snow storage

Indoor storage of snow is suitable when there is frequent snow demand during the summer season. An indoor snow storage is a well-insulated and refrigerated space. Supply snow for the storage can either be produced by TIS machines or by temperature dependent snowmakers inside the refrigerated space. In the latter case, a larger needed refrigerated volume is expected. Little research on indoor snow storage exists, however it is a principle used in indoor ski resorts.

Paul (2003) investigated the benefits of using "binary snow" instead of snow produced by methods described in this chapter. In order to conserve snow in a traditional indoor skiing hall, the air temperature is cooled to $-5\,^{\circ}\mathrm{C}$. Equally important is the freezing of the floor, to prevent snowmelt at the floor surface. If the floor is on the ground, rather than on beams, insulation is very important, to avoid ground freezing and an unnecessary increase in cooling load. Producing temperature independent snow inside the hall represents a large heat gain. The cooling load of such a hall is enormous: a 500 m long, 60 m wide and 60 m high hall has an annual electricity demand of 4 000 MWh, which corresponds to 133 $\mathrm{kWh/m^2}$ (Paul, 2003). The alternative snow system, using binary snow, is found to have only 65 % of the energy demand compared to a similarly sized hall. Snow is produced from an ice slurry containing an additive called Turin. In addition to a lower electricity consumption, it has a better snow quality, similar to that of natural snow (Paul, 2003). However, as a central part of the binary snow concept is a large turnover of produced snow, it is uncertain if it is a viable option for storage and outdoor use.

If snow production is to be done by temperature dependent snow machines inside a refrigerated room, sensible and latent heat will be transferred from the equipment and water droplets to the air surrounding the snowmaking equipment (Clulow, 2006). Removing this heat is important to control the dew-point conditions of the air. The typical heat gains for a ski hall are transmission load, infiltration load, internal load and defrost heat gains. The heat gain from snow production represents the largest internal load. Due to the size of the halls, the construction is often thin, resulting in large transmission gains (Clulow, 2006). For small storages, this can be avoided. Except for the snow production equipment, there will be practically no internal gain in a storage. If the snow is produced outside of the storage, the heat gain from the production is eliminated as well.

3.4 Snow demand for all year ski slopes

Alpine resorts at high altitudes or on glaciers can offer skiing conditions during summer. Hintertux, located 3000 m a.s.l. in Austria, offers year-round skiing at their resort. Also in Austria, The Olympiaregion Seefeld at 1180 m a.s.l. offers a 1500 m long, 6 m wide cross-country slope from the 1st of November, for classic and skating techniques. This is made possible by a 6000 m^3 storage using the storing technology discussed in subsection 3.3.1.

Synthetic snow cover is an alternative in lower altitudes. The Italian company Neveplast have developed synthetic surfaces for alpine skiing and snowboarding, cross-country skiing and snow tubing. Normal skiing equipment can be used on the plastic surface, designed to resemble the feel of natural snow when carving. For cross-country skiing, they offer products for both classic and skating technique (Neveplast.com, 2016)

For a concept where continuously produced snow will supply a year-round slope, the snowmelt will define the demand. The length, width and depth of the slope will need to be determined. 25 cm deep snow is often suggested as the minimum for cross-country skiing conditions (Hanssen-Bauer et al., 2015; Naturnvernforbundet, 2016). To model snow melt with short time steps, two basic models are used (Mullem et al., 2004):

- Energy balance method
- Degree-day method

Out of the two, the energy balance method is the most detailed one. It estimates the heat fluxes leaving and entering the snow layer. As it is a data-intensive method it is sometimes not used due to inadequate data or the level of detail not being necessary. The simpler degree-day method uses air temperature to index all of the energy fluxes, making it possible to estimate snowmelt with only the air temperature as the required input. In order to overcome the shortcomings of the degree-day method, Hock (1999) developed two versions of the degree-day method, which include radiation. The first variation of the method is based on clear-sky irradiance (W/m^2) while the second takes cloud cover into account, using measured global irradiance (W/m^2). In this variation of the degree-day method, the melt rate M (mm/h) is calculated by

Equation 3.1:

$$M = \begin{cases} \left(\frac{1}{n} MF + a_{snow/ice}\, I\, \frac{G_s}{I_s}\right) T & : \quad T > 0 \\ 0 & : \quad T \leq 0 \end{cases} \tag{3.1}$$

where n is the number of time steps, MF is an empirical melt factor (mm/day°C), $a_{snow/ice}$ is a dimensionless empirical irradiance coefficient for snow and ice surfaces, I is potential clear-sky irradiance at the surface (W/m^2), G_s is measured global irradiance (W/m^2), I_s is potential clear-sky direct solar irradiance (W/m^2) at the site of the global irradiance measurements and T is the air temperature (°C). If the temperature is below 0 °C, the melt is set to zero.

4. Simulation model and system design

In order to develop a simulation model to analyze the various energy flows for a hypothetical centralized refrigeration unit, one must first understand the demands which it will cover. The refrigeration unit, a transcritical CO_2 heat pump, will provide the following:

- Space heating for the hotel
- Domestic hot water for the hotel and supermarket
- Air-conditioning for the hotel
- Refrigeration for the supermarket
- Refrigeration for the TIS machine
- Refrigeration for an indoor snow storage

Figure 4.1 illustrates the applications of the centralized refrigeration unit:

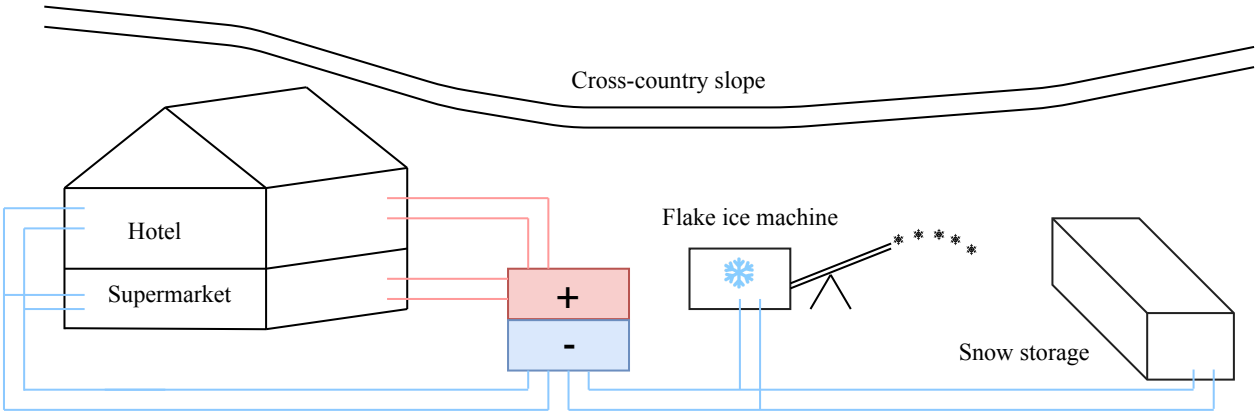

Figure 4.1: System illustration

This chapter contains theory and assumptions behind the input necessary to perform simulations of the heat pump model. Later in the chapter, the design and control strategy of the heat pump itself is presented.

4.1 Shading and snow production

Snow melt

To calculate the refrigeration demand as a result of snow production, the snow demand needs to be determined first. The annual snow demand for the cross-country slope is set equal to the snow melted. The slope is 1 km long and 6 meters wide, with a depth of 40 cm. To estimate the hourly melting of snow in the slope, the degree-day method including radiation presented as Equation 3.1 in section 3.4 is used. It is repeated here to discuss the chosen values:

$$M = \begin{cases} \left(\frac{1}{n} MF + a_{snow/ice}\, I\, \frac{G_s}{I_s}\right) T & : \quad T > 0 \\ 0 & : \quad T \leq 0 \end{cases}$$

The method requires air temperature and irradiance data as input. This data is gathered from the climate database Meteonorm, for a weather station in Værnes, 30 km east of Trondheim for the year 2005. In the calculations, the potential clear-sky irradiance at the snow surface, I, and at the location of of measured global irradiance, I_s are assumed equal, because of the geographical proximity and similar latitude of Værnes and Trondheim. The values for the empirical coefficients MF and a_{snow} are set to 2.1 $\frac{\text{mm}}{\text{day°C}}$ and 0.0007, respectively. They are obtained from a study performed by Hock (1999) on snow and ice melt on Storglaciëren, a glacier in Sweden.

Shading

Installing shading of the cross-country slope will be considered in an attempt to reduce the snow demand. The radiation from the sun becomes scattered when penetrating the atmosphere. Due to the scattering of radiation, an object on the earth's surface will receive radiation from all incident angles. However, the intensity of radiation is greater closer to the zenith angle of the sun. The scattered radiation increases with cloud cover, ranging from 10 % of total solar radiation on a clear day, to nearly 100 % on a very overcast day. The scattered component of solar radiation is commonly approximated as being independent of direction (Incropera et al., 2013). This is called diffuse radiation. The component of radiation not scattered is called direct radiation.

In the calculation of snowmelt *without* shading, measured data for global irradiance ob-

tained from Meteonorm is used directly in Equation 3.1.

In calculation of snowmelt *with* shading, it is assumed that the slope is shaded from direct radiation and that it receives the portion of the diffuse radiation which is not shaded for. This portion is found by calculating the *view factor* of the geometry of the shading. The ratio of received irradiance by the slope is 1 minus the view factor. The diffuse irradiance is also obtained from Meteonorm. The chosen shading is a roof with the same width as the slope, illustrated by a simple sketch shown in Figure 4.2. The view factor F_{ij} of two parallel plates can be calculated by the following equation (Incropera et al., 2013):

$$F_{ij} = \frac{\left((W_i + W_j)^2 + 4\right)^{\frac{1}{2}} - \left((W_j - W_i)^2 + 4\right)^{\frac{1}{2}}}{2W_i} \tag{4.1}$$

where $W_i = \frac{w_i}{L}$, $W_j = \frac{w_j}{L}$, w_i is the width of the top plate, w_j is the witdh of the bottom plate and L is the distance between them. The view factor for the chosen geometry is calculated by use of Equation 4.1 to be 0.62. Hence, the received diffuse irradiance by the ski slope is 38 % of the total diffuse irradiance.

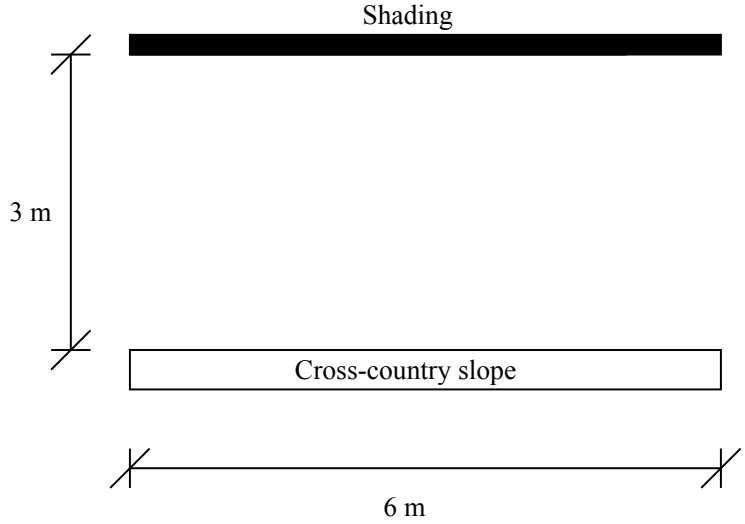

Figure 4.2: Cross-section of the cross-country slope and shading

Snow production

The snow is modeled to be produced by a flake ice machine. It requires refrigeration to cool the inlet water to 0 °C and then freeze the water. As mentioned in subsection 3.2.1, flake ice systems

produce dry ice, which means the ice will be cooled below 0 °C. Similar operational conditions in the FID as the system proposed by Bergwitz-Larsen (2017) is assumed, i.e. the ice is to be cooled to −5 °C. The refrigeration needed, $\dot{Q}_{FID}$, to achieve this cooling of water, phase change and cooling of ice is calculated using the following equation:

$$\dot{Q}_{FID} = \dot{m} \cdot c_{p,water} \cdot (T_{water} - T_{freezing}) + \dot{m} \cdot h_{sf} + \dot{m} \cdot c_{p,ice} \cdot (T_{freezing} - T_{ice}) \tag{4.2}$$

In Equation 4.2, $\dot{m}$ is the mass flow, which is assumed equal for water and ice, which implies that all the water sprayed on the FID is frozen. The specific heats of water and ice, $c_{p,water}$ and $c_{p,ice}$, are obtained from Engineering ToolBox (2001) at 0 °C. h_{sf} is the heat of solidification when water changes state from liquid to solid. The inlet temperature of water, T_{water}, is set to 7 °C, similar to the inlet city water for hot water purposes. $T_{freezing}$ is the freezing temperature of water, 0 °C. Finally, T_{ice} is the outlet temperature of the ice, discussed previously in this section.

4.2 Building models and supermarket refrigeration demand

The energy system will cover cooling and heating demands for the buildings. To estimate the space heat and cooling demands of the buildings, as well as the DHW demand, their size and construction must be decided. Additionally, the refrigeration demand of the supermarket needs to be determined.

The REMA supermarket will be on the ground floor, with the hotel on the floors above. The footprint of the building is set to 1050 m^2, similar to normal one-floor REMA supermarkets in the area. Hence, each floor of the hotel will also be 1050 m^2. The supermarket will not have a kitchen section for preparation of fresh goods.

The proposed hotel will have 200 rooms. Britannia Hotel in central Trondheim has 247 rooms and a total area of 8400 m^2. Scaling the new hotel according to the total hotel area per room of Britannia leads to a needed floor area of 6800 m^2. With each floor being 1050 m^2, the minimum number of floors needed is 7, and the total floor area of the hotel is 7350 m^2.

4.2.1 AC and space heating

Hotel

A model of the building envelope was created in the Norwegian building simulation software SIMIEN. As the hotel will be a new construction, no data of the construction is available. A key motivation for the integrated energy solution is energy-efficiency, and therefore the building is expected to meet criteria for commercial passive houses, given in NS3701:2012 (StandardNorge, 2012). Important building properties are listed in Table 4.1.

Table 4.1: Building properties

Description	Value	Unit
Combined glass, window and door area divided by floor area	13.1	%
U-value wall	0.12	W/m^2K
U-value floor and roof	0.08	W/m^2K
U-value windows	0.80	W/m^2K
Leakage number at ΔP = 50 Pa	0.60	air changes per hour
Normalized thermal bridge value	0.03	W/m^2K
Heat recovery in ventilation	80	%
Heat loss number to infiltration and ventilation	0.33	W/m^2K

The 1050 m^2 floors measure 30 x 35 meters. The height from one floor to the next is set to 4 meters, yielding an exterior wall area of 980 m^2 on the north and south facing walls and 840 m^2 on the east and west facing walls. The roof and walls are exposed to the ambient, while the floor is adjacent to the the supermarket, simulated as a zone with a temperature of 20 °C during summer and 16 °C during winter.

Snow storage warehouse

To avoid a high peak refrigeration load due to increased snow demand in the summer months, an indoor snow storage will store snow produced in the winter. This allows for an even production throughout the year, limiting the necessary installed capacity. This storage building does not need to fulfill the same criteria as the supermarket and hotel, and the cooling demand,

$\dot{Q}_{storage}$ is estimated simply as the transmission heat loss through the building envelope:

$$\dot{Q}_{storage} = \dot{Q}_{transmission} = U \cdot A \cdot \left(T_{amb} - T_{inside}\right) \tag{4.3}$$

where U and A are the U-values and areas of the walls, roof and floor. T_{amb} is the ambient temperature. The produced snow is assumed to be allocated to the storage immediately, and

Table 4.2: Snow storage building parameters

Description	Value	Unit
U value wall	0.06	W/m^2K
U value roof	0.06	W/m^2K
U value floor	0.08	W/m^2K
Inside temperature	-5	°C

the snow is to be distributed from the storage to the cross-country slope following demand due to snow melt, as described in section 4.1. The control strategy of the storage is to build up a sufficient storage with even daily production during the winter to meet the summer demand without having to increase the daily production. There will be losses related to distribution of the snow. Therefore, the storage volume at the end of the year must be larger than that of the beginning of the year, to account for these losses.

Supermarket

Supermarkets in Nordic climates are usually located in the ground floor, with few to no windows, making the indoor climate cool and the heat gain from received radiation very low. As specified in the assignment text, the supermarket will be constructed in a basement location with no AC demand, hence the refrigeration demand for rooms in the supermarket is zero. The rejected heat from the stand-alone units will cover the heat demand all year, as is common practice in supermarkets at this latitude. The supermarket's demands to be covered by the centralized heat pump are, therefore, the heating demand due to DHW and the refrigeration demand for the LT and MT display cabinets, which will be presented in subsection 4.2.2 and 4.2.3, respectively.

4.2.2 Domestic hot water

The domestic hot water heat demand for the hotel is based on area-specific heat demands for hotels from *Standard Norway* SN/TS 3031:2016 (StandardNorge, 2016). This estimation is equal for each day of the year. The hot-water demand of the supermarket is assumed to be 100 L/day, with equal distribution throughout the day as commercial buildings given in SN/TS 3031:2016. The combined heat demand estimated for the supermarket and hotel is plotted to the left-hand side axis in Figure 4.3. The temperature of the city water is assumed to be 7 °C at all times. The water is heated up to 80 °C before entering the hot water tanks. The water demand, $\dot{V}$ (L/h), is calculated from the combined DHW heat demand, $\dot{Q}_{DHW}$, in the following way:

$$\dot{V} = \frac{\dot{Q}_{DHW} \cdot 1000 \frac{L}{m^3} \cdot 3600 \frac{s}{h}}{\rho_{water} \cdot C_{p,water} \cdot \Delta T} \tag{4.4}$$

Using the mean values of density and specific heat of water between 0 °C and 80 °C: $\rho_{water} = 990$ $\left(\frac{\text{kg}}{\text{m}^3}\right)$ and $C_{p,water} = 4.19$ $\left(\frac{\text{kJ}}{\text{kgK}}\right)$, the total water demand is found. Water demand is plotted to the right-hand side axis in Figure 4.3.

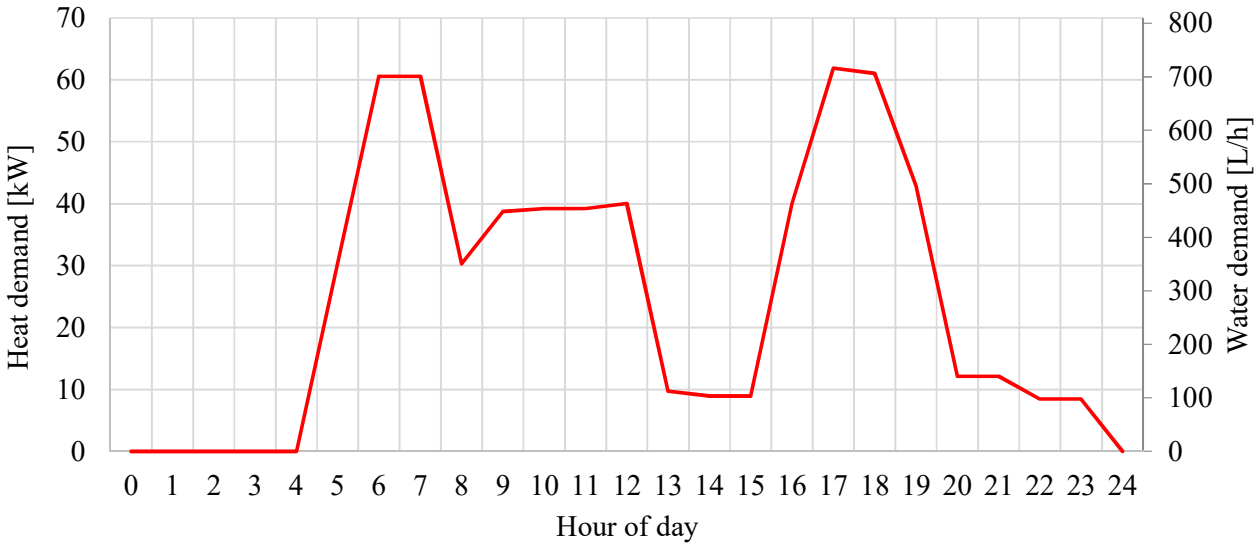

Figure 4.3: Hourly domestic hot water demand

4.2.3 Supermarket refrigeration demand

Similar principles as Selvnes (2017) are used in the estimation of the supermarket's refrigeration demand, which is assumed independent of outside temperature and equal for each opening day. It is modeled to be open 6 days a week. When the supermarket is closed, it has a constant cooling load. During opening hours, it has two peaks, one in the morning due to incoming goods and one between 15:00 and 18:00 when there are most customers. The specific MT and LT loads have been decided in cooperation with prof. Armin Hafner at NTNU. The LT and MT cooling load for each hour of the days which the supermarket is open is plotted in Figure 4.4 on the next page.

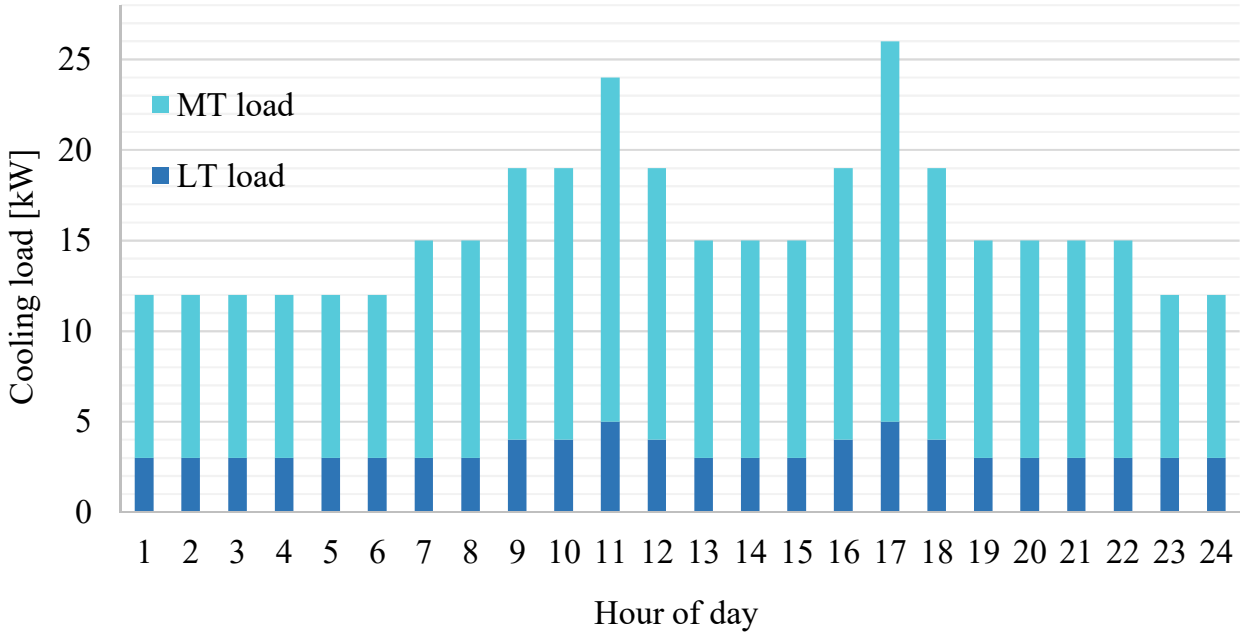

Figure 4.4: Refrigeration demand for a typical supermarket in Trondheim during a weekday

4.3 Transcritical CO_2 heat pump

The calculation tool to analyze the heat pump will be developed in Microsoft Excel, in combination with RnLib, a library containing thermodynamic data of common refrigerants including CO_2. In order to set up the calculation tool, the design of the centralized heat pump needs to be set up first.

4.3.1 Heat pump design

The design of the centralized heat pump is based on a booster system with parallel compression. A schematic drawing of the proposed design of the heat pump and connected heating subsystems is presented in Figure 4.5, while Figure 4.6 shows the thermodynamic process sketched in a logarithmic pressure-enthalpy diagram.

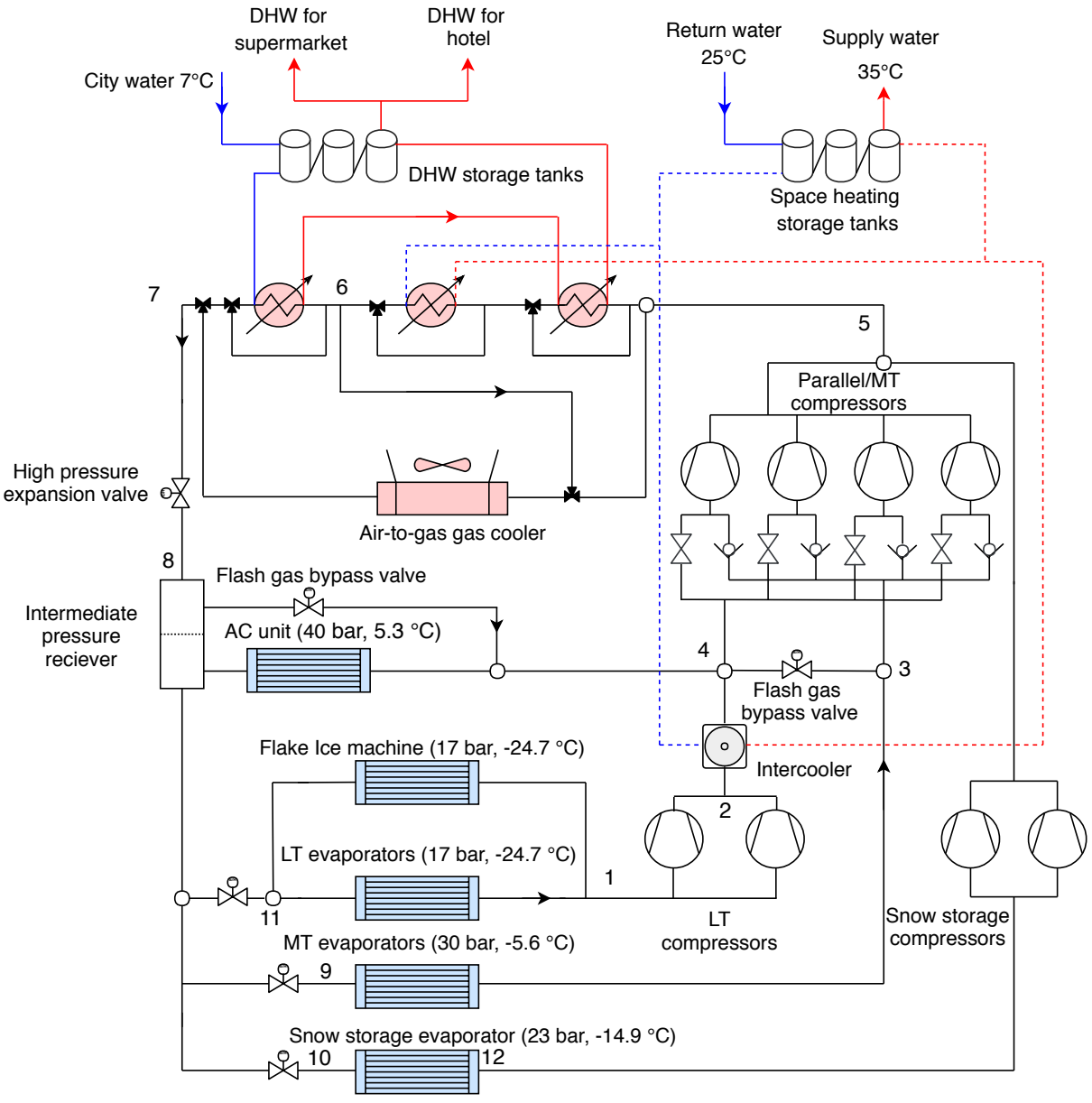

Figure 4.5: Design of the transcritical CO_2 heat pump

The numbered state points in Figure 4.5 correspond to the numbering in Figure 4.6 . The MT

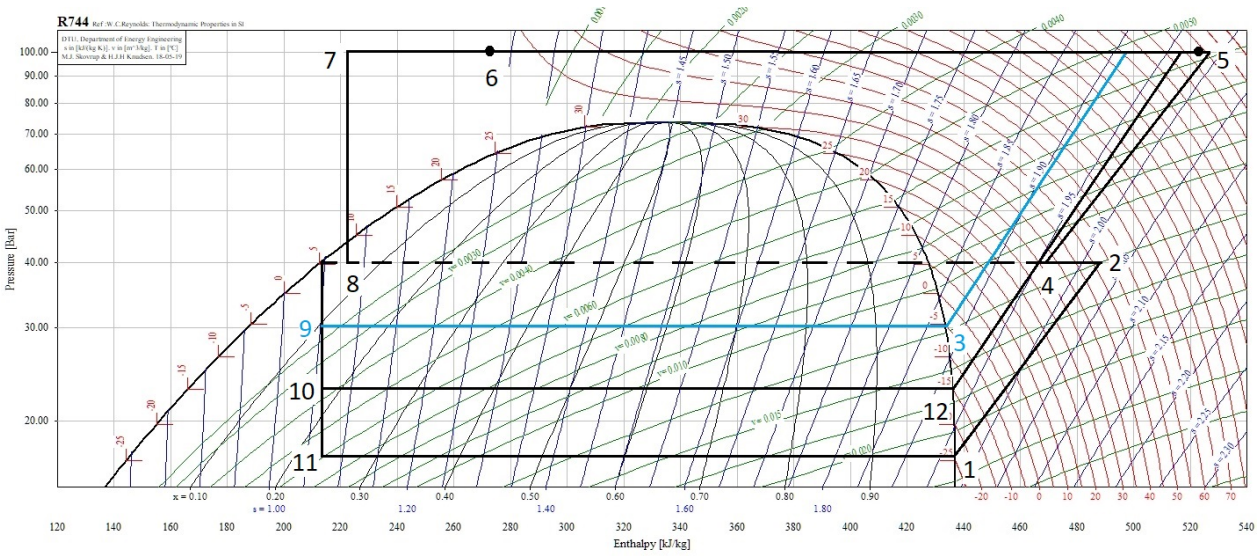

Figure 4.6: Logarithmic pressure-enthalpy diagram for the heat pump operating at 100 bar as the high-side pressure. Figure adapted from CoolPack

evaporator and compressor is sketched with a blue line in Figure 4.6 to facilitate its reading. In practice, there will be more than one of the components, such as MT evaporators and LT evaporators. The MT/Parallel compressor rack will be referred to as parallel or MT compressor according to how the rack is operated. This configuration will be discussed in detail later in this chapter. An air-to gas cooler is installed in parallel with the heat recovery units, so the heat pump can be operated in heat recovery mode or heat rejection mode. In case heat is recovered for space heating only, the air-to-gas gas cooler will provide additional cooling of the CO_2 after the outlet of the space heating heat exchanger (state point 6). Figure 4.6 is drawn without any flow in the AC unit, in order to highlight the separation of gas and liquid in the liquid pressure receiver (8). If there was flow in the AC unit, it would run equal to the dashed line between (8) and (4), at 40 bar. The AC unit is modeled to be driven by gravity, hence no pump is needed. Pump work and pressure drop is not considered in any system or subsystem in this thesis. The pressure drop in the flash gas expansion valve between (4) and (3) is 10 bar. Further system characteristics are presented in table Table 4.3 on the next page The refrigeration loads in Table 4.3 are the maximum cooling loads the heat pump needs to deliver. As the LT and MT refrigeration capacity are assumed equal each day, the installed cooling and freezing capacity in the supermarket should be dimensioned for peak loads higher than what's listed in Table 4.3. The same should be considered for the snow storage building's installed capacity. Supermarkets

Table 4.3: Heat pump characteristics

Component	Value	Unit
Refrigerant	R744	[-]
LT evaporator	-24.70	°C
Snow storage evaporator	-14.88	°C
MT evaporator	-5.56	°C
AC evaporator	5.30	°C
Intermediate pressure	40	bar
Maximum LT refrigeration load	5	kW
Maximum MT refrigeration load	21	kW
Maximum Snow storage refrigeration load	16	kW
Maximum TIS refrigeration load	420	kW
Maximum AC refrigeration load	127	kW
Minimum ΔP in the high pressure valve	5	bar
Temperature approach in heat exchangers	5.0	K

of this size typically have 60 kW cooling capacity and 15 kW freezing capacity (Selvnes, 2017). In the case of the AC unit, its peak load capacity is needed only for a few hot summer days, typical for Nordic conditions, an can be used for dimensioning the AC unit. Whenever the AC demand exceeds 20 kW, the snow production switches off to avoid high peak refrigeration loads. The 5 bar minimum pressure difference in the high-pressure expansion valve results in the minimum allowed value of the pressure in the air-to-gas gas cooler to be 45 bar.

The approach temperature in the heat exchangers is set to 5 °C. As an example, this means the refrigerant at the outlet of the DHW preheat exchanger will be 12 °C, as the city water is assumed to be 7 °C all year. The intercooler is installed to reduce the outlet temperature of the LT compressors, which will, in turn, reduce the outlet temperature of the MT and Parallel compressors. It is beneficial to restrict the outlet temperature of the compressors to reduce heat loss. A low discharge temperature will make it likely that valves and other components in the compressor last longer.

Figure 4.7 and Figure 4.8 shows the design of the heat recovery circuits. One key difference is that the space heat loop is a closed one, recirculating the water. The supply water is returned at 25 °C. The DHW subsystem is an open system, always receiving water at 7 °C. The hot water, stored at 80 °C, is mixed before reaching the faucet or shower and is emptied into the drain. Drainage water heat recovery is not implemented in the model.

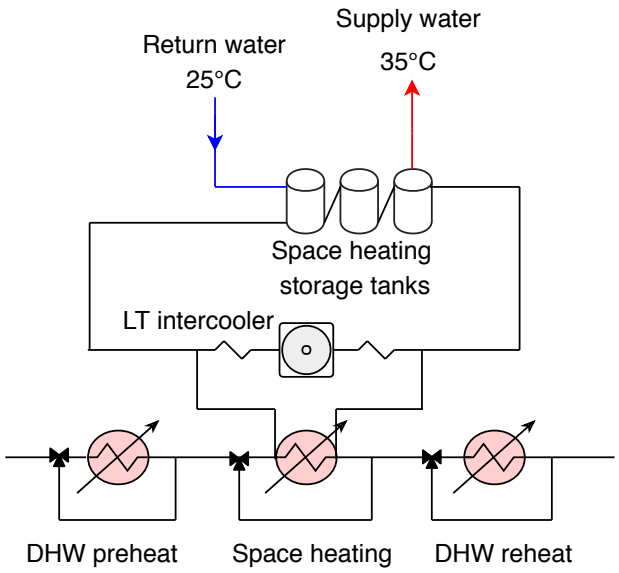

Figure 4.7: Space heat subsystem

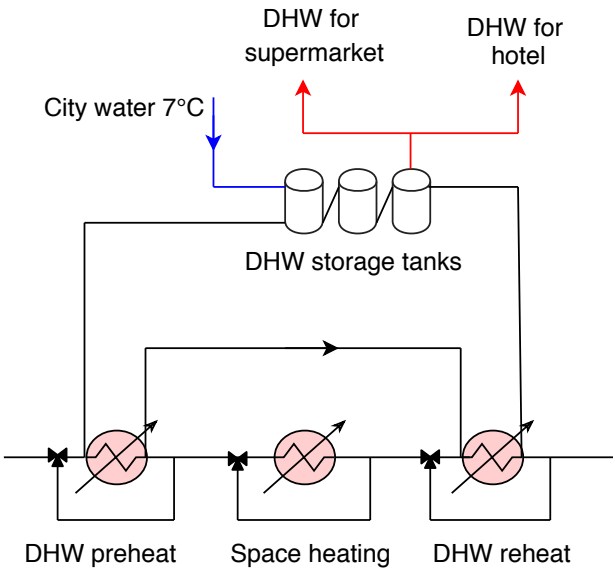

Figure 4.8: DHW subsystem

What makes CO_2 an excellent refrigerant for heating hot water is its gliding temperature in the transcritical region. A good temperature fit is possible for heating DHW, as seen is the temperature-entropy diagram in Figure 4.9. The blue line represents CO_2 at 100 bar, the red line represents water for DHW purposes, heated from 7 °C to 80 °C. In systems where both storages can be charged at the same time, an even better fit is possible.

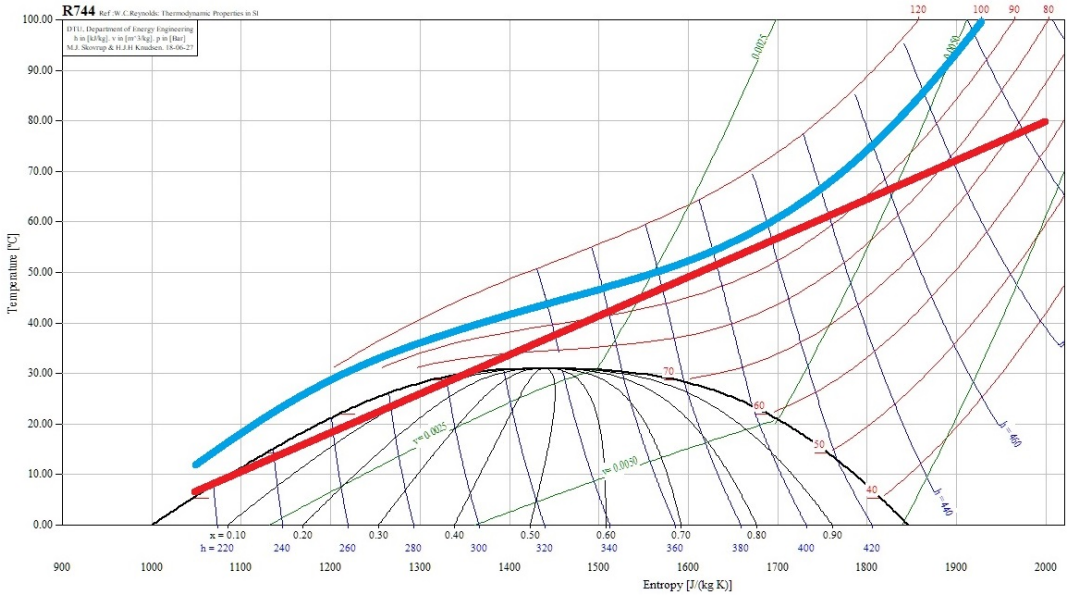

Figure 4.9: Temperature-entropy diagram illustrating heating of DHW

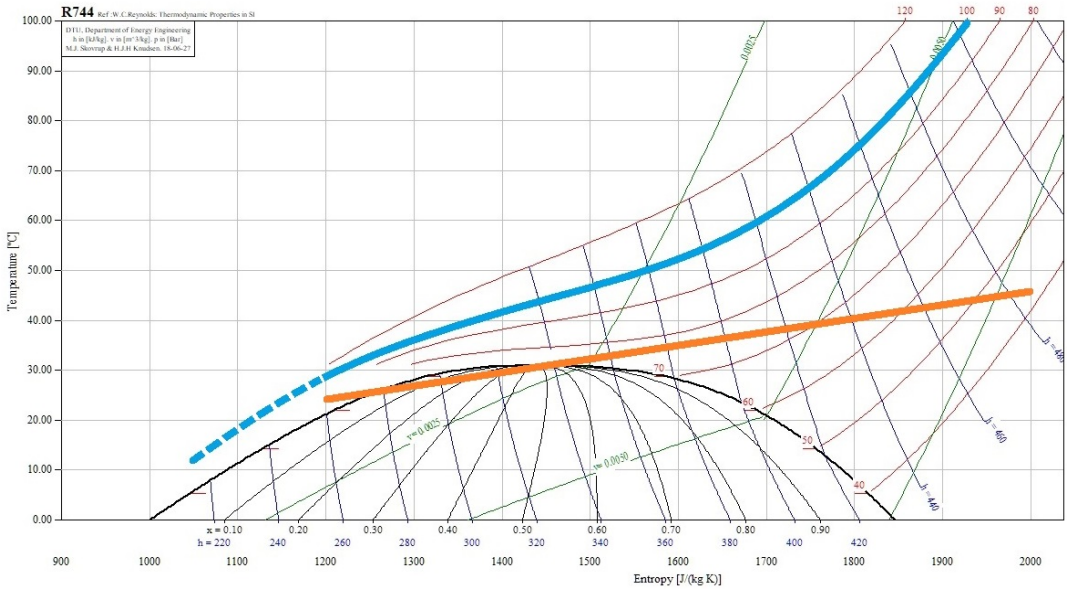

Figure 4.10: Temperature-entropy diagram illustrating the heating of space heating water

The heating of water for space heating has a worse temperature fit (Figure 4.10), as this water is heated from 25 °C to 35 °C. The orange line represents the space heating water. The dashed part of the blue line represents additional cooling of the refrigerant by the air-to-gas gas cooler, after leaving the space heating heat exchanger. This configuration is illustrated later, in Figure 4.19. The intercooler also heats water for space heating purposes. The refrigerant inlet temperature to the intercooler is 43 °C, while the outlet temperature is set to 30 °C, similar to the outlet of the space heating unit. Further water temperatures in the heat recovery units and AC unit are presented in Table 4.4. In the heat exchangers, heat transfer from the exchanger to its

Table 4.4: Water temperatures in heating and cooling subsystems

	Water temperature [°C]	
Heat exchanger	Inlet	Outlet
Preheat DHW	7	25
Space heating	25	35
Reheat DHW	25	80
AC	17	13

surroundings are neglected. So is the change in potential and kinetic energy of the fluid. With these assumptions, the heat transfer rate, $\dot{Q}$, in a heat exchanger is calculated by the following

equation (Incropera et al., 2013):

$$\dot{Q} = \dot{m} \cdot \left(h_{in} - h_{out}\right) \tag{4.5}$$

where h_{in} and h_{out} are the inlet and outlet enthalpies of the fluid on one side of the exchanger, in kJ/kg. $\dot{m}$ is the mass flow of the fluid, in kg/s. Another useful relation in modelling and design of heat exchangers relates the heat transfer rate, $\dot{Q}$, to the temperature difference, heat transfer area and overall heat transfer coefficient:

$$\dot{Q} = UA\Delta T_{lm} \tag{4.6}$$

The overall heat transfer coefficient U (W/m^{2}K), is defined in terms of the total thermal resistance to heat transfer between the fluids. A (m^2) is the heat transfer surface area in the heat exchanger. ΔT_{lm} is the logarithmic mean temperature difference between the fluids, in K.

A brazed plate heat exchanger is a good option for recovering heat at the high-pressure side of the system. The AXP series from Alfa Laval (Figure 4.11) is particularly well-suited for R744 applications at high pressures (Alfa Laval, 2016). The series is approved by the European Pressure Equipment Directive (PED) for pressures up to 130 bar at temperatures between −10 °C and 150 °C, which are suitable values for heat exchangers to be used for heat recovery at the proposed heat pump conditions. The maximum capacity is 300 kW. Recalling the 629 kW gas cooler heat duty in the flake ice system proposed by Bergwitz-Larsen, it is likely that two or more heat exchangers need to be installed in parallel in the subsystems to ensure sufficient heat recovery.

Figure 4.11: The AXP brazed plate heat exchanger series from Alfa Laval (2016)

4.3.2 Control strategy

Heat recovery mode Sale of excess heat is considered. The suppliers of district heating in the area were contacted and expressed an interest to purchase excess heat. However, as the return temperature in the district heating network is around 70 °C, it would not provide sufficient cooling of the refrigerant in the gas cooler. Production of hot water can cool the refrigerant to 12 °C with the assumed approach temperature in the heat exchangers. Therefore, selling hot water to local customers is the chosen strategy. The high-side pressure during heat recovery is set to 100 bar to ensure a sufficiently high temperature for preparation of DHW. The parallel compressors are utilized in heat recovery mode, preventing the refrigerant to be expanded unnecessarily, thus reducing the required power input. They will be operating at an acceptable pressure ratio of 2.5 during heat recovery. This means that the valve between point 4 and 3 will be closed and the parallel compressors will compress the flow from the intercooler, AC unit and the gas from the intermediate pressure receiver.

Heat rejection mode When heat is not recovered, it is rejected to the ambient by the air-to-gas gas cooler. In this mode, the parallel compressors are not operating, because they will in the worst case operate with a pressure ratio of 1.125 (45 bar/40 bar), due to the minimum pressure in the gas cooler being 45. Therefore, the flash gas, the discharge from the AC unit and intercooler are flashed down to 30 bar and compressed by the MT compressor rack, operating at a higher pressure ratio. When heat is rejected to the ambient, the gas cooler pressure will vary. For increased efficiency, the pressure should be chosen to minimize the gas fraction out of the high-pressure valve. This pressure will depend on the ambient temperature. The modeled strategy is to choose a pressure which corresponds to a saturation temperature 3 K higher than the temperature the refrigerant can reach out of the gas cooler. This temperature difference is a safety measure to ensure that phase change always happens in the gas cooler. If not, one could risk that saturated gas instead of saturated liquid would enter the high-pressure expansion valve, which would reduce the cooling capacity greatly. As the ambient temperature increases, this method results in a higher gas fraction. When the refrigerant temperature in the gas cooler approaches and exceeds the critical temperature of CO_2 (31.1 °C), the result is a gas fraction higher than what's most efficient for the total system. Therefore, when the ambient temperature exceeds

20 °C, which corresponds to a refrigerant temperature of 28 °C, another principle to choose the gas cooler pressure is implemented. After discussions with Dr. Ángel Álvares Pardiñas at NTNU, the pressure in the gas cooler during heat rejection is chosen after the following relation:

$$P(T_{amb}) = \begin{cases} \frac{(T_{amb}+5)-25}{40-25} \cdot (100-70.5)+70.5 & : \quad T_{amb} > 20 \\ P_{sat}(T_{amb}+8) & : \quad T_{amb} \leq 20 \end{cases} \tag{4.7}$$

where $P(T_{amb})$ is the gas cooler pressure in bar, $P_{sat}(T_{amb})$ is the pressure of saturated liquid in bar and T_{amb} is the ambient temperature in °C. This relation is sketched in a logarithmic pressure-enthalpy diagram in Figure 4.12. The orange line corresponds to ambient temperatures above 20 °C and the red line for ambient temperatures below 20 °C

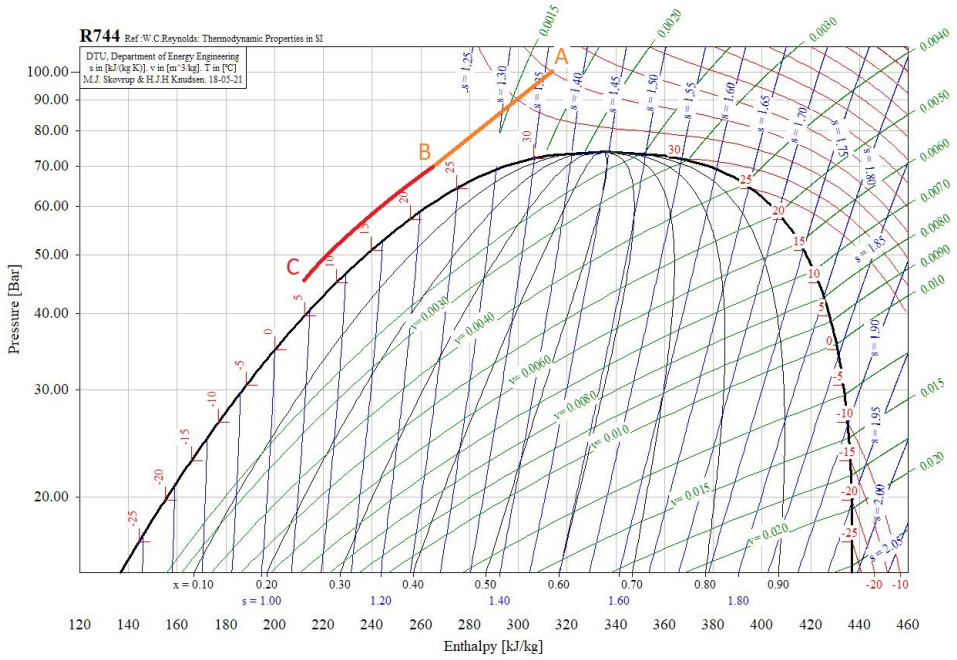

Figure 4.12: The gas cooler pressure sketched in a logarithmic pressure - enthalpy diagram

The gas cooler pressure follows a straight line drawn between point A at 100 bar and 40 °C and point B at 70.5 bar and 25 °C. Point C denotes the lowest possible pressure out of the gas cooler, 45 bar, due to the minimum pressure difference required for the high-pressure expansion valve. A suitable gas cooler model for this application is the Alfa-V VXF industrial V-type CO_2 gas cooler, by Alfa Laval (2018), shown in Figure 4.13. Its capacity range is 160-1000 kW,

assuming an air temperature of 35 °C, CO_2 at 90 bar and cooling of the gas from 120 to 30 °C. The largest model is 8.2 meters long and 2.2 meters wide, making installation on the roof a possibility.

Figure 4.13: The Alfa Laval Alfa V VXD gas cooler (Alfa Laval, 2018)

Compressor considerations

A consequence of the varying pressure in the gas cooler is that all the compressors will operate at varying pressure ratios, except for the LT compressors. A compressors' isentropic efficiency changes with changing pressure ratios. An empirical equation developed by Prof. T. M. Eikevik at NTNU based on measurements of piston compressors is used to model the isentropic efficiency of compressors, η_{is}, as a function of the pressure ratio, PR (Bergwitz-Larsen, 2016):

$$\begin{aligned}\eta_{is} = &-0.00000461 \cdot PR^6 + 0.00027131 \cdot PR^5 - 0.00628605 \cdot PR^4 + 0.0737025 \cdot PR^3 - \\ &0.46054399 \cdot PR^2 + 1.406653347 \cdot PR - 0.87811477\end{aligned} \tag{4.8}$$

This dependency is presented graphically in Figure 4.14.

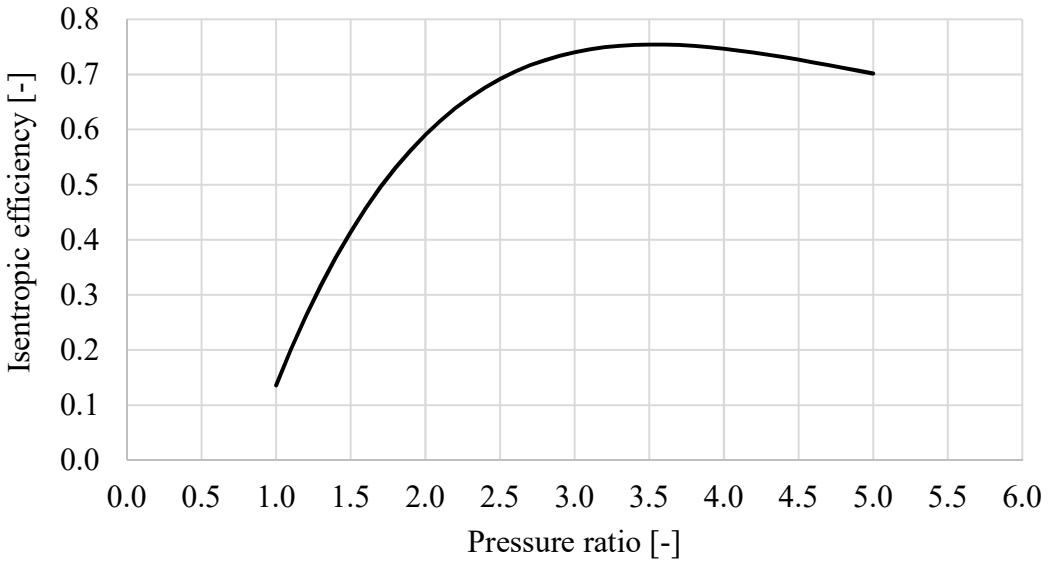

Figure 4.14: Isentropic efficiency as a function of pressure ratio

The isentropic efficiency drops quickly for low pressure ratios, which is preferably avoided. The indermediate pressure P_m should be set to reduce the compression work. In isentropic compression, the minimum compression work occurs when the pressure ratio PR is equal for each of the two compression stages (Eikevik et al., 2017):

$$PR = \frac{P_{heat\ recovery}}{P_m} = \frac{P_m}{P_{LT}} \tag{4.9}$$

$$P_m = \sqrt{P_{heat\ recovery} \cdot P_{LT}} \tag{4.10}$$

With a heat recovery pressure of 100 bar and a LT pressure of 17 bar, Equation 4.10 yields an intermediate pressure of 41 bar. As stated in Table 4.3, the intermediate pressure is set to 40 bar. Once the pressure ratio is calculated and isentropic efficiency is found, the outlet enthalpy of each compressor can be found, using the definition of the isentropic efficiency (Moran et al., 2012):

$$\eta_{is} = \frac{h_{out,s} - h_{in}}{h_{out} - h_{in}} \tag{4.11}$$

where $h_{out,s}$ is the outlet enthalpy at isentropic compression. When the outlet enthalpy is found, the power input per unit mass flowing through the compressor is found using the following relation (Moran et al., 2012):

$$\dot{W}_{cv} = \dot{m} \cdot \left(h_{out} - h_{in}\right) \tag{4.12}$$

where W_{cv} is the power input to the control volume inside the compressor cylinder, which is then compressed by the piston. Heat loss in the compressors also needs to be considered when modeling compressors. The heat loss,$\dot{Q}_{cv}$, is the difference between the compressor power and the *actual* energy increase of the fluid, $\left(h_{out,fluid} - h_{in}\right)$ (Moran et al., 2012):

$$\dot{Q}_{cv} = \dot{W}_{cv} - \dot{m} \cdot \left(h_{out,fluid} - h_{in}\right) \tag{4.13}$$

Introducing the heat loss factor as $f_{heat\ loss} = \frac{\dot{Q}_{cv}}{\dot{W}_{cv}}$ and dividing Equation 4.13 by $\dot{W}_{cv}$, the enthalpy of the fluid leaving the compressor is found the following way:

$$h_{out,fluid} = h_{in} + (1 - f_{heat\ loss}) \cdot \left(h_{out} - h_{in}\right) \tag{4.14}$$

All the compressors are modeled with a heat loss factor of 0.1. This means that 10 % of the compressor work cannot be recovered as heat, as it is lost through the surface of the compressors. The factor (1-$f_{heat\ loss}$) is commonly referred to as adiabatic efficiency. The sum of the total cooling load and power input should be equal to the excess heat in an ideal process, as described in Equation 2.1. This can be used to verify the calculations by the model. With 10% heat loss, the excess heat should be the sum of the cooling load and 90% of the power.

Due to the proposed heat recovery and heat rejection strategies, a large portion of the refrigerant flow will be directed either to the MT compressors or the parallel compressors, but not both at the same time. When the flash gas bypass valve between the suction of the parallel compressors (4) and the MT compressors (3) is open, there is no flow in the parallel compressors. To avoid an unnecessarily high investment cost, it would be beneficial to utilize the parallel compressors operating as MT compressors when the flash gas bypass valve is open. This would reduce the total number of compressors needed. The proposed MT/parallel compressor rack design is presented in Figure 4.15.

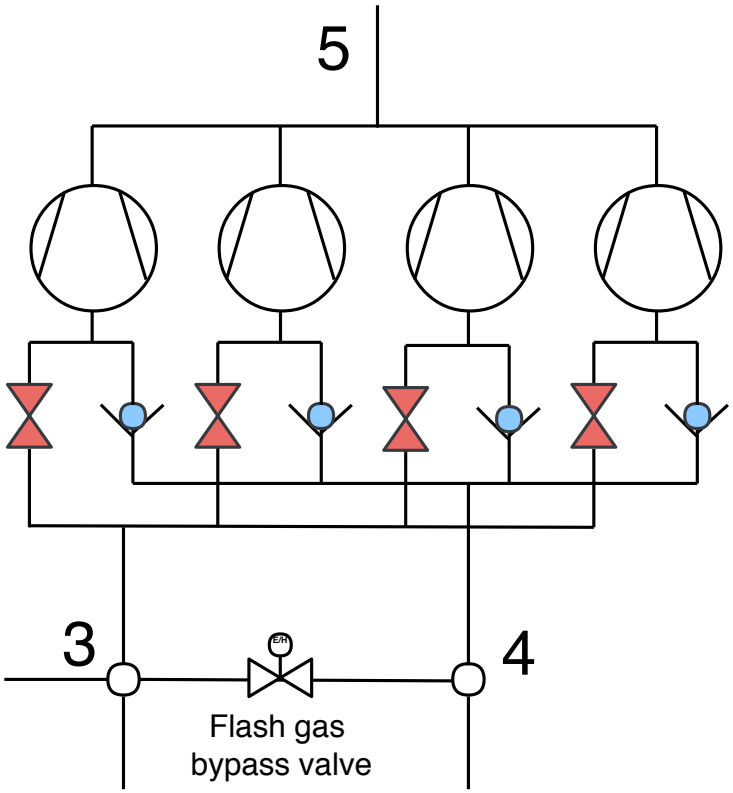

Figure 4.15: MT and parallel compressor rack design

This compressor rack design uses the principle of pivoting compressors, similar to a CO_2 refrigeration system proposed by Han (2017). The numbering of the state points corresponds to Figure 4.5. The compressors are operated to minimize the electricity consumption. To achieve this, the flash gas bypass valve is opened and the red valves are closed when the pressure ratio, and thus, the isentropic efficiency for the parallel compressors is low. The blue check valves will open as the suction pressure of the compressors drop. The rack is utilized as an MT compressor rack, due to a higher pressure ratio, in this configuration. During heat recovery mode, the pressure ratio of the parallel compressors is acceptable. The red valves are opened and the flash gas bypass valve is closed. The blue check valves remain closed due to a higher downstream pressure. One compressor always remains in MT configuration to compress the fluid from the MT evaporators.

A suitable compressor is the BITZER Ecoline+, designed for transcritical CO_2 applications, shown in figure Figure 4.16 (BITZER, 2018). The smallest model, 4PTEU-7LK, of the Ecoline+ has a maximum geometric displacement of 4.5 m^3/hour at 50 Hz with the possibility to run at 20 % capacity, yielding a lower limit of 0.9 m^3/hour. The largest model, 6CTEU-50LK, has a geometric displacement of 39.5 m^3/hour at 50 Hz.

Figure 4.16: The Ecoline+ compressor by BITZER

4.3.3 Hourly electricity price variation and power fees

The TIS machine will produce snow all year round to meet the snow demand. In order to cut costs, it can be beneficial to systematically turn off the machine during periods with high electricity prices and turn it on when the price is lower. Therefore, the median spot price of electricity is calculated for each hour of the day, based on a full year. It is presented in Figure 4.17 together with a future scenario. The data is downloaded from Nord Pool (2017). The electricity prices gathered from Nord Pool are the exchange prices on the Nordic market. The price of electricity for the end-user is higher and depends on fees from the power supplier. A fee of 0.70 NOK/kWh is used in calculations, based on phone correspondence with a local power supplier (TrønderEnergi Marked, 2018).

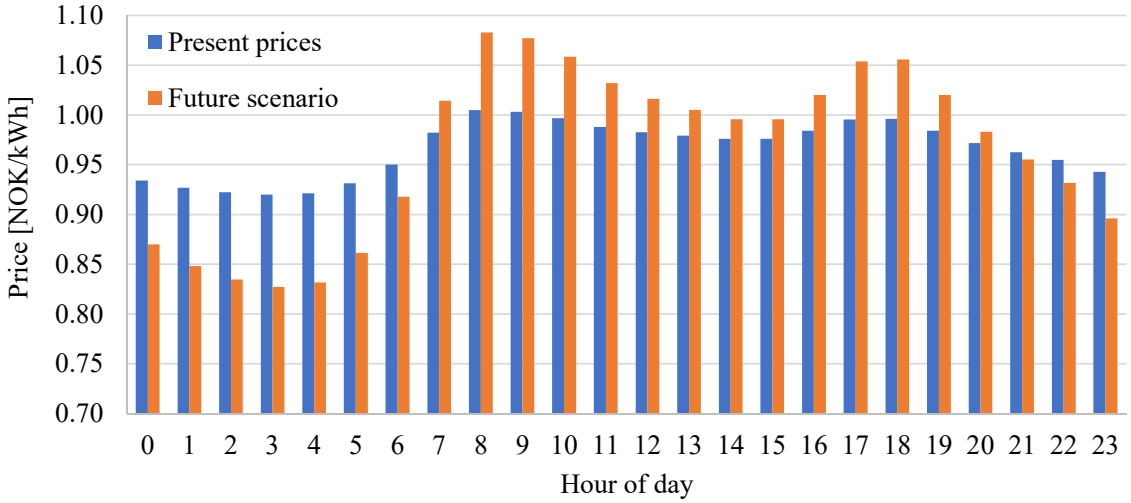

Figure 4.17: Calculated hourly median electricity spot price

The European power market will be more connected in the future and import and export of energy are expected to increase. An interconnector scheduled for completion in 2020 will connect Norway directly the German power marked (Norwegian Ministry of Petroleum and Energy, 2017). The German power market is to a greater extent influenced on weather-dependent energy sources, such as wind and solar power, than the Norwegian power market. Larger fluctuations in spot prices occur in Germany. Therefore, the result of a direct connection between Germany and Norway could be larger fluctuations in the spot price in Norway. Figure 4.18 shows the German spot price varies more than in Norway.

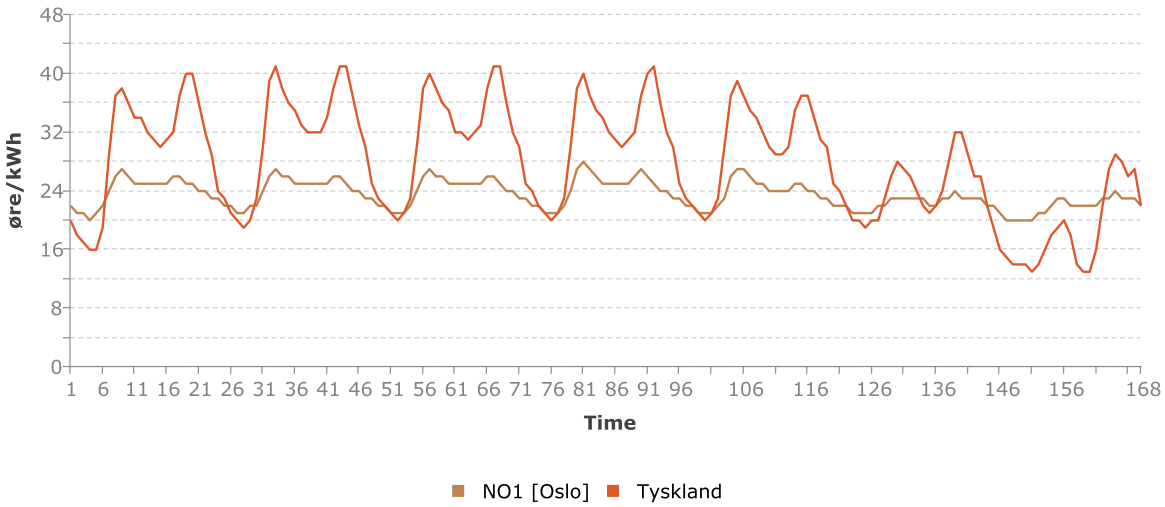

Figure 4.18: Comparison of electricity prices in øre/kWh in Norway and Germany (Norwegian Ministry of Petroleum and Energy, 2017)

The time axis shows hours. It can be observed that the price profile each day resembles the hot water demand presented in Figure 4.3. The future scenario is created by doubling the hourly difference to the yearly mean of the present prices. This means that the average price stays the same, but the variations are larger.

Power companies operate with a fee for business customers with high peak loads on the power grid. Table 4.5 shows fees for low-voltage businesses charged by the local power company (TrønderEnergi Nett, 2018). The highest hourly load is measured by the power company each month and used to calculate a monthly fee, differentiating between summer and winter. Additionally, an annual fee of NOK 8 800 is charged for low-voltage businesses.

Table 4.5: Load fees [NOK/kW/month] charged by Trønder Energi Nett

	0-200 kW	200-500 kW	500-800 kW	>800 kW
Winter (Nov-Feb)	60	53	47	40
Summer (Mar-Oct)	45	40	35	30

4.4 Thermal storages and PCM integration

Thermal storages are needed in the DHW and space heat subsystems. The thermal storages will be charged with use of heat exchangers transporting energy from the refrigerant to water, discussed on page 46. The pipelines with flow are marked green figures Figure 4.19 and Figure 4.20 during charging of the space heat storage and the DHW storage, respectively.

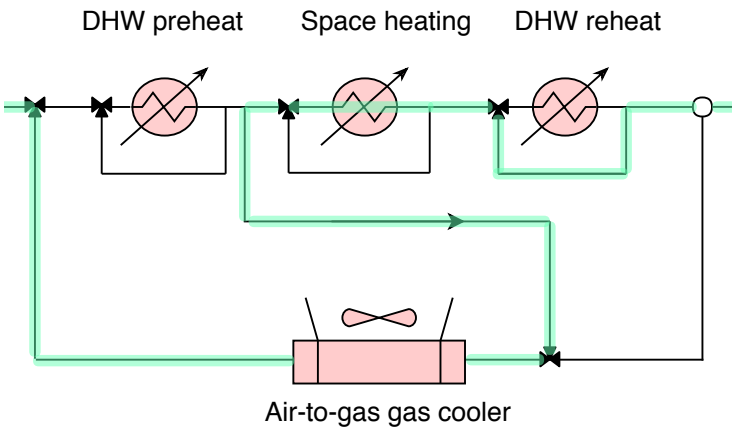

Figure 4.19: Flow lines during space heat storage charging

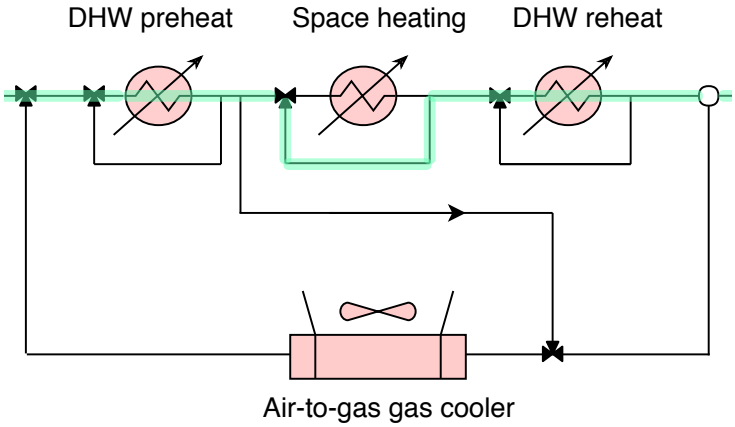

Figure 4.20: Flow lines during DHW storage charging

The tanks will be modeled to be charged when the water level, and thus stored energy, drops below a set value optimized manually, to cover the heat demand and minimize the storage size. During charging, the outlet pressure of the parallel, MT and snow storage compressors is set to 100 bar and all the excess heat is allocated to either space heating or DHW. Hence, only one

heat storage can be charged at the time. This is due to limitations in the calculation model. In practice, it would be possible to recover heat both for DHW and space heating purposes at the same time. As the resolution of the model is one hour, it is not of much importance for the operation of the storages, as they will rarely need charging the same hour. The DHW storage is prioritized, as it is considered more important to be able to cover the DHW demand than the space heat demand for the hotel. Running out of hot water is more critical for a hotel than not being able to meet the heat demand for one or two hours.

When PCM is used in the model, it will be modeled to be integrated in the hot water tanks, similar to Nkwetta and Haghighat (2014), as seen in Figure 4.21. For space heating, the PCM S34 by PCM Products (2013) will be the chosen PCM. As it has a melting temperature of 34 °C, it will be charged when water at 35 °C is admitted to the storage. This 1 K temperature difference works in theory but may prove to be too little in practice. When the space heat storage is emptied, return water at 25 °C enters the storage and heats up as the PCM changes phase from liquid to solid. It is assumed that the water heated by the PCM reaches 34 °C. For simplicity, the supply space heat water is modeled to always be 35 °C. With the use of PCMs, more heat can be stored in a smaller volume. The purpose of the PCM in this application is to increase storage capacity while maintaining the tank size at an acceptable level, as opposed to Nkwetta and Haghighat (2014), where the purpose was to shift peak loads. For the DHW tanks, PCM integration is not considered necessary. The size of the DHW tanks is modeled to be able to cover one day's total demand, in case of failure. The space heating storages are modeled to be as small as possible while still covering the heat demand.

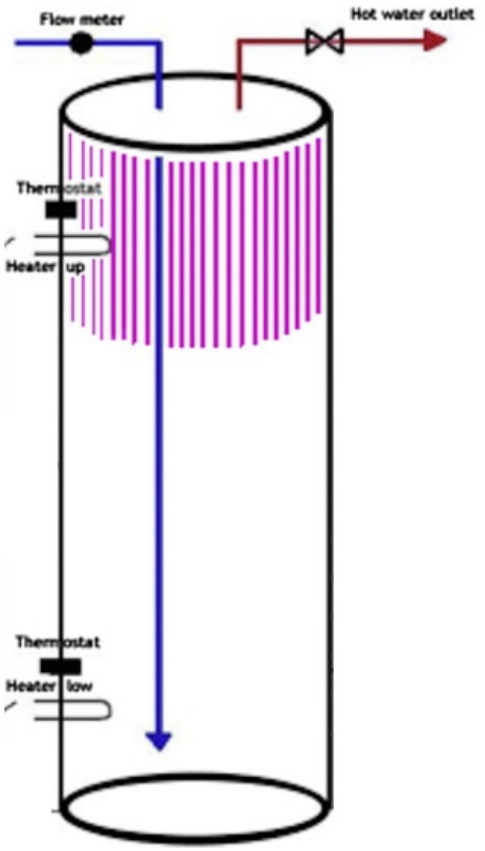

Figure 4.21: Hot water tank integrated with PCM

5. Results and discussion

This chapter contains results of calculations and simulations. The snow melt and corresponding snow demand are presented first, followed by the result of the building simulation. Once all the necessary data is obtained, four cases for the operation of the heat pump are defined and results of their simulations are presented and compared.

5.1 Shading and snow production

With temperature and radiation data from Meteonorm, the hourly snowmelt for one year is found both with and without the shading arrangement presented in section 4.1. Figure 5.1 shows the results from the calculation of snowmelt using the degree-day method including radiation presented in section 3.4.

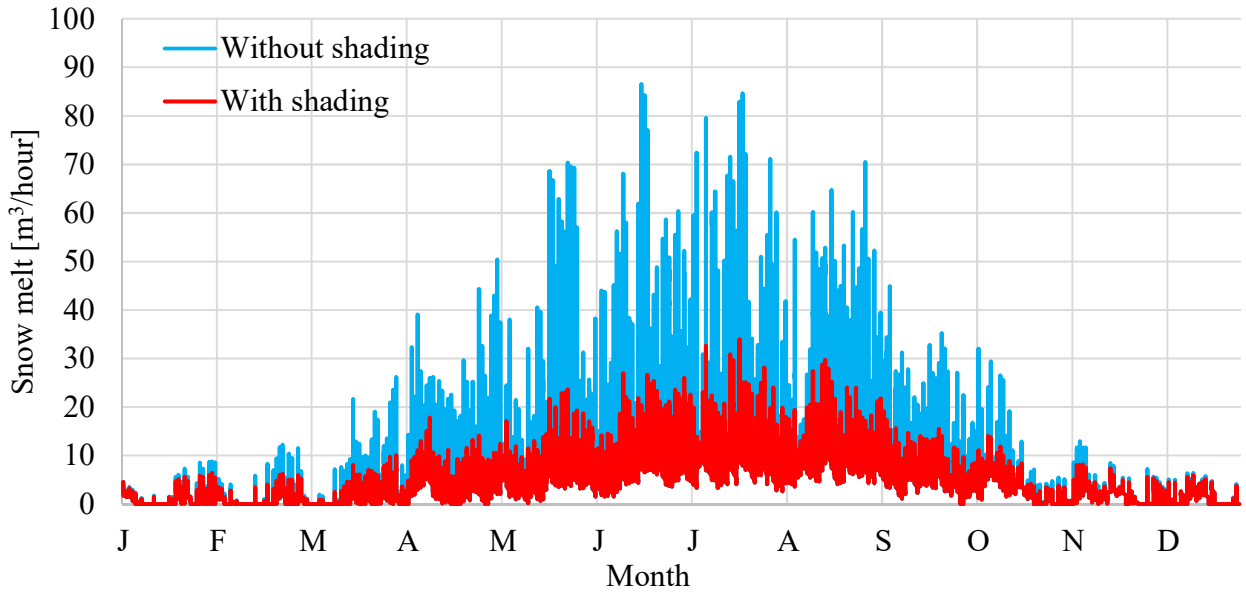

Figure 5.1: Hourly snowmelt with and without shading

The calculated snowmelt without shading is always equal to, or greater than, the snowmelt with shading. As expected, the difference is much larger during the summer months, when the sun is higher, radiating on the snow longer each day. The total volume of snow calculated to melt during one year both with and without shading are presented in Table 5.1. Sun shading results

in a 42 % reduction of the annual snow demand. The model is also tweaked to be compared with the results found by Lintzén (2016), discussed in subsection 3.3.1. With the same volume and snow depth, the average hourly snowmelt from April the 15th to May the 27th is 0.14 m^3/h in this thesis (without shading), compared to 0.19 m^3/h in the study by Lintzén, also without shading. With climate data for Arjeplog in 2013 (Şahin et al., 2016), the average temperature for this period is calculated to be 5.22 °C, while the average temperature in Granåsen during the same period is 7.93 °C. Thus, the model calculates a lower melt rate than experiments, even though the average temperature was higher than the experiment. The amount of melted snow

Table 5.1: Necessary snow production and storage volume due to snow melt

	Without shading	With shading
Total snow melt[m^3]	80406	47036
Necessary production rate [m^3/h]	9.42	5.85
Required storage volume [m^3]	34000	20000

will represent the minimum snow demand. Some snow will be lost in distribution and some will, possibly, melt when the storage is opened to fetch snow for the slope. This is assumed to be 2000 m^3 per year, regardless of shading. Figure 5.2 shows the required storage levels during the simulated year to ensure not running out during the summer.

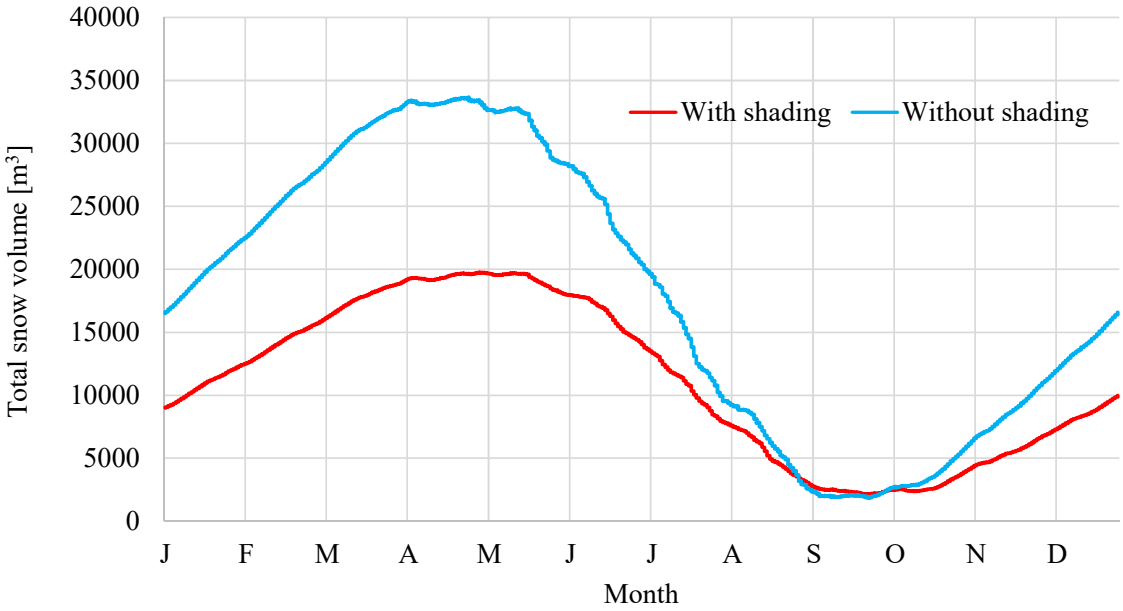

Figure 5.2: Snow storage volume throughout the year

The cross-country slope will be operated all year. Therefore, the strategy in operation of the snow storage should be that the storage level at the end of the year is equal to what it was at the beginning of the year. The storage should also never be empty. The minimum value of the storage in the simulation is set to 1500 m^3, which is considered a suitable buffer.

In order to meet the demand for snow during summer, the storage is filled up during the winter. If there is no shading of the cross-country slope, the necessary storage volume is larger, resulting in a higher required snow production capacity. Building the shading arrangement will represent a one-time investment cost, but it will also reduce the investment needed for the snow storage. It will also reduce the operational cost, as less snow is required for the ski track. Based on these consequences, shading will be considered the chosen solution moving forward in this work.

5.2 Building simulation

Simulation of the hotel was performed in SIMIEN. Figure 5.3 shows the energy budget of the building. Heating makes up 32.3 % of the energy demand of the hotel, while cooling represents 10.8 %. DHW represents 23 % of the energy demand. In total, 66.1 % of the hotel's energy demand will be covered by the centralized heat pumping unit. The remaining power consuming activities in the hotel will be covered by electricity.

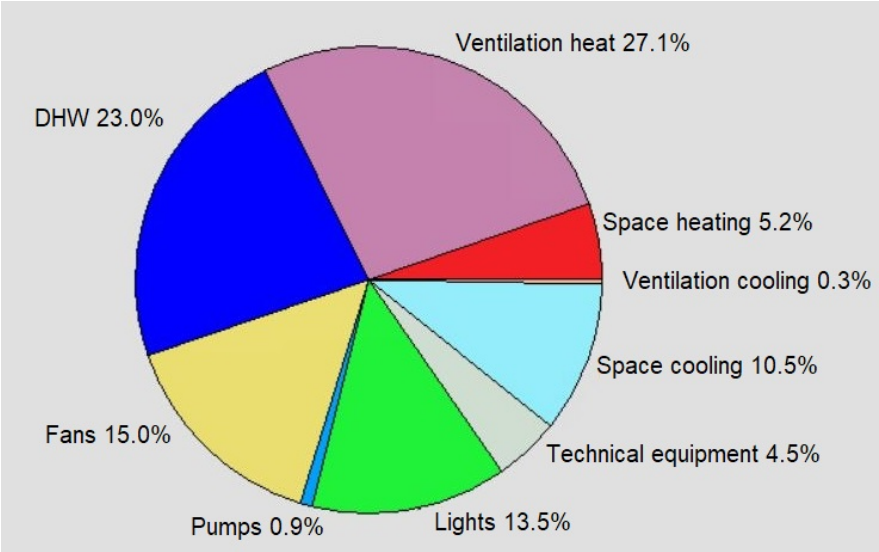

Figure 5.3: Energy budget for the hotel

From the output file produced by the simulation, the required space heating and ventilation heating for the hotel can be obtained on an hourly basis.

Other useful data, such as the hotels' cooling demand and inside air temperature can also be obtained. Both space- and ventilation heating are modeled to be met by the low-temperature space heating system presented in Figure 4.7, with a 35 °C supply temperature and 25 °C return temperature. The building's heating demand was investigated further, as it seemed to fluctuate a lot. A reason for this could be the combination of the supply temperature of ventilation air (after being heated by the heating battery) and the change in ventilation rate from opening hours of the hotel to closing hours. The inside set-point temperature is 21 °C and the effects of increasing the supply temperature from 19 °C to 21 °C were found. The indoor air temperature is equal for both choices of supply air temperature. Changing the temperature to 21 °C did even out the heat demand slightly, as can be seen in Figure 5.4. It also increased the total heat demand marginally, from 239 MWh/year at a supply air temperature of 19 °C, to 243 MWh at 21 °C. Raising the supply temperature reduces the peak heat demand from 177 to 170 kW. The more probable reason for the decrease in heat demand during closing hours is the decrease in ventilation air flow rates, 2 m^3/hm^2 during closed hours and 7 m^3/hm^2 during open hours, as listed for hotel buildings in *Standard Norway* SN/TS 3031:2016 (StandardNorge, 2016).

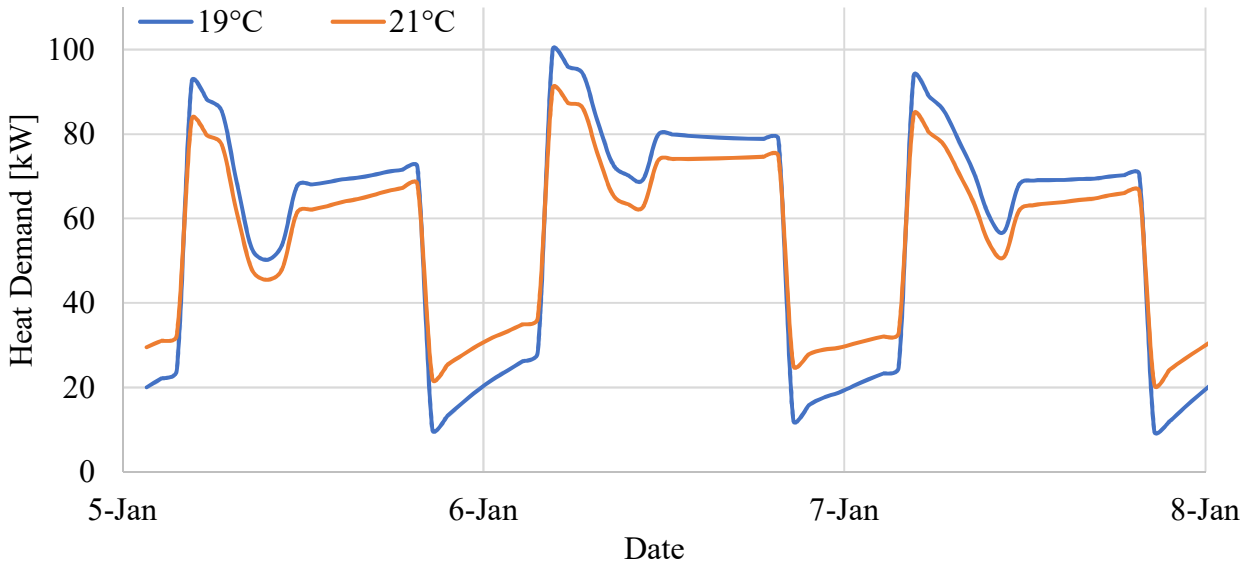

Figure 5.4: Heat demands during three winter days for 19 °C and 21 °C supply air temperature and indoor temperature

As mentioned in the literature survey, the heat demand increases linearly with the ventilation airflow rate (Selvnes, 2017). This explains the large fluctuations in heat demand between closing and opening hours. The air exchange rate during opening and closing hours of the hotel in this thesis is 1.75 and 0.5, respectively, which are considered reasonable values compared to those suggested by Selvnes (2017). The results of the hotel building simulation in this thesis are comparable to those done by Smitt (2017) on Britannia Hotel. The area-specific space heat demand of Britannia Hotel is 30.07 kWh/m^2/year. The simulations of the proposed hotel in this thesis yielded an area-specific space heat demand of 32.47 kWh/m^2/year. The cooling demand, however, proved to be much smaller for the hotel simulated in this thesis. Its area-specific cooling demand is 3.08 kWh/m^2/year, compared to 20.79 kWh/m^2/year at Britannia Hotel.

The required volume for storing the snow was discussed in section 5.1. A snow storage building with a volume of 21 000 m^3 was modeled, with length, width and height of 250, 12 and 7 m, respectively. To reduce transmission heat loss, a building shape with a large volume to surface area ratio, such as a cube or a building with a square footprint, would be most efficient, but pose challenges for construction. Carrying the roof would be the main challenge. A narrow and long building will be the more likely option and is, therefore, the chosen shape. The calculation of the refrigeration demand for the snow storage building resulted in an annual cooling demand of 65 316 kWh. This demand will be linearly dependent only on the ambient temperature due to the simplicity of the model. This refrigeration demand is expected to be the minimum demand required for the snow storage building, as it doesn't take into consideration infiltration losses when the entrance is opened to collect snow for distribution. Other variables such as radiation on the building surface and humidity are also not considered.

All demands to be covered by the centralized heat pumping unit, both heating and refrigeration, are presented as load-duration curves in Figure 5.5. Heating is plotted as a positive demand and cooling as a negative. The load duration curves make it easy to compare the characteristics of the different demands. The most significant feature is the dominating cooling demand due to snow production. It will give a stable supply of available excess heat, excluding the hours when the AC demand exceeds 20 kW. Fittingly, this occurs during hot summer days when there is no space heat demand. The AC demand is zero most of the year, while the snow storage refrigeration and supermarket refrigeration demands are quite similar in magnitude and peak load.

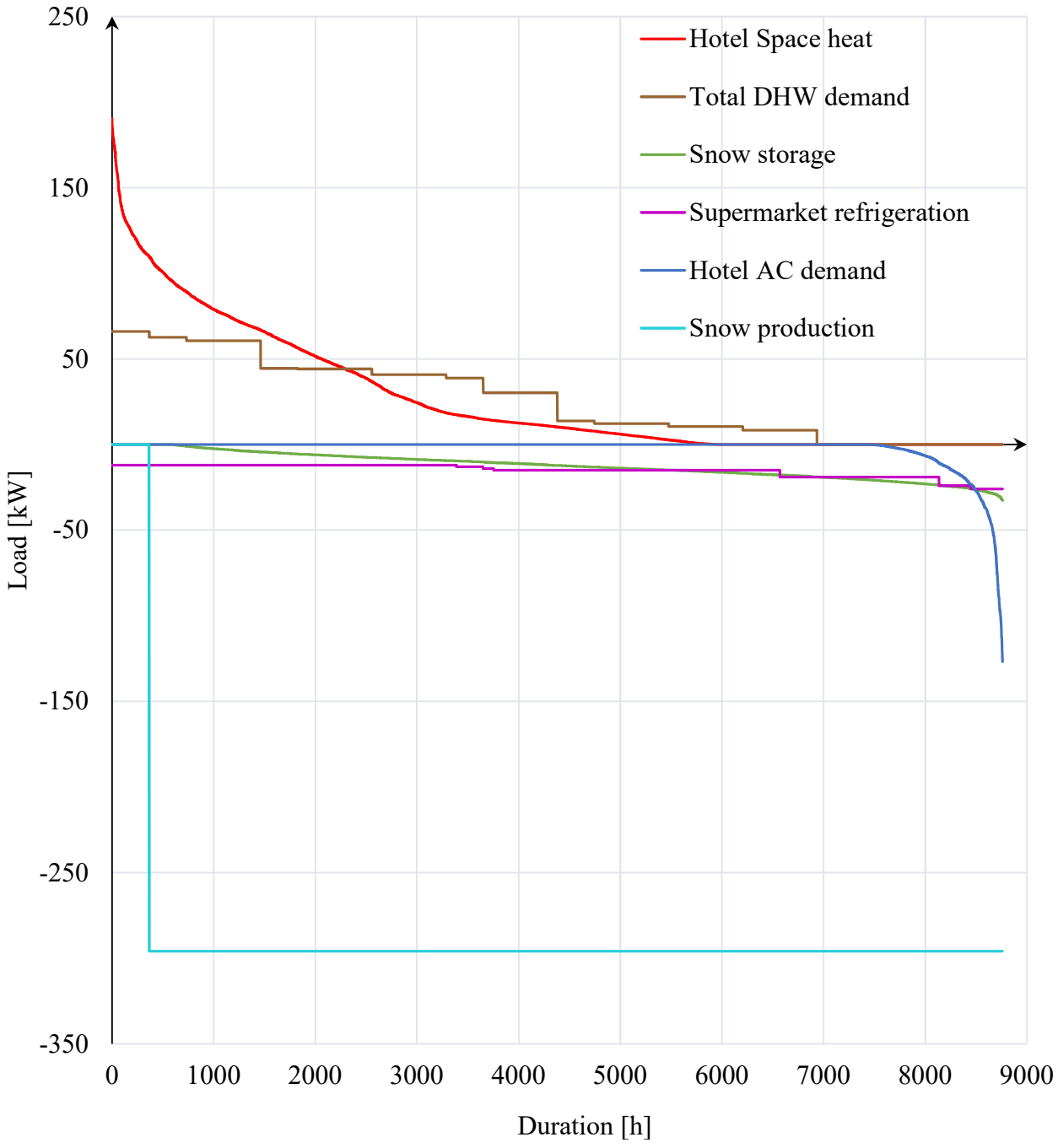

Figure 5.5: Load-duration curves for the heating and cooling demands

The total space heating demand is similar in magnitude to the DHW demand, but with a higher peak demand. Due to the total refrigeration demand being much higher than the total heating demand, the operation of the heat pumping unit will be focused firstly on covering the refrigeration demand, while using the resulting excess heat to cover the heating demands. In Table 5.2 the exact values of all the annual demands are listed.

Table 5.2: Total refrigeration and heating demands

Demand	Value [MWh]
Hotel space heat	239
Total DHW	222
Total heat demand	472
Snow storage refrigeration	65
Supermarket refrigeration	133
Hotel AC	23
Snow Production	2531
Total refrigeration demand	2751

5.3 Transcritical CO_2 heat pump

Different cases for the heat pump are simulated. As evident by the load duration curves in Figure 5.5, more surplus heat than the total heating demand is expected. The heat not needed can either be rejected or recovered for sale. Therefore, investigating the heat pump with total heat recovery and only partial heat recovery, to meet the demand, will be done. In both of these cases, two different strategies are considered: producing snow continuously and producing snow when the electricity spot prices are lower. The motivation for even production of snow is to minimize cost due to a lower heat storage needed and a lower capacity of the flake ice machine. This yields four cases:

- Case 1: Total heat recovery and even snow production, minimizing storage
- Case 2: Total heat recovery with snow production during low electricity prices
- Case 3: Partial heat recovery and even snow production, minimizing storage
- Case 4: Partial heat recovery with snow production during low electricity prices

In cases 1 and 2, the excess heat not needed by the hotel or supermarket is used to produce hot water, as described in subsection 3.2.4. In cases 3 and 4, this heat is rejected to the ambient through the air-to-gas gas cooler. In cases 2 and 4, with snow production during low electricity prices, heat storages and integration with PCM are considered to guarantee the supply of heat when there is not sufficient excess heat from the system. Case 1 is considered the base case. The annual energy efficiency (E.E.) for all cases are presented in Table 5.3. It is defined in Equation 5.1 as all useful thermal contributions divided by the work done by the compressors for one full year

$$E.E. = \frac{H_{space\ heat} + H_{DHW} + C_{TIS} + C_{LT} + C_{MT} + C_{snow\ storage} + C_{AC}}{W_{LT} + W_{MT} + W_{parallel} + W_{snow\ storage}} \tag{5.1}$$

where H and C represent heating and cooling contributions, respectively. The annual cooling efficiency is found as the sum of the cooling contributions divided by total work. Similarly, the annual heating efficiency is found as the sum of recovered heat divided by total work. The total

Table 5.3: Annual energy performance of the 4 cases

Case	1	2	3	4
Electricity demand [MWh]	1452	1452	1291	1280
Cooling [MWh]	2752	2752	2752	2752
Heat recovered [MWh]	3957	3960	461	461
Total available heat [MWh]	*4059*	*4058*	*3915*	*3906*
Cooling efficiency	1.90	1.90	2.13	2.15
Heating efficiency	2.73	2.73	0.36	0.36
Energy efficiency	4.62	4.62	2.50	2.52

cooling for all cases is the same. The heat recovered in cases 1 and 2 requires external demand for heat, for example from a swimming hall and a hotel. In cases 3 and 4, less work is required by the compressors compared to cases 1 and 2, due to a lower high-side pressure during heat rejection. Consequently, cases 3 and 4 boast better cooling efficiencies than cases 1 and 2. However, as most of the available heat in cases 3 and 4 is rejected, the heating efficiency is very low. This gives an annual energy efficiency around 2.5, much lower than that of cases 1 and 2. In cases 3 and 4, only 12% of the available heat is recovered. There are not any notable differences in how the heat pump performs between case 1 and 2. In these cases, only 2.5% of the heat is rejected. This is heat rejected in the intercooler when there is no space heat demand, and heat rejected in

the gas cooler when the space heat storage is charged, as shown in Figure 4.19. Equation 2.1 in the very beginning of this thesis states that the available heat in an ideal heat pump cycle should be the sum of the heat entering the cycle in the evaporators and the work input. It is observed in all cases that the total available heat is the sum of the cooling and work, minus the 10% heat lost to the ambient by the compressors, strengthening the reliability of the model.

The performance of the heat pump with a snow production capacity of 100 tonnes/day is compared to those of the flake ice system modelled by Bergwitz-Larsen (2017), as discussed in subsection 3.2.4. The loads in the evaporators and gas cooler are almost identical, however the required power input is higher in the flake ice system, which is modelled with a higher level of detail. For example, pressure drops in the flake ice drum, pipelines and heat exchangers are accounted for by Bergwitz-Larsen (2017), but neglected in this thesis, which agrees with a lower power input in this thesis. A comparison of the loads and COPs are presented in Table 5.4.

Table 5.4: Comparison of loads between the flake ice system modelled by Bergwitz-Larsen (2017) and the centralized refrigeration unit modelled in this thesis

Characteristic	Flake ice system	Centralized refrigeration unit	Unit
Cooling efficiency	2.37	2.64	[-]
Heating efficiency	1.66	1.87	[-]
$\dot{Q}_{gas\ cooler}$	629	621	kW
$\dot{Q}_{evaporators}$	442	440	kW
$\dot{W}_{compressors}$	266	235	kW

To compare the work done by each compressor category for total and partial heat recovery, cases 1 and 3 are used. Their annual electricity consumption is presented in Table 5.5. In case 1, the high-side pressure is kept at 100 bar and the parallel compressors are always utilized, never needing to flash down to the suction pressure of the MT compressor. Therefore, the parallel/MT compressor rack is mostly utilized as parallel compressors. The opposite is true for case 3, where the parallel

Table 5.5: Work by compressor category [MWh]

Case	1	3
LT	594	594
MT	32	595
Parallel	800	86
Snow Storage	26	15
Sum	1452	1291

compressor is only utilized during heat recovery and the parallel/MT compressor rack is mostly utilized as MT compressors. In this case, gas is expanded down from 40 to 30 bar. This negative effect on the performance is inevitably dwarfed by the effect of less heat being recovered in case 3. The snow production represents the largest demand by a healthy margin. To further investigate the performance of the heat pump, it is therefore evaluated during hours with snow production and hours without. The results are presented in Table 5.6. Surprisingly, the

Table 5.6: Performance during and not during snow production

	During snow production		Not during snow production	
Case	2	4	2	4
Work [MWh]	1421	1254	31	26
Cooling [MWh]	2663	2663	89	89
Recovered heat [MWh]	3918	459	42	2
Recovered + rejected heat [MWh]	*3942*	*3793*	*116*	*113*
Cooling efficiency [-]	1.87	2.12	2.83	3.40
Heating efficiency [-]	2.76	0.37	1.32	0.06
Energy efficiency [-]	4.63	2.49	4.15	3.46
E.E. counting all available heat [-]	*4.65*	*5.14*	*6.61*	*7.77*

snow production has a different effect on the annual energy efficiency for cases 2 and 4. Case 2 records a higher efficiency during snow production, while case 4 records a drop in efficiency. To understand these numbers better, one must realize that heat is recovered when the storages drop below a pre-defined level, and it is arbitrary if that happens during snow production or not. Thus, it is of more relevance to evaluate either the cooling efficiency or the sum of the cooling, recovered *and* rejected heat divided by work. It is observed that both cases experience an increase in the cooling efficiency when snow is not produced. The same is true for the energy efficiency if all available heat is counted. The result would be an energy efficiency of 6.61 in case 2. Case 4 reports a higher efficiency, but the heat rejected in the gas cooler is not at a temperature level suitable for recovery. These results show that the snow production has a negative effect on the energy efficiency of the heat pump.

5.3.1 Seasonal performance

The demands of space heat, AC, snow storage refrigeration, as well as the gas cooler outlet temperature during heat rejection, are dependent on the ambient temperature. Therefore, the heat pump is expected to perform differently according to the season. In order to evaluate the seasonal performance, the operation of the heat pump's heat recovery is presented in the following pages, followed by a comparison of the energy efficiency during winter and summer.

Figures 5.6 and 5.7 show the available heat, recovered heat and total heat demand for both DHW and space heating for three winter and three summer days, respectively. The chosen winter days are the 1st to 3rd of January and the summer days are the 16th to 18th of June.

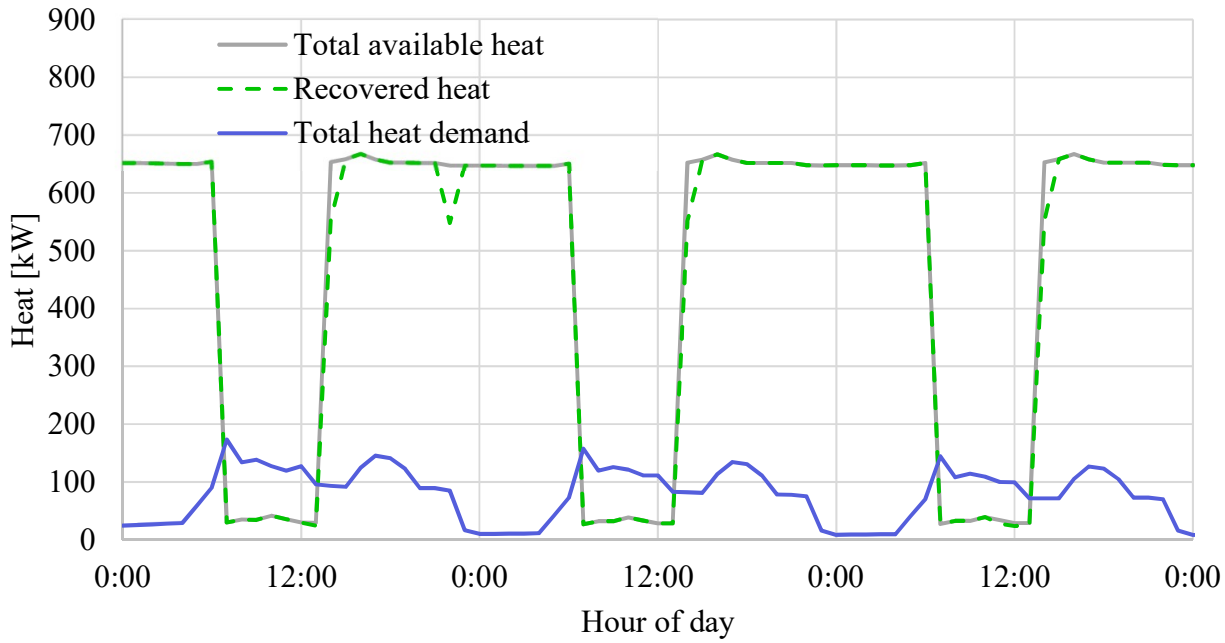

Figure 5.6: Available and recovered heat plotted with heat demand for three winter days, case 2

Figures 5.6 and 5.7 represent case 2, with snow production during hours of cheaper electricity and total heat recovery. A key difference between the graphs is a smaller heat demand during summer. Also, The effect of switching off the snow production when the AC demand exceeds 20 kW is seen during the third day in Figure 5.7. The small dips in recovered heat in Figure 5.6 are due to the space heat storage being charged. These dips are not present in Figure 5.7, as the space heat storage does not require charging during these summer days. Figures 5.8 and 5.9 show similar graphs, produced with data from case 3. The difference in heat recovery strategy

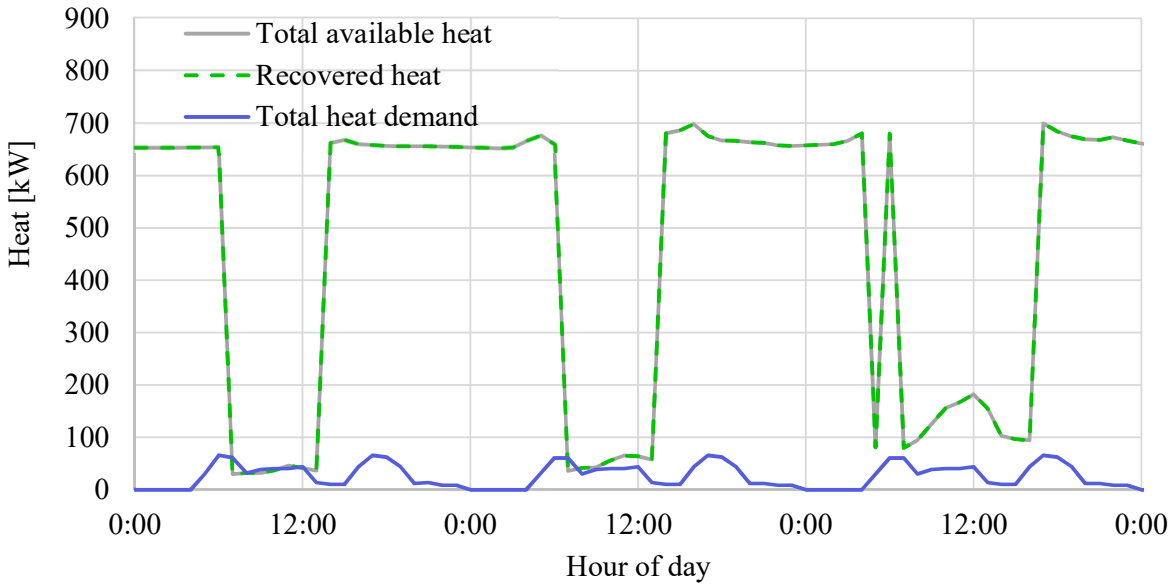

Figure 5.7: Available and recovered heat plotted with heat demand for three summer days, case 2

is highlighted here, as heat is recovered to a much smaller degree. Additionally, the effect of increasing the pressure during heat recovery can be seen in the small peaks in the grey line representing total available heat in Figure 5.8. In January, the gas cooler pressure lies typically around 50 bar. The increase in pressure to 100 bar during heat recovery is necessary to raise the temperature for DHW heat recovery but does not increase the amount of available heat more than 8-10 %.

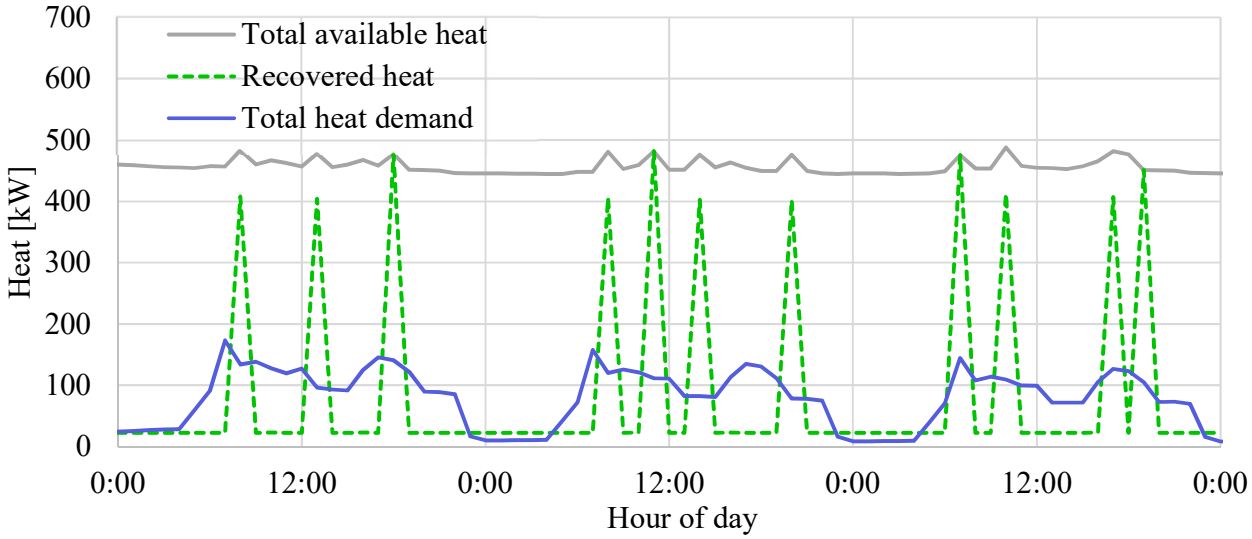

Figure 5.8: Available and recovered heat plotted with heat demand for three winter days, case 3

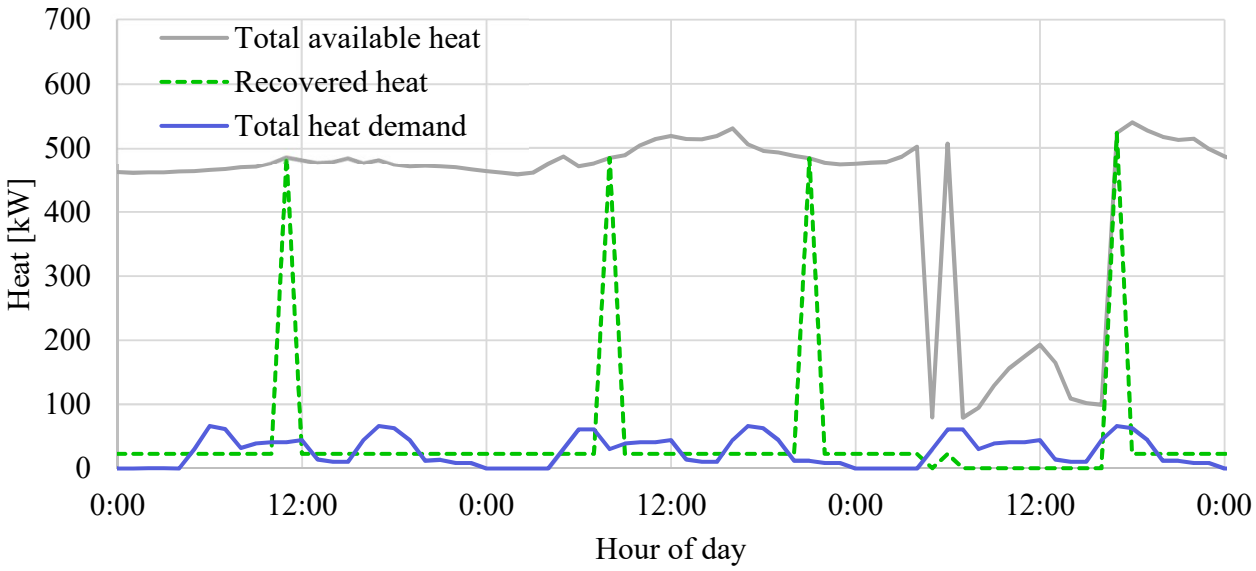

Figure 5.9: Available and recovered heat plotted with heat demand for three winter days, case 3

When the snow production stops due to a high AC demand during the third day in Figure 5.9, a jump in the available heat can be observed. This is due to the gas cooler pressure strategy, raising the pressure to restrict the gas fraction during high ambient temperatures, thus increasing the amount of heat rejected in the gas cooler. Figure 5.8 shows that the space heat storage is charged two or three times per day on a winter day, while the DHW storage is charged once or twice.

To calculate the seasonal performance during summer, April to September is defined as the summer season. Consequently, October to March is defined as the winter season. The calculated annual energy efficiency for the summer season is 4.61 for case 1. For the winter season, it is 4.63. More heat is rejected in the intercooler during summer, resulting in a slightly lower efficiency. In case 3, the annual energy efficiencies in summer and winter are 2.22 and 2.80, respectively. The difference in performance from winter to summer is larger due to heat only being recovered to cover the heat demand, which is larger in winter. To further understand how the seasons influence the performance, the energy efficiency for case 1 is plotted in Figure 5.10 for the same three winter and three summer days as in figures 5.6 to 5.9. Other than two types of exceptions, the performance during summer and winter is very similar. The first type of exception is during space heat storage charging when drops in energy efficiency can be seen on the graph representing winter. The other exception represents a more drastic increase in energy efficiency, during some summer hours. It occurs when the AC demand exceeds 20 kW and snow

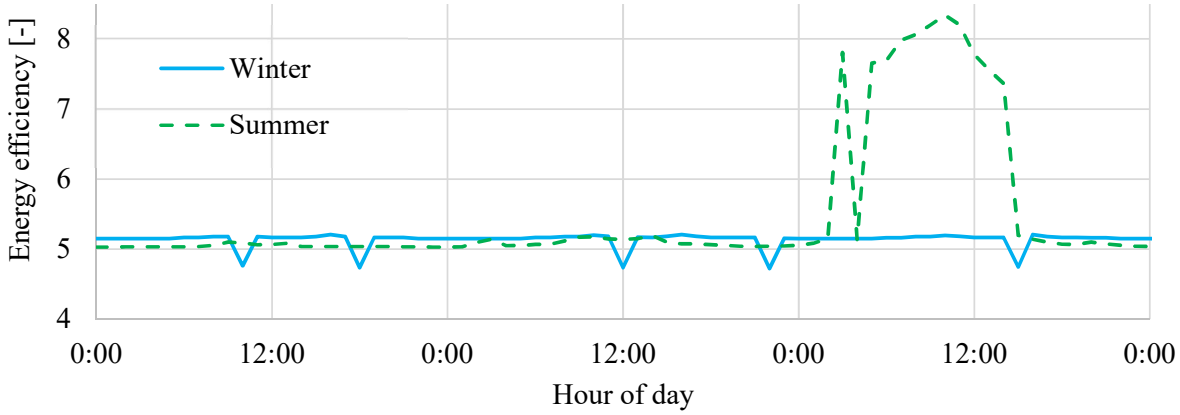

Figure 5.10: Energy efficiency for case 1 during three summer and three winter days

production switches off. During these hours, all heat is recovered for hot water production and the gas fraction in the intermediate pressure receiver is at 5 %. It has already been discovered that the snow production has a negative effect on the energy performance. These findings confirm that. They also indicate that the energy performance is at its highest when there is no snow production and the AC demand is high, yielding energy efficiencies up to 8. For case 3, the cooling efficiency is used to present the seasonal differences in system efficiency (Figure 5.11), as the arbitrarily distributed heat recovery makes the trends more difficult to read if the total energy efficiency was plotted. The cooling efficiency is generally higher in winter, due to a lower outlet temperature reached in the gas cooler. Jumps in the cooling efficiency occurs during summer, when the AC unit is active. The frequent dips in winter are due to heat recovery, when the high side pressure is raised, resulting in more compressor power demand.

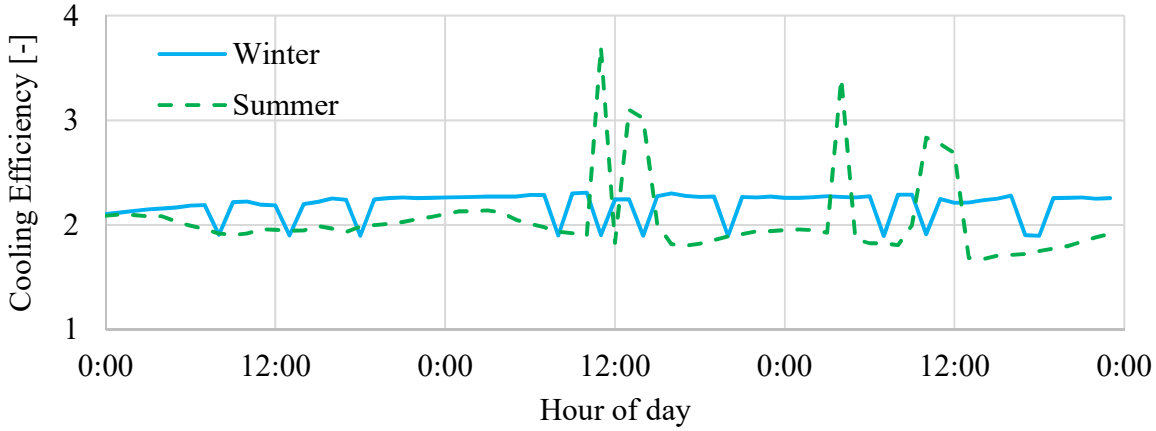

Figure 5.11: Cooling efficiency for case 3 during three summer and three winter days

5.3.2 DHW and space heat storages

After the heat pump model was set up, the storage sizes needed to be determined. As a way to guarantee DHW in case of a failure, the minimum size of the DHW storage is set to what is required to cover one day's DHW demand without being charged. Due to a large amount of available heat each day, neither of the cases need a larger DHW storage volume than one day's demand in order to never be emptied. The volume corresponding to one day's demand is 7527 L. There are commercially available DHW tanks in this size range.

Cold energy storage devices are not considered. Cooling represents the largest demand and the heat pump will, therefore, be operated to cover this. There are no periods where the heat pump produces excess refrigeration which could be stored.

The space heat demand has a much higher peak than the DHW demand. This results in a larger amount of energy needed to be stored in order to meet the peak demands during cold periods. The required space heat storage volume for each case is presented in Table 5.7, for water-only storing.

Table 5.7: Required space heat storage volume

Case	Storage volume [m^3]
1	30
2	100
3	30
4	100

The continuous access to surplus heat in cases 1 and 3 yields a smaller required storage volume. In cases 2 and 4, a larger storage is required to cover the space heat demand during the hours when snow production is switched off and the space heating demand is high. A 30 m^3 storage corresponds to a cube with sides 3.11 m, while each side of a 100 m^3 cube-shaped storage would be 4.64 m. PCM integration in the space heat storage is evaluated. One of the benefits of PCM is to reduce the necessary installed compressor capacity, as peak loads can be covered by the thermal storage. In this case, however, the heat pump's required capacity is determined by the refrigeration load, thus, implementing PCM in the hot thermal storage would not lower the necessary capacity of the heat pump. Integrating the S34 by PCM Products (2013) in the storage tanks resulted in an effective reduction in the storage volume requirement. The results for different PCM volume fractions of the total storage volume

are presented in Table 5.8.

Table 5.8: Required storage volumes with PCM integration in space heat storage

Cases 2 and 4	
PCM volume fraction [%]	Total storage volume [m^3]
10	67
20	51
30	41
40	34
50	30
60	26
Cases 1 and 3	
PCM volume fraction [%]	Total storage volume [m^3]
10	20
20	15
30	12

The results of the calculated reduction of storage volume were used to produce Figure 5.12, showing the reduction of storage volume according to PCM volume percentage. A 30 % volume fraction of PCM yields close to a 60 % reduction in total storage volume. In cases 2 and 4 this corresponds to a total storage volume of 41 m^3, whereas 12.3 m^3 are occupied by PCM.

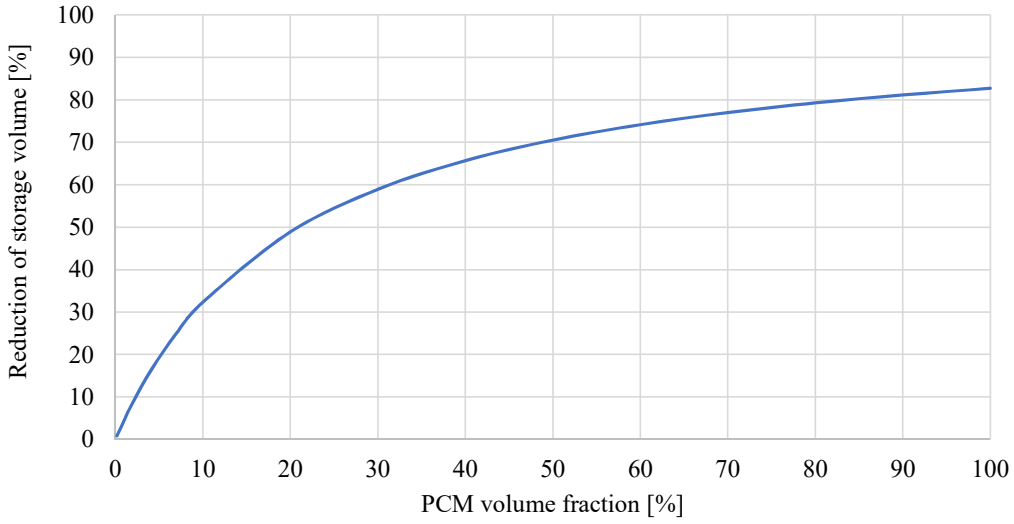

Figure 5.12: Reduction of storage space according to PCM volume fraction in the space heating thermal storage

5.3.3 Economical considerations

In deciding which case is most attractive, cost plays an important role. To compare the cases, the focus will be on operational costs and earnings from the sale of excess hot water.

Operational costs

The essential difference separating the even-numbered cases from the odd-numbered cases is the strategy to use hours of cheap electricity to do the most power-consuming activities. Cases 3 and 4 have a lower total electricity consumption than cases 1 and 2, as the high-side pressure is reduced to achieve a better energy efficiency. The costs of electricity consumption for the four cases are presented in Table 5.9. Shifting the bulk of the power demand to periods with cheaper

Table 5.9: Annual electricity cost for all cases at present prices and future scenario

	Case			
	1	2	3	4
Electricity consumption [MWh]	1452	1452	1291	1280
Annual cost, present prices [NOK]	1 402 477	1 388 621	1 247 434	1 225 289
Annual cost, future prices [NOK]	1 370 630	1 329 060	1 250 561	1 202 029

electricity does reduce the energy cost. With the present electricity prices, the electricity consumption cost is reduced by NOK 14 009 from case 1 to case 2. This corresponds to a reduction of 1.0%. Cases 1 and 2 have equal electricity consumption. Therefore, their comparison gives an accurate description of the effect of shifting the bulk of the power demand to periods with cheaper electricity. As the electricity consumption in case 4 is lower than in case 3, greater savings can be expected. With current prices, the cost of electricity is reduced by NOK 22 145 from case 3 to 4, a reduction of 1.8 %. In the future scenario, the reduction in cost is NOK 41 570 (3.0 %) from case 1 to 2 and 48 532 (3.8 %) from case 3 to 4. Also worth noting from these numbers is that the results of reducing the high-side pressure when the storages do not need charging correspond to annual savings of NOK 155 043 and 163 332 (Case 1/3 and 2/4, respectively). However, the earnings of hot water sale will influence the profitability of the cases, which will be treated later in this chapter.

Shifting the snow production to hours with cheaper electricity means that more snow is pro-

duced per operational hour. This causes the peak loads in power demand to increase, which will raise the power cost due to fees by the power companies. These fees were presented in Table 4.5. The monthly peak loads of the heat pump for all cases and total power fees are presented in Table 5.10. Considering today's electricity prices and comparing cases 1 and 2, it is seen that the

Table 5.10: Peak power demand in kW for each month and total power fees

	Case			
Month	1	2	3	4
Jan	176	240	174	238
Feb	176	240	174	238
Mar	177	241	173	238
Apr	178	242	177	242
May	184	249	206	278
Jun	183	248	215	301
Jul	184	248	223	303
Aug	184	248	225	304
Sep	182	245	193	262
Oct	178	242	180	246
Nov	176	241	174	237
Dec	176	240	174	238
Total power fee [NOK]	107 592	143 085	113 127	150 916

additional fee due to increased power, NOK 35 493, is greater than the savings of producing snow during hours of cheaper electricity, NOK 14 009. In the future scenario, however, the savings are NOK 41 570, greater than the fees. The total costs of power with the present prices are presented in Table 5.11. To evaluate the economical potential of selling hot water, the selling price must be

Table 5.11: Total power costs in NOK

	Case			
	1	2	3	4
Electricity consumption cost	1 402 477	1 388 621	1 247 434	1 225 289
Peak load fee	107 592	143 083	113 127	150 916
Total power cost	**1 510 069**	**1 531 704**	**1 360 561**	**1 376 205**

decided. For it to be beneficial for the customers, it must be cheaper than what it would cost to heat the water themselves. In the present scenario, the yearly mean price per kWh used in this thesis is NOK 0.97. It is assumed that the customers have access to the same city water, at 7 °C.

If they require water at a different temperature than the DHW produced by the CO_2 heat pump system, this could be achieved by configuring the heat recovery differently during production to sale. A lower temperature would yield more produced water with the available heat. Therefore, evaluating how much excess energy can be sold is done. A selling price of 0.4 NOK/kWh is assumed, as it is uncertain what energy source the different customers have. Cases 1 and 2 produce the same amount of excess heat. The calculated earnings are presented in Table 5.12. The available excess heat is enough to produce 112 239 L/day of water heated from 7 °C to 80 °C.

Table 5.12: Earnings from hot water sale

	Daily	Annually
Excess energy [MWh]	9.5	3 478
Earnings [NOK]	3 811	1 391 015

With delivery in tanks as proposed by Bergwitz-Larsen (2016), this correspond to 4.68 containers per day. The annual earnings from hot water sale are NOK 1 391 015, which corresponds to 92 % of the total power cost in case 1.

Necessary investments

The difference in investment cost between the cases will be discussed briefly. Integrating PCM in the space heat storage in cases 2 and 4 is evaluated. The price of the PCM S34 is £7 per kilo (PCM Products, 2018), and the density is 2 100 kg/m^3 (PCM Products, 2013). If the total space heat storage volume is 41 m^3 implemented with 12.3 m^3 of PCM, it would require 25 830 kg of the PCM. Hence, the material cost of the PCM is £180 810, which is NOK 1 949 888 as of June the 5th, 2018. This is only the material cost, thus a higher total cost of implementation is expected.

In cases 2 and 4, more compressors are needed due to a higher capacity demand. Additionally, heat exchangers in the heat recovery subsystems with a higher capacity are needed. Furthermore, the flake ice machine in cases 2 and 4 needs a higher production capacity. This will increase the investment cost in cases 2 and 4, compared to cases 1 and 3.

5.4 Parameter study

In further evaluation of the pump's performance, parameter studies of the high-side pressure during heat recovery and evaporation temperature in the flake ice machine are performed.

5.4.1 High-side pressure during heat recovery

In attempt to increase the performance of the heat pump, the high-side pressure is varied while still enabling heat recovery at the temperatures needed. A study on case 1 of was performed for pressures lower than 100 bar. The DHW supply temperature is 80 °C, therefore the high-side temperature needs to be above 85 °C due to the minimum temperature difference assumed in the heat exchangers. This proved to be true for a great reduction in the high-side pressure. At 75 bar, the refrigerant temperature is 86 °C and the CO_2 stays supercritical in the gas cooler. The total electricity consumption and annual energy efficiency for different high-side pressure values are plotted in Figure 5.13.

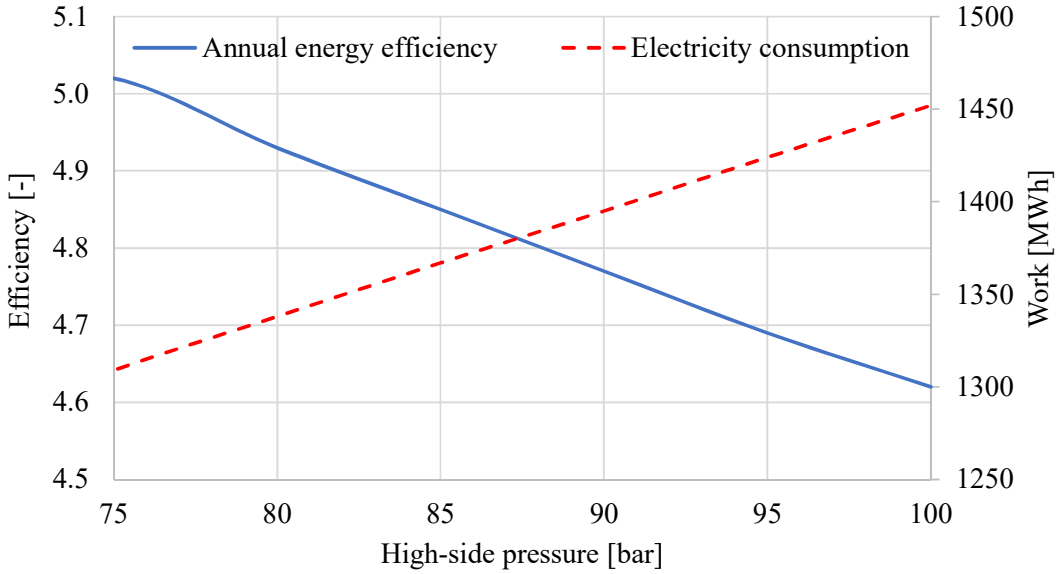

Figure 5.13: Annual energy efficiency and total electricity consumption at different high-side pressures

The result shows that the high-side pressure should be reduced to 75 bar. This will reduce the annual electricity consumption by 125 MWh and increase the annual energy efficiency from

4.62 to 5.02. With this reduction of the high-side pressure, the intermediate pressure should be 36 bar, according to Equation 4.10.

5.4.2 Evaporation temperature in the flake ice machine

Also in attempt to increase the performance of the heat pump, the different evaporation temperatures in the flake ice machine are evaluated. The governing equations for heat exchange are presented in section 4.3. If one assumes that the overall heat transfer coefficient remains unchanged, the mean logarithmic temperature difference can be reduced if the heat transfer area is increased, keeping the heat transfer constant. The LT evaporators in the supermarket are kept at the original temperature level, while the effects of varying the evaporating temperature and pressure in the flake ice machine are investigated. In this parameter study, the refrigerant discharge from the flake ice machine is compressed separately from the discharge from the LT evaporator. Figure 5.14 shows how the annual energy efficiency related to higher evaporating temperatures in the flake ice machine. The annual cooling efficiency is plotted to values on the vertical axis on the right-hand side.

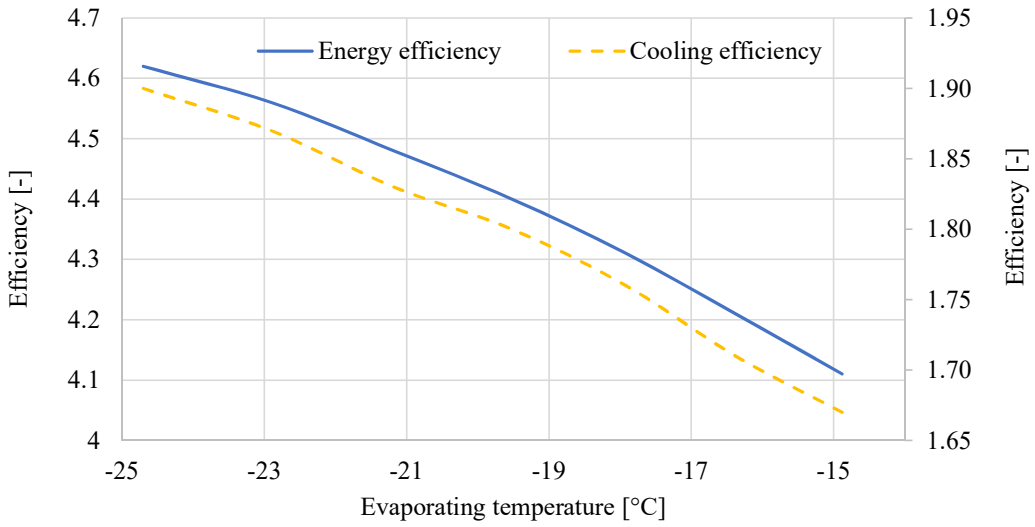

Figure 5.14: Energy efficiency and cooling efficiency at different evaporating temperatures in the flake ice machine

Surprisingly, the efficiencies drop when the evaporating temperature is increased. The explanation is that the compressors connected to the discharge of the flake ice machine already operate at a low pressure ratio. Increasing the suction temperature and pressure results in an even lower

pressure ratio. This results in such a low isentropic efficiency for the compressors that the average energy efficiency is reduced.

In further attempt to improve performance, a reconfiguration of the system is done by connecting the discharge of the flake ice machine evaporator to the suction of the snow storage compressor, operating at a much higher isentropic efficiency. With the proposed reconfiguration, the annual energy efficiency is calculated for different evaporating temperatures in the flake ice machine. The study is performed for case 1 and the results are plotted in Figure 5.15.

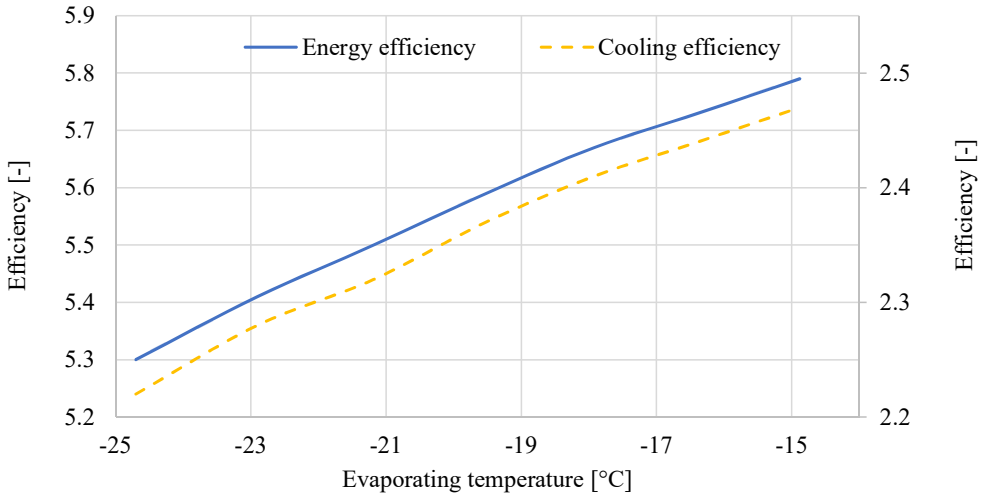

Figure 5.15: Energy efficiency and cooling efficiency at different evaporating temperatures in the flake ice machine with reconfiguration of the heat pump

In the case where the evaporation temperature is increased from −24.70 °C to −14.88 °C, the energy efficiency rises from 4.62 to 5.79. Cooling remains unchanged, while the annual electricity consumption is reduced by 23 % and the recovered heat is reduced by 6.4 %. Further details are presented in Table 5.13. In this case, the evaporation pressure is raised from 17 bar to 23 bar. A consequence is less hot water will be produced for sale, but as this is in abundance it is not considered a negative effect of the reconfiguration. In the cases where the evaporation temperature is lower than −14.88 °C, the discharge from the snow storage evaporators is expanded down to the discharge pressure of the flake ice machine before entering the suction of the snow storage compressors. This is not the ideal configuration regarding energy efficiency, but is seen in Figure 5.15 to be of little consequence for the results of the calculations, as the annual mass flow of CO_2 through the snow storage evaporator is only 3 % of the mass flow through the FID.

Table 5.13: Annual effect on heat pump performance by reconfiguration and increasing the evaporation temperature in the flake ice machine

Evaporation temperature [°C]	-24.70	-14.88
Electricity consumption [MWh]	1452	1115
Cooling [MWh]	2752	2752
Heat recovered [MWh]	3957	3702
Cooling efficiency [-]	1.90	2.47
Heating efficiency [-]	2.73	3.32
Energy efficiency [-]	4.62	5.79

5.5 Remarks and further discussion

Several assumptions were made in calculations of inputs to the model and the model itself. Snowmelt calculations will be discussed first, followed by the building simulations and finally simulations of the heat pump.

In the calculation of received radiation on the cross-country slope with the proposed shading installation, it is assumed that no direct solar radiation enters the snow layer. With only roof shading, direct radiation can enter the snow layer, especially at high latitudes. A shading construction with both a roof and a wall to shade primarily towards the south should be considered. This would require detailed modeling of the entire cross-country circuit and its design, which is considered outside the scope of this work. In the calculation of the snowmelt, coefficients from a study on a glacier in northern Sweden were used. These coefficients are expected to be different for a low-land location in central Norway. Comparing the results with experimental data suggests that the calculated snowmelt is slightly low. Precipitation is not accounted for in evaluation of the snow demand, neither as snow nor as rain. Natural snowfall reduces the snow demand, while rain is expected to increase the snowmelt, and thus, snow demand. Therefore, not considering precipitation is expected to not influence the annual snow demand much, as it both increases and decreases the snow demand. However, it will reduce demand in winter and increase demand in summer, which results in a larger volume requirement for the snow storage.

The cooling demand of the snow storage building is modeled as the transmission heat loss through the walls, roof and floor. The real cooling demand will be higher due to infiltration

losses in the summer and potential internal heat gains from lights and other equipment used to collect snow. Infiltration losses will be increased when snow is collected for distribution and the storage doors are opened. The calculated cooling demand for the snow storage building is very likely lower than the actual demand of a snow storage building of this size. In the simulation of the hotel, interior walls and surfaces were not accounted for. Therefore, the thermal constant of the building is low and the thermal responsiveness high. This means that the simulated building cools down and heats up faster than it would in real life. Additionally, hotels of this size normally have conference rooms and possibly a spa area. A conference room would require refrigeration from the AC when occupied, increasing the total refrigeration demand. The refrigeration demand of the hotel is very low compared to other hotels, and the validity of this particular result is therefore questionable. A spa section is expected to increase the DHW demand. The hotel's DHW demand is solely based on values from building standards.

cases 3 and 4, where excess heat is not sold, do not compete well with cases 1 and 2 in terms of annual energy efficiency and profitability, due to a lot of heat being rejected to the ambient. However, if heat cannot be sold, their internal comparison is of relevance.

Creating the heat pump model in Excel proved to bring certain challenges. The problem of circular references occurred during modeling of the high-side while trying to model flow in the gas cooler, space heat recovery and DHW recovery at the same time. This lead to simplifying the model into charging only one thermal storages at the time. Interestingly, this exact strategy was proposed by Smitt and Hafner (2018) to reduce the amount of heat rejected in the gas cooler of a centralized energy system for a hotel. Due to the 25 °C return temperature in the space heat subsystem in this work, some heat needs to be rejected by the air-to-gas gas cooler with this configuration as well, in order to achieve the desired temperature out of the gas cooler. This additional cooling of the refrigerant is found to reduce the annual compressor work by 9000 kWh. Adding the heat rejected in the intercooler when there is no space heat demand, 2.5 % (102 000 kWh) of the available heat is rejected compared to 9.0 % (ca. 55 768 kWh) in the system modeled by Smitt. The space heat recovery unit and DHW recovery unit are connected in series in the model but operated as if they were connected in parallel, made possible by bypasses and valves. With this configuration, two stages of DHW heating is not needed, and one heat exchanger could be sufficient for DHW heating, if its capacity is high enough.

The heat pump was initially modeled with a suction gas heat exchanger, but the problem of circular references occur here as well. It was finally modeled without it and also modeled without superheating out from the evaporators.

The equation used for calculating the isentropic efficiency of the compressors yields a very low efficiency for low-pressure ratios. Reducing the discharge pressure of the LT compressors when the MT compressors are in use was considered, but the work input of the LT was found to increase even though the pressure ratio was decreased from 2.35 to 1.76. This corresponds to compression from 17 bar to 40 bar and 30 bar, respectively. In line with these results, the reconfiguration from a two-stage to a one-stage compression done in the parameter study of the evaporation temperature in flake ice machine suggests that a one-stage compression yields a better annual energy efficiency than a two-stage compression. However, this requires further investigation of the necessary heat transfer capacity in the FID to produce flake ice at higher evaporation temperatures, should it be implemented. Lowering the high-side pressure during heat recovery was also found to increase efficiency. The temperature fit in the gas cooler should be evaluated further before implementing this configuration.

Not considering pump work and pressure drop in the heat pump model will lead to a lower power demand and thus better performance values. The calculated energy efficiencies are therefore higher than real values will be.

The PCM implementation is considered with a low level of detail. Evaluation of the time it takes to heat up the water during phase change should be done in order to reveal if a storage with the suggested PCM volume fraction can provide water at the desired temperature quickly enough.

6. Summary and conclusion

In this thesis, state-of-the-art supermarket refrigeration systems are introduced along with the motives for reintroducing CO_2 as a refrigerant. A presentation of heat pump systems for hotels follows, including concepts to increase energy efficiency and reduce costs. Then, snow production methods both dependent and independent of the ambient temperature are explained. This is followed by a brief presentation of snow storage methods and a review of snow demands for all year cross-country slopes, which includes a suggested method to calculate snowmelt.

A simulation model of a transcritical R744 heat pump intended to cover several thermal demands is set up. These demands are found by calculation or simulation and include the DHW demand for a supermarket and a hotel, the space heating and cooling demand for a hotel, refrigeration of food and beverages for a supermarket, temperature independent snow production for an all year cross-country slope and refrigeration for a snow storage building. The R744 heat pump is designed based on the principle of a booster system with parallel compression. Heat recovery for space heating and DHW are implemented in the high-pressure side of the system, in addition to heat recovery from an intercooler at the discharge of the LT compressors for space heating purposes. Operation strategies for heat recovery and heat rejection are planned.

The annual snow demand for the cross-country slope is calculated to be 80 406 m^3, which requires a snow storage building capable of storing 34 000 m^3 of produced snow to meet the demand during summer. With a suggested shading construction of the cross-country slope, the annual snow demand is reduced by 42 % to 47 036 m^3 which requires a 20 000 m^3 snow storage. Simulation of the 7350 m^2 hotel yields a space heat demand of 32.47 kWh/m^2/year and a cooling demand of 3.08 kWh/m^2/year. The space heat demand is similar to another hotel in the region, while the cooling demand is found to be much smaller. In the simulation of the heat pump's performance, four cases are defined. In cases 1 and 2, heat is recovered both to cover the heat demands of a hotel and supermarket and to produce hot water for sale. In cases 3 and 4, heat is only recovered to cover the supermarket's and the hotel's heat demands. Cases 2 and 4 are modeled to produce snow during hours when the spot price of electricity is low. Cases 1 and 3 are modeled with even snow production. Cases 3 and 4 records annual energy efficiencies of 2.50 and 2.52, respectively. Due to more heat being recovered, cases 1 and 2 perform better.

Both cases record an annual energy efficiency of 4.62.

The system is found to perform better without snow production. Therefore, a parameter study of the evaporation temperature in the flake ice machine is performed in attempt to improve the heat pump's performance. Raising the temperature by 10 K and reconfiguring the system to accommodate the temperature rise resulted in an increase of the annual energy efficiency from 4.62 to 5.79 in case 1. A parameter study of the high-side pressure during heat recovery is also performed. The results indicate that reducing the high-side pressure increases the annual energy efficiency. A reduction from 100 bar to 75 bar increases the annual energy efficiency from 4.62 to 5.02. Both of these reconfigurations are recommended for the system, however further investigation should be done to prove their feasability.

To further evaluate the cases, operational costs are compared. The results show that the effect of shifting snow production is marginal, as electricity consumption is reduced by only 1 %. The corresponding savings are found to be less than the increase in fees charged by the power companies for peak loads. Cases 2 and 4 also require larger thermal storages. Integration of PCMs is considered but found not to be economically attractive. On the basis of these two considerations, cases 2 and 4 are found not to be competitive with cases 1 and 3. Annual operational costs in case 3 are NOK 149 508 lower than in case 1, but no hot water is sold. The estimated annual earnings from the sale of produced hot water are NOK 1 391 015, making case 1 the preferred case, with case 3 as the next best option. However, costs of distributing the water to be sold are not taken into consideration and are expected to bring cases 1 and 3 closer in regards to economic potential.

6.1 Suggestions for further work

- Investigate the possibility to use the excess heat for a local heating network in the neighborhood surrounding Granåsen
- Estimate the costs of distributing produced hot water to customers by container transportation
- Investigating the effect of connecting the discharge of the snow storage compressors to

the parallel compressors with the reconfiguration done in the parameter study

- To further take advantage of the cheaper electricity prices, modify the model to calculate the economic advantage of only charging the storage during night-time to reduce electricity consumption by the compressors during the day, in cases 3 and 4, when the high-side pressure can be optimized
- At a high-side pressure of 75 bar, perform a parameter study of the intermediate pressure to find its optimal value
- Evaluate the temperature fit in the gas cooler for heat recovery to DHW and space heating at 75 bar
- Investigate the consequence of raising the evaporation temperature in a flake ice machine with regards to necessary FID area and production capacity
- Implement and evaluate the potential of drainage water heat recovery
- Include pressure drop and pump work in the heat pump model
- Evaluate the cooling demand of the snow storage building using a more sophisticated method

Bibliography

Alfa Laval (2016). *Alfa Laval AXP52 Product Leaflet*. Retrieved from https://www.alfalaval.ca/products/heat-transfer/plate-heat-exchangers/brazed-plate-heat-exchangers/axp/, Accessed 15 June 2018.

Alfa Laval (2018). *Alfa-V VXD Product Leaflet*. Retrieved from https://www.alfalaval.com/products/heat-transfer/finned-coil-air-heat-exchangers/finned-coil-gas-coolers/Alfa-V-VXD/, Accessed 29 May 2018.

Arias, J. (2005). *Energy Usage in Supermarkets - Modelling and Field Measurements*. Doctoral thesis, Royal Institute of Technology, KTH.

Baek, N. C., Shin, U. C., and Yoon, J. H. (2005). A study on the design and analysis of a heat pump heating system using wastewater as a heat source. *Solar Energy*, 78(3):427–440.

Bédécarrats, J. P., David, T., and Castaing-Lasvignottes, J. (2010). Ice slurry production using supercooling phenomenon. *International Journal of Refrigeration*, 33(1):196–204.

Bergwitz-Larsen, K. (2016). *Energy Efficient and Environmental Friendly Snow Production Equipment at Ambient Temperatures above 0 ° C*. Project assignment, Norwegian University of Science and Technology (NTNU).

Bergwitz-Larsen, K. (2017). *Energy Efficient and Environmental Friendly Snow Production by Refrigeration systems*. Master's thesis, Norwegian University of Science and Technology (NTNU).

BITZER (2018). *Ecoline+ Transcritical*. Retrieved from: https://www.bitzer.de/gb/en/reciprocating-compressors/ecoline-1-transcritical/ Accessed 28 May 2018.

Chow, T. T., Bai, Y., Fong, K. F., and Lin, Z. (2012). Analysis of a solar assisted heat pump system for indoor swimming pool water and space heating. *Applied Energy*, 100:309–317.

Clulow, M. G. (2006). Indoor snowmaking. *ASHRAE Journal*, 48(7):18–23.

Danfoss (2016). *Norwegian supermarket with Danfoss CO_2 heat recovery solution receives award*. page 2016, Retrieved from: http://www.danfoss.com/newsstories/cf/norwegian-supermarket-with-danfoss-co2-heat-recovery-solution-receives-award/?ref=17179879839#/ Accessed 17 February 2018.

Dieseth, J.-B. R. (2016). *Snow production equipment at ambient temperatures above zero*. Master's thesis, Norwegian University of Science and Technology (NTNU).

Eikevik, T. M., Bredesen, A. M., and Nekså, P. (2017). Compendium tep4255. Trondheim: NTNU.

Elbel, S. and Hrnjak, P. (2004). Effect of internal HX on performance of transcritical CO_2 systems with ejector. *International Refrigeration and Air Conditioning Conference at Purdue*, R166:1–8.

Emerson Climate Technologies (2010). *Refrigerant Choices for Commercial Refrigeration - Finding the Right Balance*. Retrieved from http://www.emersonclimate.com/europe/Documents/Resources/TGE124_Refrigerant_Report_EN_1009.pdf, Accessed 02 March 2018.

Emerson Climate Technologies (2015). *Commercial CO2 Refrigeration Systems - Guide for Subcritical and Transcritical CO_2 Applications*. Retrieved from http://www.emersonclimate.com/en-us/Market_Solutions/By_Solutions/CO2_solutions/Documents/Commercial-CO2-Refrigeration-Systems-Guide-to-Subcritical-and-Transcritical-CO2-Applications.pdf, Accessed 03 March 2018.

Engineering ToolBox (2001). [online]. Retrieved from https://www.engineeringtoolbox.com, Accessed 24 April 2018.

European Union (2016). *EU legislation to control F-gases*. In *Climate Action*, Retrieved from: https://ec.europa.eu/clima/policies/f-gas/legislation_en#top-page, Accessed 22 February 2018.

Fauve, M. and Rhyner, H. U. (2004). Physical Description of the Snowmaking Process using the Jet Technique. In Bartelt, P., Adams, E., Christen, M., Sack, R., and Sato, A., editors, *Snow Engineering V: Proceedings of the Fifth International Conference on Snow Engineering, 5-8 July 2004, Davos, Switzerland.*, pages 215–218. A.A. Balkema Publishers.

Gisselman, F. and Cole, S. (2016). Samhällsekonomisk analys av snötillverkning i Östersund.

Gjerland, M. and Olsen, G. Ø. (2014). Snøproduksjon og snøpreparering. Retrieved from: https://www.regjeringen.no/no/dokumenter/Veileder—Snoproduksjon-og-snopreparering-V-0965/id764367/, Accessed 27 February 2018.

Graham, J., Johnston, W., and Nicholson, F. (1993). *Ice in fisheries*. FAO Fisheries Technical Paper. No. 331. Rome, FAO.

Graver, S. (2016). *Akkumulatortank skal gi mer miljøvennlig avfallsvarme i Trondheim*. Retrieved from: http://www.energi.no/akkumulatortank-skal-gi-mer-miljovennlig-avfallsvarme-i-trondheim Accessed 1 May 2018.

Grünewald, T., Wolfsperger, F., and Lehning, M. (2018). Snow farming: Conserving snow over the summer season. *Cryosphere*, 12(1):385–400.

Hafner, A., Poppi, S., Nekså, P., Minetto, S., and Eikevik, T. M. (2012). Development of Commercial Refrigeration Systems with Heat Recovery for Supermarket Building. *10th IIR Gustav Lorentzen Conference on Natural Refrigerants*, (January 2016).

Hägg, C. (2005). *Ice Slurry as Secondary Fluid in Refrigeration Systems*. Number November. Stockholm: KTH.

Han, Y. (2017). *Energy-efficient Supermarket CO2 Compressor Pack with Ejectors*. Master's thesis, Norwegian University of Science and Technology (NTNU).

Hanssen-Bauer, I., Førland, E., and Haddeland, I. (2015). Klima i Norge 2100. Kunnskapsgrunnlag for klimatilpasning oppdatert i 2015. *Norwegian Environment Agency*, (2):204.

Hanssen-Bauer, I., Førland, E., Haddeland, I., Hisdal, H., Mayer, S., Nesje, A., Nilsen, J., Sandven, S., Sandø, A., Sorteberg, A., and Ådlandsvik, B. (2009). Klima i Norge 2100. *M-406 | 2015 Klima*, (2):204.

Hock, R. (1999). A distributed temperature-index ice- and snownelt model including potential direct solar radiation. *Journal of Glaciology*, 45(149):101–111.

Incropera, F., Dewitt, D., Bergman, T., and Lavine, A. (2013). *Principles of Heat and Mass Transfer*. John Wiley & Sons Singapore Pte Ltd, 7th edition.

Johnsen, A. H. (2013). *Optimal drift av energisystem i et supermarked*. Master's thesis, Norwegian University of Science and Technology (NTNU).

Katsumi, H. (2006). Technology and market development of CO2 heat pump water heaters (ECO CUTE) in Japan. *IEA Heat Pump Centre Newsletter*, 24(3):12–16.

Kleven, M. H. (2012). *Analysis of Grey-water Heat Recovery System in Residential Buildings*. Master's thesis, Norwegian University of Science and Technology (NTNU).

Lam, J. C. and Chan, W. W. (2003). Energy performance of air-to-water and water-to-water heat pumps in hotel applications. *Energy Conversion and Management*, 44(10):1625–1631.

Lintzén, N. (2016). *Properties of Snow with Applications Related to Climate Change and Skiing*. Doctoral thesis, Luleå University of Technology.

Moran, M. J., Shapiro, H. N., Boettner, D. D., and Bailey, M. B. (2012). *Principles of Engineering Thermodynamics*. John Wiley & Sons (Asia) Pte Ltd.

Mullem, J. a. V., Garen, D., and Woodward, D. E. (2004). Part 630 - Hydrology. In *National Engineering Handbook*, chapter 11, pages 11–21.

Müller, O. B. (2015). *Får kritikk for tidlig snøproduksjon*. Retrieved from: https://www.gd.no/nyheter/reiseliv/ringsaker/far-kritikk-for-tidlig-snoproduksjon/s/5-18-165116, Accessed 27 February 2018.

Naturnvernforbundet (2016). *Klimaendringer i Norge (2016)*. Retrieved from \url{https://naturvernforbundet.no/__cparticleid__16032/, Accessed 02 March 2018.

Nekså, P., Walnum, H. T., and Hafner, A. (2010). CO2 - A Refrigerant From the Past With Prospects of Being One of the Main Refrigerants in the Future. *9th IIR Gustav Lorentzen Conference*.

Neveplast.com (2016). *Product information of NP50: Nordic Skiing*. Retrieved from: http://www.neveplast.com/prodotti/np50/, Accessed 02 March 2018.

Ni, L., Lau, S. K., Li, H., Zhang, T., Stansbury, J. S., Shi, J., and Neal, J. (2012). Feasibility study of a localized residential grey water energy-recovery system. *Applied Thermal Engineering*, 39:53–62.

Nkwetta, D. N. and Haghighat, F. (2014). Thermal energy storage with phase change material—A state-of-the art review. *Sustainable Cities and Society*, 10:87–100.

Nord Pool (2017). *Historical Market Data*. Retrieved from https://www.nordpoolgroup.com/historical-market-data/, Accessed 13 April 2018.

Norwegian Ministry of Petroleum and Energy (2017). *Kraftmarkedet*. Retrieved from https://energifaktanorge.no/norsk-energiforsyning/kraftmarkedet/, Accessed 17 June 2018.

Paul, J. J. (2003). Concept of Operating Indoor Skiing Halls with " Binary Snow " as a Snow Substitute. *Main*, pages 1–8.

PCM Products (2013). *Type of Phase Change Materials*. Retrieved from: http://www.pcmproducts.net/Phase-Change-Material-Solutions.htm Accessed 11 May 2018.

PCM Products (2018). RE: Mail correspondence. Type to Birkeland, J.

Ratnik Industries (2014). *Sky Giant III*. Retrieved from: http://ratnik.com/product/sky-giant-iii/ Accessed 28 February 2018.

Selvnes, H. (2017). *Energy distribution concepts for Urban Supermarkets including energy hubs*. Master's thesis, Norwegian University of Science and Technology (NTNU).

Smitt, S. M. (2017). *Integrated Energy concepts for high performance hotel buildings*. Master's thesis, Norwegian University of Science and Technology (NTNU).

Smitt, S. M. and Hafner, A. (2018). Integrated energy concepts for high performance hotel buildings. Proceedings of the 13th IIR Gustav Lorentzen Conference on Natural Refrigerants, Valencia, Spain, IIF/IIR.

Snowell Ice Systems (2016). *20T/day flake ice drum*. Retrieved from: http://www.snowell-icemachine.com/products_detail/productId=75.html, Accessed 28 February 2018.

Spandre, P., François, H., George-Marcelpoil, E., and Morin, S. (2016). Panel based assessment of snow management operations in French ski resorts. *Journal of Outdoor Recreation and Tourism*, 16(February):24–36.

StandardNorge (2012). NS 3701:2012 Kriterier for passivhus og lavenergibygninger - yrkesbygninger.

StandardNorge (2016). SN/TS 3031:2016 Bygningers energiytelse - Beregning av energibehov og energiforsyning.

Strand, R. (2014). Optimalisering av snølagring om sommeren. Technical report, Høgskolen i Gjøvik.

Tasiou, S. (2014). *MHI CO2 hot water heat pumps reduce central London hotel costs by 40%*. Retrieved from: http://www.r744.com/articles/5370/mhi_co_sub_2_sub_hot_water_heat_pumps_reduce_ce ntral_london_hotel_costs_by_40, Accessed 23 February 2018.

Tassou, S. A., Ge, Y., Hadawey, A., and Marriott, D. (2011). Energy consumption and conservation in food retailing. *Applied Thermal Engineering*, 31(2-3):147–156.

The Linde Group (2017). Managing refrigerants the responsible way. *The Linde Group*.

TrønderEnergi Nett (2018). *Nettleie for bedriftskunder fra 1. januar 2018*. Retrieved from: https://tronderenerginett.no/nettjenester/vilkar-og-nettleie/nettleie-bedrift-2018 Accessed 6 May 2018.

Trondheim Kommune (2018). *Granåsen 2023*. Retrieved from https://www.trondheim.kommune.no/granasen-2023group-2, Accessed 28 June 2018.

TrønderEnergi Marked (2018). Phone correspondence. to Birkeland, J.

United Nations Environmental Program (2016). The Kigali Amendment to the Montreal Protocol: HFC Phase-down, OzonAction Fact Sheet. In *28th Meeting of the Parties to the Montreal Protocol, 10-14 October, 2016, Kigali, Rwanda*, pages 1–7, Nairobi, December 2016. Retrieved from http://web.unep.org/africa/news/kigali-amendment-montreal-protocol-another-global-commitment-stop-climate-change Accessed 13 February 2018.

Vagle, B. H. (2016). *Utilization of surplus heat from snow producing machines*. Master's thesis, Norwegian University of Science and Technology (NTNU).

Van Orshoven, D., Klein, S. A., and Beckman, W. A. (1993). An Investigation of Water as a Refrigerant. *Journal of Energy Resources Technology*, 115(4):257.

Şahin, C. D., Coşkun, T., Gülhan, Ö., Arsan, Z. D., and Akkurt, G. G. (2016). Aalborg Universitet CLIMA 2016 - proceedings of the 12th REHVA World Congress Heiselberg , Per Kvols. *CLIMA 2016 - proceedings of the 12th REHVA World Congress*.

Appendices

A. Risk Assessment

NTNU HSE	Hazardous activity identification process	Prepared by	Number	Date
		HSE section	HMSRV2601E	09.01.2013
		Approved by		Replaces
		The Rector		01.12.2006

Unit: Energy and Process Engineering **Date:** 05.02.2018

Line manager: Olav Bolland

Participants in the identification process (including their function)**:**

Short description of the main activity/main process: Master project for student Jostein Birkeland. Integrated energy system for Granåsen Snow Arena, Hotel and Supermarket.

Is the project work purely theoretical? (YES/NO): YES *Answer "YES" implies that supervisor is assured that no activities requiring risk assessment are involved in the work. If YES, briefly describe the activities below. The risk assessment form need not be filled out.*

Signatures: *Responsible supervisor:* *Student:* Jostein Birkeland

ID nr.	Activity/process	Responsible person	Existing documentation	Existing safety measures	Laws, regulations etc.	Comment

B. Draft Scientific Paper

INTEGRATED ENERGY SYSTEM FOR GRANÅSEN SNOW ARENA, HOTEL AND SUPERMARKET

Jostein Birkeland, Armin Hafner
Norwegian University of Science and Technology,
Kolbjørn Hejes vei 1D, 7491 Trondheim Norway
josteibi@stud.ntnu.no, armin.hafner@ntnu.no

ABSTRACT

Large investments will soon be made to further develop the skiing area around Granåsen in Trondheim, including a building comprised of a supermarket in the basement and a hotel on the floors above. Centralized heat pumping units are common in supermarkets, but not widely applied in hotels. Developing such systems to cover the thermal demands of multiple buildings can reduce their combined environmental footprint and reduce their cost of ownership.

This work aims to describe how a centralized heat pumping unit should be designed to cover all major heating and cooling demands of a supermarket and a hotel, in addition for snow production for a 1 km all-year cross-country slope. Relevant thermal demands, including temperature independent snow production, are obtained before a numerical model of the heat pump is created and used to perform annual simulations of the energy system.

The annual average energy efficiency of the system is found to be 4.62, with 8 times more available heat than the total heating demand of the building. A proposed shading installation for the cross-country slope is calculated to reduce the annual snow demand of the cross-country slope by 42 %. Optimizing the high-side pressure and increasing the evaporation temperature in the snow machine can increase the efficiency of the heat pump to 5.02 and 5.79, respectively. These values agree with similar CO_2 systems, reaching higher efficiencies than traditional heat pump systems in hotels. Recovering useful energy from centralized systems in urban areas can benefit the surrounding community while reducing the areas' total environmental footprint.

Keywords: Transcritical CO_2 heat pump, commercial refrigeration, integrated energy system, temperature independent snow production, snow storage, phase change material

1. INTRODUCTION

Days with snow conditions in central Norway is expected to drop from 150 to 70-80 during this decade (Hanssen-Bauer et al., 2009). One method to ensure skiing conditions near cities in the future is temperature independent snow production (TIS), which has been criticized by the media for not being environmentally friendly, thus adding to the very problem it is trying to overcome (Müller, 2015). This has led to research on making this type of snow production more environmental friendly, for example by integrating different snowmaking technologies with combined refrigeration and heat recovery systems (Dieseth, 2016; Bergwitz-Larsen, 2017). The research focuses on using natural refrigerants such as CO_2, ammonia and hydrocarbons, motivated by regulations aiming to phase out refrigerants with high GWP and ODP values, (UNEP, 2016; European Union, 2016). CO_2 has a low GWP and ODP value, is non-flammable and non-toxic and is very well suited for heating of domestic hot water (DHW), which makes it the preferred refrigerant for such systems.

CO_2 heat pump systems have been studied recently both for hotel and supermarket applications (Smitt, 2017; Selvnes, 2017). This paper seeks to develop the design of a combined heat pump and refrigeration system for a supermarket, a hotel and for snow production. The design is based on a transcritical CO_2 booster system with parallel compression. An important aspect of the system design is to recover the available heat from the refrigeration and snow production, in contrast to commercially available TIS machines, where this heat is rejected to the ambient. The following section contains descriptions of how the specific thermal loads are found and assumptions made in the development of the heat pump model used for an annual simulation of the system with an hourly resolution.

2. METHODOLOGY

The method to calculate the different demands which the centralized refrigeration unit will cover are obtained before its design is presented.

2.1. Snow Demand and Production

The annual snow demand is estimated as the snowmelt from the cross-country slope plus an assumed 2000 m^3 lost in distribution. The snowmelt is calculated hourly using a degree-day method developed by Hock (1999). The method requires air-temperature and irradiance data, which is obtained from the climate database Meteonorm. To reduce the snow demand, especially during summer, a shading construction is proposed (Fig. 1). The calculated view factor of the shading construction is 0.62. Once the annual snow demand is estimated both with and without shading, the refrigeration required by the flake ice machine to produce the required snow is calculated. Flake ice machines produce dry, subcooled ice. The evaporation temperature in the flake ice drum (FID) is often modeled as -30 °C, cooling the ice to -5 °C. The supply water is set to a constant value of 7 °C. Consequently, the refrigeration load per unit mass required by the flake ice machine is estimated as the heat transfer necessary to cool water 7 K, freeze it and cool ice 5 K.

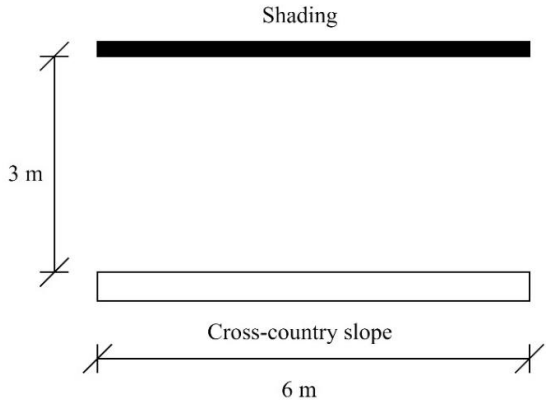

Figure 1: Cross section of the shading construction

2.2 Building Modeling and Load Estimations

A model of the proposed building was needed to estimate its heating and cooling demands. The footprint of the supermarket is 1050 m^2, with the hotel occupying the floors above. The supermarket is in a basement location, therefore modeled without an AC demand. The heat demand of the supermarket is covered by heat rejected from stand-alone refrigeration units, as is common practice for supermarkets at this latitude. A simulation model of the 200-room hotel building envelope is created in the building simulation software *SIMIEN*[1]. Each floor of the hotel has the same floor area as the supermarket. Four floors are needed to accommodate all facilities and rooms. The building is expected to meet the Norwegian Standard for commercial passive houses NS3701:2012 (Standard Norway, 2012). The hotel is simulated as a single temperature zone with 18-hour operation, as specified in the standard. The supermarket adjacent to the bottom floor is modeled to hold 20 °C during summer and 16 °C during winter. To obtain an hourly resolution of the DHW heating demand, estimated values were collected from Energy Performance of Buildings SN/TS 3031:2016 (Standard Norway, 2016). Additionally, the cooling demand of a snow storage building capable of storing a maximum of 21 000 m^3 snow is estimated as the transmission heat loss through the snow storage building envelope. The thermal demands of buildings to be covered by the centralized heat pump are all found smaller than the required refrigeration to produce snow (Fig. 2.)

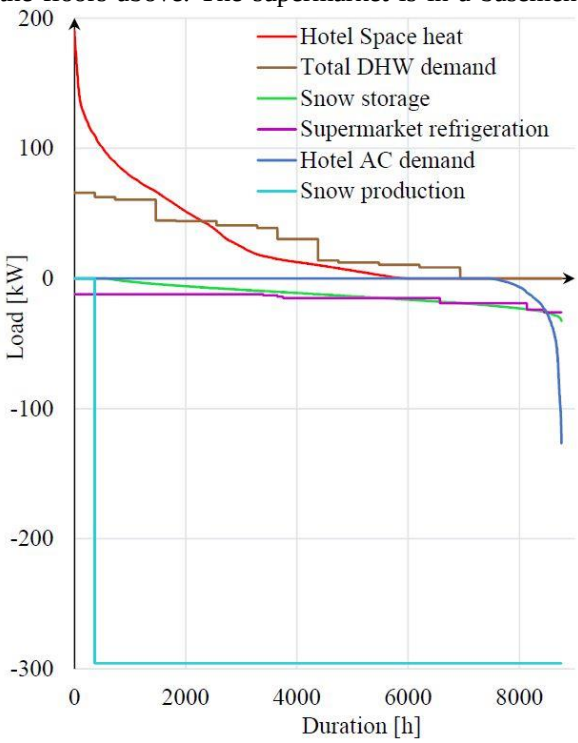

Figure 2: Load-duration curves for snow production and thermal demands of the buildings.

[1] Building energy simulation software by *ProgramByggerne*, http://www.programbyggerne.no/ .

2.3 Energy System and Heat Pump Design

Before a numerical model of the energy system was created in Microsoft Excel, the heat pump design had to be determined. The heat pump is operated according to the cooling demand, recovering heat from the high-side to be stored in thermal energy storage tanks. The gas cooler is designed with three heat exchangers in series for heat recovery to space heating and DHW. An air-to-gas heat exchanger is connected in parallel for heat rejection to the ambient, if necessary (Fig. 3.). The energy storage tanks are charged when the contained energy level drops below 20 %. Only one thermal storage is charged at the time, due to challenges modeling in Excel. The middle heat exchanger is bypassed when the DHW storage is charged, and vice versa. In practice, the storages can be charged at the same time. The DHW tank is sized to cover one day's hot water demand, to guarantee hot water for hotel guests in case of failure. The space heating tank is sized to be as little as possible while still covering the demand. The DHW is heated to 80 °C and the water for space heating is heated to 35 °C. An approach temperature of 5 °C is assumed in the heat exchangers in the gas cooler configuration. After the gas cooler, the fluid is expanded to an intermediate pressure receiver at 40 bar, where the vapor is removed through a bypass valve. Liquid CO_2 is expanded to the appropriate pressure level for the different evaporators, except for the gravity-driven AC evaporator, also at 40 bar. The heat pump is designed with three compressor

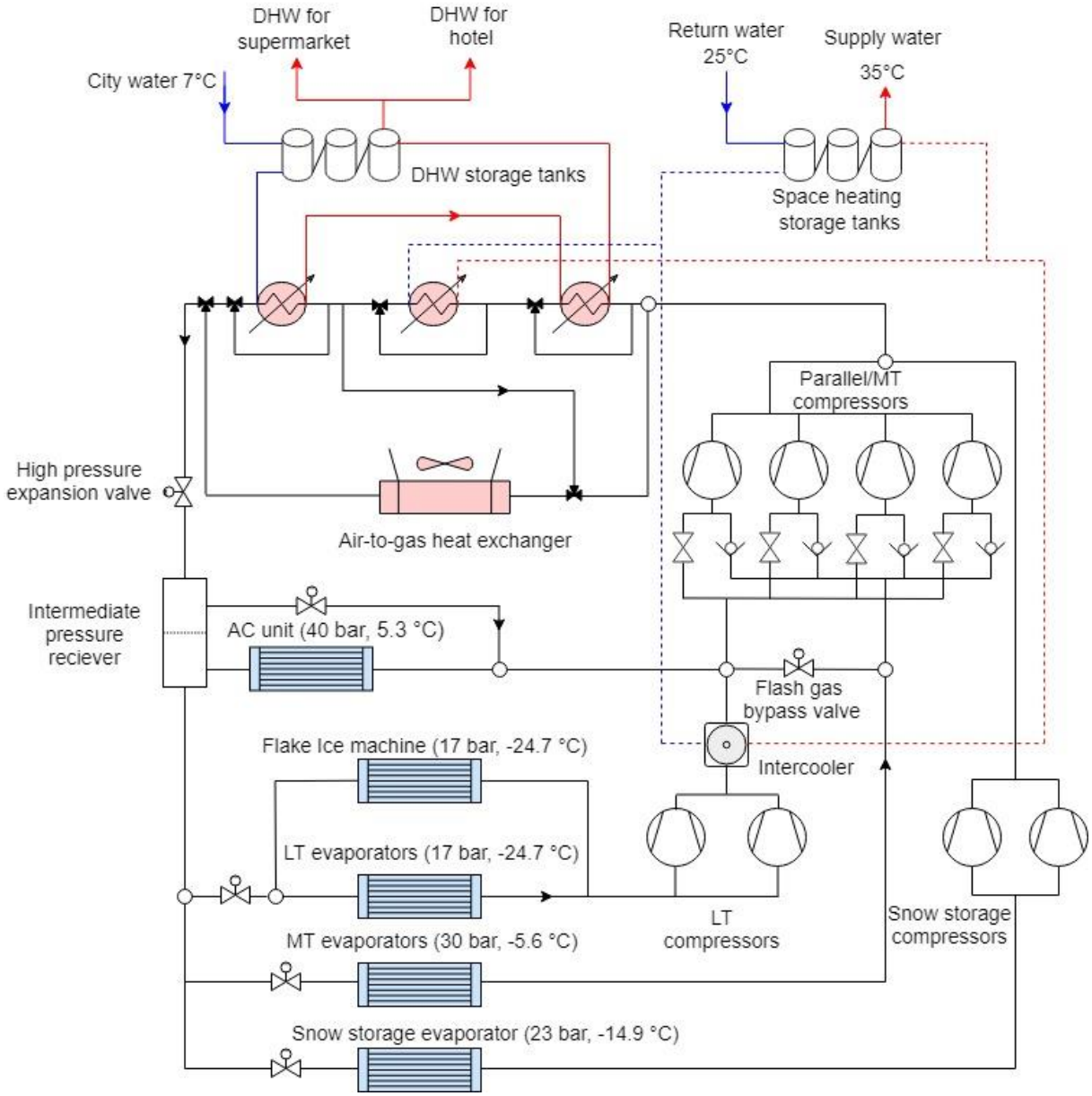

Figure 3: Heat pump design with space heating and DHW sub-systems.

racks. The suction line of the compressors in the parallel/MT compressor rack can be alternated to allocate compressors to be operated as MT compressors in periods where the parallel compressors would operate at a too low pressure ratio. All compressors are modeled with a 10 % heat loss and an isentropic efficiency depending on the pressure ratio (Fig. 4.). This relation is developed by Prof. T. M. Eikevik at NTNU, using measurements on piston compressors (Bergwitz-Larsen, 2016). To reduce the required size of the space heating tank, integrating PCM in the thermal storage is considered. The supply water for space heating purposes is 35 °C. A hydrated salt PCM melting at 34 °C is chosen for this evaluation. The PCM will melt when the storage is charged with water at 35 °C. When the storage is drained, return water at 25 °C is admitted to the storage, receiving latent heat from the solidifying PCM.

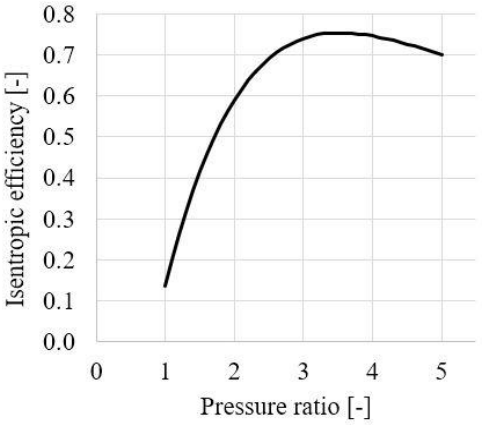

Figure 4: Isentropic efficiency of compressors as a function of pressure ratio

2.4 Simulation cases and control strategy

Different cases are defined to compare the performance and operational costs of the energy system. To reduce the cost of electricity, the potential of shifting snow production to hours of the day with cheaper electricity spot prices is investigated. Additionally, the system is considered both to only recover heat for the heating demands of the building plot and to recover all available heat. This yields four cases:

Case 1: Complete heat recovery and continuous snow production

Case 2: Complete heat recovery and snow production to low electricity prices

Case 3: Partial heat recovery and continuous snow production

Case 4: Partial heat recovery and snow production to low electricity prices

In all cases, snow production is switched off when the AC demand exceeds 20 kW to reduce peak loads. The heat not needed by the building plot in case 1 and 2 is used for heating hot water to be sold to local clients such as hotels and swimming halls. This heat is rejected to the ambient in case 3 and 4. In all cases, electricity prices from the Nordic power market are used (Fig. 5.). These prices are obtained from Nord Pool (2017), and the hourly median is calculated from data for the full year of 2017. Norway will have direct connections to the British and German power grid by 2020 (Norwegian Ministry of Petroleum and Energy, 2017). This can cause the spot prices in Norway to fluctuate more, due to weather, dependent production in Germany. Therefore, a future price scenario is created to evaluate the energy system with higher variations in the spot prices. During heat recovery mode, the high side pressure is set to 100 bar and the parallel compressors are utilized. No gas is expanded in the flash gas expansion valve in this mode. In the high-side, the fluid is cooled down to 12 °C by the inlet city water, which is heated for DHW purposes. During heat rejection mode (case 3 and 4 only), the pressure in the air-to-gas heat exchanger, P_{GC}, is controlled according to the ambient temperature to optimize the energy efficiency. The modeled strategy (eq. 1) is developed in cooperation with Dr. Ángel Álvarez Pardiñas at NTNU.

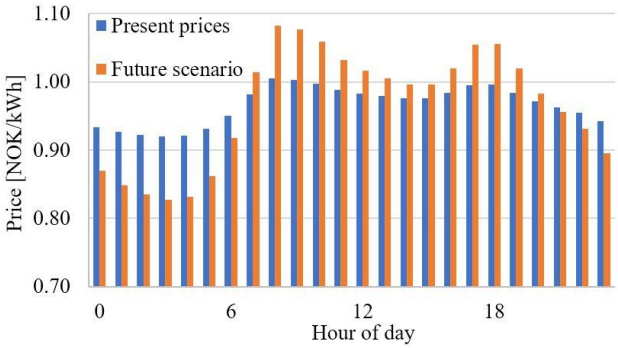

Figure 5: Daily spot price variations for the Nordic power market, including a future price scenario

$$P_{GC}(T_{amb}) = \begin{cases} \frac{(T_{amb} + 5)\text{K} - 25\text{K}}{(40 - 25)\text{K}} \times (100 - 70.5) + 70.5 & T_{amb} > 20\ ℃ \\ P_{sat}(T_{amb} + 8\text{K}) & T_{amb} \leq 20\ ℃ \end{cases} \quad (1)$$

3. RESULTS AND DISCUSSION

3.1 Snow Demand

The energy system is simulated with an hourly resolution for a full year. The annual snow demand of the cross-country track was found to be 80 406 m^3. With the proposed shading construction, the snow demand is reduced by 42 %, to 47 036 m^3. It is evident that the difference in snowmelt is greatest during summer, due to higher radiation values. The simulation shows that the required storage volume with and without shading is 20 000 m^3 and 34 000 m^3, respectively (Fig. 6.). The snow production rate is set to achieve the same storage level at the end of the year as the initial level. The model is used to calculate melt of a snow pile of similar geometry as an experiment in Sweden by Lintzén (2016). During a 42-day period in the spring, the model yields a melt rate of 0.14 m^3/hour, compared to 0.19 m^3/hour in the experiment. The average temperature in the experiment was lower than in the calculation by the model, suggesting that the calculated melt is somewhat low.

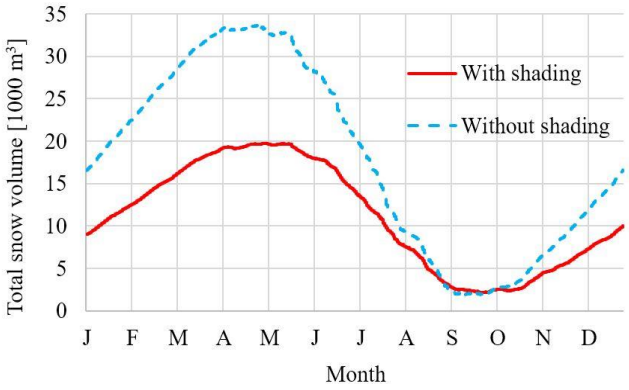

Figure 6: Simulated annual snow storage stock

3.2 Heat Pump Performance

The focus of the simulated results is to evaluate the heat pump's performance and operational costs within the four cases. Case 1 is considered the base case. The average annual energy efficiency (E.E.) of the system is defined as all useful thermal demands divided by the total compressor work as stated in equation 2:

$$E.E. = \frac{H_{space\ heat} + H_{DHW} + C_{TIS} + C_{LT} + C_{MT} + C_{snow\ storage} + C_{AC}}{W_{LT} + W_{MT} + W_{parallel} + W_{snow\ storage}} \quad (2)$$

H and C represents heating and cooling contributions, respectively, and W represents compressor work. The cooling efficiency is found by only considering the cooling contributions. In all cases, the provided cooling is equal. Case 1 and 2 both record an energy efficiency of 4.62. Only 2.5 % of all heat is rejected. This happens during charging of the space heat storage while the gas is cooled further by the air-to-gas heat exchanger. Case 3 and 4 record lower efficiencies, 2.50 and 2.52, respectively, due to less heat recovered. In these cases, the heat demand of the hotel and supermarket amount to only 12 % of the total heat available in the gas cooler, hence, 88 % of the heat is rejected. For equal snow production rate, the system is compared to a flake ice system with heat recovery modeled by Bergwitz-Larsen (2017) (Tab. 1.).

Table 1: Comparison of component loads

	Flake ice system	CO_2 Heat Pump	Unit
$\dot{Q}_{Gas\ coolers}$	629	621	kW
$\dot{Q}_{Evaporators}$	442	440	kW
$\dot{W}_{compressors}$	266	235	kW

The load in the gas cooler and evaporator are similar, strengthening the reliability of the model. The heat pump modeled in this work has a lower power requirement, due to less level of detail regarding thermodynamic losses. The effects of the flake ice drum on system performance is evaluated. To obtain reasonable results, the energy efficiency is calculated with all available heat in the gas cooler, as it is arbitrary if the storages are charged during snow production or not. In case 2, the calculated efficiency rises from 4.65 during snow production to 6.61 without snow production. In case 2 and 4, the cooling efficiency is found to rise 51 % and 60 %, respectively. These results suggest that the snow production lowers the system performance. The system is found to have almost identical efficiency in summer and winter in case 1 and 2. However, frequent peaks are observed in summer due to the AC demand exceeding 20 kW and the snow production switching.

The required DHW storage for covering one day's hot water demand is 7.5 m^3. The required space heat storage size is larger, due to a higher peak demand and lower temperature in the supply water. In case 1 and 3, the required storage is found to be 30 m^3. Due to less stability in the available heat, a larger volume, 100 m^3, is required in case 2 and 4. In these cases, integration of PCM capsules in the water tanks can reduce the storage volume (Fig. 7). A 100 % volume fraction of PCM means no water present in the tank, and distribution through the pipe network is impossible. Hence, there needs to be water present in the tanks, however how much is unknown. A 30 % volume fraction of PCM is considered, which results in a 59 % reduction of required storage space. This requires 25 830 kg of the PCM, which represents a material cost of NOK 1 949 888.

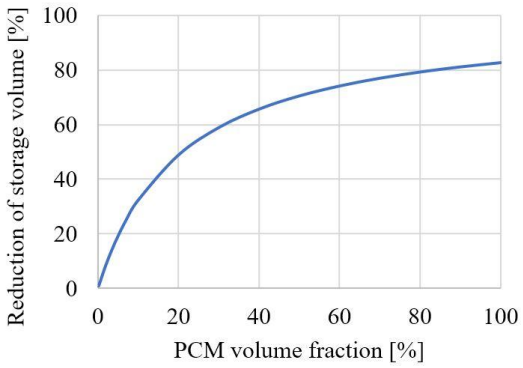

Figure 7: Reduction of storage volume due to implementation of PCM

In the comparison of operational costs, shifting the snow production to periods of cheaper spot prices was found to reduce the electricity consumption cost marginally (Tab. 2.). Doing so also results in a higher peak power demand. Power companies normally charge a fee related to a business customer's peak demand (TrønderEnergi Nett, 2018). This fee was found to increase more than the electricity consumption cost decreased in all cases. In case 1 and 2, the estimated revenue of hot water sale is 1 391 015.

Table 2: Total power costs for all cases, in NOK

Case	1	2	3	4
Electricity consumption cost	1 402 477	1 388 621	1 247 434	1 225 289
Peak load fee	107 592	143 083	113 127	150 916
Total power cost	**1 510 069**	**1 531 704**	**1 360 561**	**1 376 205**

The temperature of CO_2 at the inlet to the gas cooler was found to be around 120 °C. This is higher than necessary for heating water to 80 °C. Therefore, a parameter study was performed to see the effect of reducing the high-side pressure, which was initially set to 100 bar. The restricting condition is the temperature of the CO_2 entering the gas cooler, which needs to be higher than 80 °C. The result of the study shows that the electricity consumption of the compressors drops linearly with decreasing high-side pressure (Fig. 8.). The annual energy efficiency can be increased above 5.0 when the high-side pressure is reduced to 75 bar. In this case, the CO_2 enters the gas cooler at 86 °C. As mentioned, the snow production was found to have a negative impact on the system's annual energy efficiency. In an attempt to increase the heat pump's performance, an additional parameter study was performed, altering the evaporation temperature in the FID. If one assumes that the overall heat transfer coefficient in the FID remains unchanged, the logarithmic mean temperature difference between the refrigerant and the water/ice can be reduced if the heat transfer area is increased. Initially, raising the evaporation temperature in the FID decreased the overall efficiency of the system. The explanation lies with the LT compressor, now operating at a lower pressure ratio. With a reconfiguration of the system to a single-stage compression after the flake ice machine, the annual energy efficiency and cooling efficiency was found to increase with higher evaporation temperatures (Fig. 9).

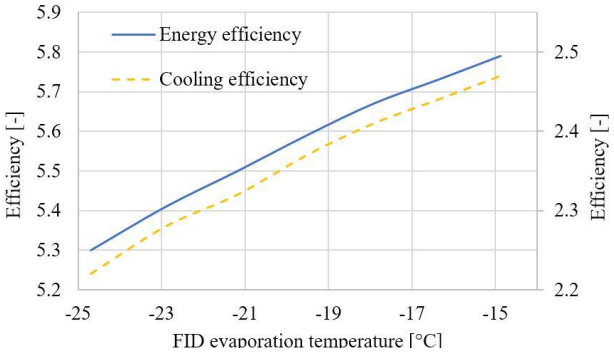

Figure 9: Energy- and cooling efficiency at different evaporation temperatures in the FID

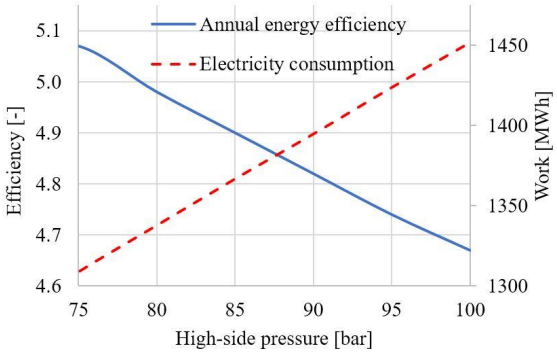

Figure 8: Annual energy efficiency and electricity consumption at different high-side pressures

3.3 Further remarks

In the calculation of received radiation on the cross-country slope with the proposed shading installation, it is assumed that no direct solar radiation enters the snow layer. With only roof shading, direct radiation can enter the snow layer, especially at high latitudes. A shading construction with both a roof and a wall to shade primarily towards the south should be considered. This would require modeling of the entire cross-country circuit, outside the scope of this work.

Precipitation is not accounted for in evaluation of the snow demand, neither as snow nor as rain. Natural snowfall reduces the snow demand, while rain is expected to increase the snowmelt, and thus, snow demand. Therefore, not considering precipitation is expected to not influence the annual snow demand much, as it both increases and decreases the snow demand. However, it will reduce demand in winter and increase demand in summer, which results in a larger volume requirement for the snow storage. On a related note, the cooling demand of the snow storage building is estimated in a simple manner, as the transmission heat loss through the building envelope. A higher cooling demand is expected in practice.

The strategy of only charging one heat storage at the time was implemented due to challenges modeling in Excel. Interestingly, this strategy was proposed by Smitt (2018) to reduce the amount of heat rejected in the gas cooler of a centralized energy system for a hotel, including a transcritical CO_2 heat pump and heat recovery to DHW and space heating storages. Due to the 25 °C return temperature in the space heat subsystem in this work, some heat needs to be rejected with this configuration as well, in order to achieve the desired temperature out of the gas cooler. This is found to reduce the annual electricity consumption by 9000 kWh. Adding the heat rejected in the intercooler when there is no space heat demand, 2.5% (102 000 kWh) of the available heat is rejected compared to 9.0 % (ca. 55 768 kWh) in the system modeled by Smitt.

4. CONCLUSIONS

The proposed system is able to cover all heating and cooling demands of the supermarket, hotel and for snow production. This is made possible by operating the system to cover the cooling demands while recovering heat to hot thermal storages. The peak loads of the system are determined by the cooling demands. Thus, hot thermal storages will not reduce the necessary installed capacity. As there are no periods where more refrigeration than the demand is produced, cold thermal storages are not implemented. The snow production is found to have a negative impact on system performance. To minimize this impact, a shading construction of the cross-country slope is implemented and found to reduce the snow demand by 42 %. With shading, the necessary snow storage to meet the summer demand is found to be 20 000 m^3. The system is shown to have an annual energy efficiency of 4.62, assuming a possible sale of hot water to nearby clients. This sale generates an estimated annual revenue equal to 92 % of the annual electricity cost, which is NOK 1 510 069. Shifting snow production to periods with lower electricity spot prices is found to increase the annual costs due to the increased peak load and the corresponding increase in fees. A proposed system improvement is reducing the high-side pressure during heat recovery from 100 bar to 75 bar. This will increase the annual energy efficiency from 4.62 to 5.02. Raising the evaporation temperature in the flake ice machine and reconfiguring the discharge to a one-stage compression increases the efficiency from 4.62 to 5.79. However, this requires an investigation of the possibility to produce flake ice at higher evaporation temperatures.

NOMENCLATURE

AC	Air Conditioning	LT	Low Temperature (-24.70 °C)
C	Cooling load (kW)	MT	Medium Temperature (-24.70 °C)
CO_2	Carbon Dioxide	ODP	Ozon Depletion Potential
DHW	Domestic Hot Water	PCM	Phase Change Material
E.E.	Average Annual Energy Efficiency	$\dot{Q}$	Heat Transfer Rate (kW)
FID	Flake Ice Drum	TIS	Temperature-independent snowmaking
GWP	Global Warming Potential	W	Work (kWh)
H	Heating Load (kW)	$\dot{W}$	Power (kW)

REFERENCES

[1] Bergwitz-Larsen, K. 2016. Energy Efficient and Environmental Friendly Snow Production at Temperatures above 0 °C. Project assignment, Norwegian University of Science and Technology (NTNU).

[2] Bergwitz-Larsen, K. 2017. Energy Efficient and Environmental Friendly Snow Production by Refrigeration Systems. Master's thesis, Norwegian University of Science and Technology (NTNU).

[3] Dieseth, J.-B. R. 2016. Snow Production Equipment at Ambient Temperatures Above Zero Degrees Celsius. Master's thesis, Norwegian University of Science and Technology (NTNU).

[4] European Union, 2016. EU legislation to control F-Gases. In *Climate Action.* Available at: <https://ec.europa.eu/clima/policies/f-gas/legislation_en> [Accessed 26 June 2018].

[5] Hock, R. 1999. A distributed temperature-index ice- and snowmelt model including potential direct solar radiation. *Journal of Glacialogy*, 45(149):101-111.

[6] Lintzén, N. 2016. Properties of Snow with Applications Related to Climate Change and Skiing. Doctoral thesis, Luleå University of Technology.

[7] Müller, O. B. 2015. Får kritikk for tidlig snøproduksjon. Available at: <https://www.gd.no/nyheter/reiseliv/ringsaker/far-kritikk-for-tidlig-snoproduksjon/s/5-18-165116> [Accessed 27 February 2018].

[8] Nord Pool 2017. Historical Market data. Available at: <https://www.nordpoolgroup.com/historical-market-data/> [Accessed 13 April 2018].

[9] Norwegian Ministry of Petroleum and Energy 2017. Kraftmarkedet. Available at: <https://energifaktanorge.no/norsk-energiforsyning/kraftmarkedet/> [Accessed 17 June 2018].

[10] Selvnes, H. 2017. Energy distribution concepts for Urban Supermarkets including energy hubs. Master's thesis, Norwegian University of Science and Technology (NTNU).

[11] Smitt, S. M. 2017, Integrated Energy concepts for high performance hotel buildings. Master's thesis, Norwegian University of Science and Technology (NTNU).

[12] Smitt, S. M., Hafner, A., 2018. Integrated Energy concepts for high performance hotel buildings, Proceedings of the 13th IIR Gustav Lorentzen Conference on Natural Refrigerants, Valencia, Spain, IIF/IIR

[13] Standard Norge 2012. NS 3701:2012 Kriterier for passivhus og lavenergibygninger – yrkesbyginger.

[14] Standard Norge 2016. SN/TS 3031:2016 Bygningers energiytelse – Beregning av energibehov og energiforsyning.

[15] TrønderEnergi Nett 2018. Nettleie for bedriftskunder fra 1. januar 2018. Available at: <https://tronderenerginett.no/nettjenester/vilkar-og-nettleie/nettleie-bedrift-2018> [Accessed 6 May 2018]

[16] United Nations Environmental Program (2016). The Kigali Amendment to the Montreal Protocol: HFC Phase-down, Ozon Action Fact Sheet. In 28th Meeting of the Parties to the Montreal Protocol, 10-14 October, 2016, Kigali, Rwanda, pages 1–7, Nairobi, December 2016. Available at: <http://web.unep.org/africa/news/kigali-amendment-montreal-protocol-another-global-commitment-stop-climate-change> [Accessed 13 February 2018].